PHYSICO-CHEMICAL STUDIES ON DUSTS:

"THE SUPPRESSION OF AIRBORNE DUST BY AQUEOUS SPRAYS"

by

Rajendram Varadachari GOPALAKRISHNAN, B.E.

A thesis submitted to the University of Glasgow in fulfilment of the requirements for the degree of Ph.D. in Science.

SEPTEMBER, 1962.

ACKNOWLEDGEMENTS

The author gratefully acknowledges the valuable guidance and the constant encouragement given by Professor P.D. Ritchie and Dr. W. Gibb during the course of this work.

Thanks are also due to Professor G. Hibberd and Mr. A.W.K. Stewart of the Mining Department of the Royal College of Science and Technology for helpful discussion on the use of the Automatic Particle Counter; to Messrs. Bauchop, G.S., Deshpande, A.K. and Sweetin, R.M. for assistance in carrying out some special experiments; and to Mr. A. Clunie and Staff of the Chemical Technology Department Workshops for help in preparing various pieces of apparatus.

The author also wishes to take this opportunity for thanking the Council of Scientific and Industrial Research, Government of India, for the award of an 'Assam Oil Company' Scholarship for the first two and a half years and Professor Ritchie for a maintenance grant for the remainder of the period.

oooooo

CONTENTS

SUMMARY

This study is concerned with the capture of airborne dust particles by sprayed liquid droplets, with particular reference to the airborne coal dust encountered in mining practice. The particle size range 0.5 - 5.0 microns, of physiological importance in causing occupational health hazard, has been investigated.

The significance of dusts and their harmful particle-size and concentration are discussed and the incidences of coal-miners' pneumoconiosis and existing methods of dust suppression in mines are surveyed. The general mechanism of liquid spray formation from nozzles is investigated and the theoretical probability of capture of dust particles by spray droplets is discussed.

Experiments on dust suppression were carried out on moving dust clouds in a wind-tunnel of 45.72 cm. (18 in.) diameter and 20 metres (65 ft.) long, under controlled conditions. Dust clouds, of concentrations in the range 300 and 3000 p.p.c.c., were produced using Hattersley's laboratory type dust generator. A three-throw reciprocating pump provided spray pressures up to about 210 kg./sq.cm. (3,000 p.s.i.g.) and the spray nozzles were

operated at the axis of the tunnel against the flow of dust-laden air. Simultaneous dust sampling was done by two thermal precipitators located ahead of and beyond the spray nozzle.

Distribution of air velocity in the tunnel was studied and modifications in the tunnel were made to straighten out the air flow. The effect on air flow pattern of baffle plates suitably placed in the tunnel is illustrated in the form of iso-velocity curves.

Distribution of dust concentration in the tunnel was studied with salicylic acid filters and the rate of decay of dust concentration with distance along the tunnel was found to be constant. The probable mechanisms of dust fall-out are discussed.

A system for counting the thermal precipitator dust slides using a five-channel Automatic Particle Counter and Sizer was developed and an analysis of variance for the machine was made.

Simultaneous dust sampling by thermal precipitator and salicylic acid filter was carried out in the tunnel and a correlation factor was derived on the basis of proportional number percentage size frequencies in both the samples.

Measurment of Average Droplet Size was carried out for water sprays in the range 35.15 - 190.16 kg./sq.cm. (500 - 2,750 p.s.i.g.) using a solid cone spray nozzle and the relationship

$$A.D.S. \quad \alpha \quad p^{(-0.28)}$$

was obtained. A functional non-dimensional relationship was also derived between the characteristics of the spray and the Average Droplet Size.

The dust suppression work was mainly concerned with small high pressure spray nozzles and the following issues were brought to focus: The effects on the efficiency of dust suppression of,

(a) hollow cone and solid cone spraying,

(b) high spray pressures,

(c) surface tension of sprayed liquid,

(d) counterflow air velocity, and

(e) a tandem arrangement of spray nozzles.

The effect of spray throughput on dust-water ratio was also studied. Solid cone spraying was found to be about 5 per cent more efficient than the hollow cone spray for the same nozzle. Maximum dust suppression was effected at 140.6 kg./sq.cm. in both the cases. (53.58 per cent and 48.5 per cent).

Surface active agent solutions were found to give only a small increase in dust suppression efficiency, E. The wetting power of different types of surface active agents is discussed. A relationship was obtained between the efficiency, spray pressure and the surface tension of the sprayed liquid.

Tandem spraying was found to give the best dust suppression efficiencies without much increase in water throughput. The rate of increase in E with number of spray nozzles in tandem was found to be maximum (about 6.5 per cent) at 140.6 kg./sq.cm.

An increase in air velocity resulted in a rapid decrease of E. The rapid deceleration of droplets on discharge into the gaseous medium, its lowered efficacy of impact on dust particles and the consequent reduction of the "capture cross-section" are discussed.

The dust-water ratio was calculated for all spray pressures and nozzles employed and was found to generally decrease with increase in throughput.

The sprayed droplets did not appear to be selective in suppressing any particular size-range of dust particles.

An improved type of dust feeding machine was put into operation and is discussed in the Appendix.

LIST OF SYMBOLS AND ABBREVIATIONS

Symbols			Units
A.D.S.	=	average droplet size of sprays	micron
A.P.C.	=	automatic particle counter	
C_D	=	drag coefficient	
C_d	=	coefficient of discharge in nozzles	
D	=	diameter of wind tunnel (45.72)	cm.
D_o	=	orifice diameter of spray nozzle	cm.
D_p	=	diameter of droplet	micron
D_{po}	=	diameter for grazing capture cross-section.	micron
d_p	=	diameter of dust particle	micron
$\bar{d}$	=	mean size of particle oversize z	micron
E	=	dust suppression efficiency	
E_c	=	collection efficiency	
$\overline{FN}$	=	flow number	$(gal/hr)/\sqrt{p.s.i.g.}$
g	=	acceleration due to gravity	cm/sec/sec.
H	=	dynamic pressure of air	inches w.g.
h	=	particle size projection in A.P.C.	micron
h^1	=	height of fall of particles in sedimentation.	cm.
K	=	Particle parameter	
k_1, k_2, k_3	=	proportionality constants	
K.E.	=	kinetic energy	ergs.
L	=	length scanned	mm.

Symbols			Units
M	=	magnification in A.P.C.	
n	=	number of particles	
n_o, n_1	=	initial and final dust concentrations.	p.p.c.c.
P	=	spray pressure	kg./sq.cm.
p	=	amplitude discriminator value in A.P.C.	
p.p.c.c.	=	particles per cubic centimeter of air	
Q_w	=	throughput of sprays	litres/min.
Q_a	=	rate of air flow	c.c./sec.
Re	=	Reynolds Number	
$(Re)_C$	=	Reynolds Number for critical velocity	
r_m	=	nearest distance of approach of grazing trajectory of the particle to the centre of the droplet.	
S	=	penetration of a liquid droplet	cm.
S_i	=	adhesion tension between coal particle and spray droplet.	dyne/cm.
t	=	time	sec.
T.P.	=	thermal precipitator	
U_c	=	critical velocity	cm./sec.
V_r	=	fluid velocity relative to liquid droplet at large distances from the liquid droplet.	cm./sec.
V_s	=	terminal velocity of aerosol, as given by Stokes' law.	cm./sec.
V_s'	=	terminal velocity of aerosol, after applying Cunningham's correction.	cm./sec.
$\phi(W)$	=	number of intercepts in A.P.C. for particular slit width W	

Symbols			Units
y_o^2	=	Fonda and Herne's dimensionless capture cross-section	
$\bar{y}_o^2$	=	average value of capture cross-section over the range of penetration S of spray	
z	=	sensitivity	micron
$\bar{z}$	=	distance from wall of tunnel	cm.
α	=	angle of contact of liquid on solid surface	degree
θ	=	spray cone angle	degree
γ	=	surface tension	dyne/cm.
ρ	=	density	gm./c.c.
η	=	absolute viscosity	poise
a,l,s	=	subscripts for air, liquid and dust particle	
σ	=	standard deviation	
λ	=	mean free path of gas molecules	cm.
μ	=	micron	

oooooo

1. INTRODUCTION

1.1 Definition and Significance of dusts in Industry

The generic term 'aerosols' was coined by Professor F.G. Donnan[1] towards the end of the first World War to cover all the various disperse systems in air, such as dusts, smokes, fumes and mists. Dusts, in a colloid sense, consist of solid particles, dispersed in a gaseous medium as the result of the mechanical disintegration of matter.

Dust-producing processes in industry are too numerous to mention, but some typical examples are the processes of drilling and blasting in mines, quarrying and screening of granite, sand-blasting and "fettling" in foundries. The sizes of dust particles range widely from the submicroscopic to the visible and those larger than 76 microns in diameter are defined as 'grits' by the British Standards Institution[2]. (1 micron (1μ) = 10^{-3}mm.). Generally 'settled' dusts are above 20μ in diameter, while the lower range of 'air-borne' dusts may well extend into submicroscopic region. The percentage composition of air-borne dusts is liable to differ from that of the parent substance, on account of differential disintegration and selective settling of the dispersed particles.[3] Some pathologists prefer to include 'fumes' in the category of 'dusts' "to designate a pathological entity",[4] since fumes are also solid particles, mostly generated by the condensation of vapours of solid matter after volatilization from the molten state. Fumes, however, are usually below 1μ in size and in contrast to dusts, they often flocculate vigorously. A general classification of aerosols is given in Table 1.1 with particular reference to the size range of dusts and spray droplets used by the author in the work which led to this thesis.

Dusts from industrial atmospheres may require to be suppressed or recovered for the following reasons:-

(1) Certain dusts, notably metallic powders and organic dusts, may cause violent explosions, if they are present in appropriate concentrations in air.(5)(6)(7) This explosion hazard owes itself to the increased rate of oxidation and chemical activity, which result from an increase of surface area per unit volume with reduction of particle size. In a coal-pit, dust concentrations greater than 50 grams/cu.m. are considered dangerous.(8)

(2) Fine air-borne dusts (size less than 5μ) contribute to unhygienic working conditions and are the cause of many occupational diseases, leading progressively to total disability of the worker. This disease of the lung produced by the inhalation of dust is given the general name "Pneumoconiosis"(9). Dusts, known to cause pulmonary disability are siliceous dusts such as quartz, talc, diatomaceous earth and asbestos, other inorganic dusts such as beryllium, iron and

TABLE 1.1 CHARACTERISTICS OF AEROSOLS

(A list of symbols is given in pages v-vii)

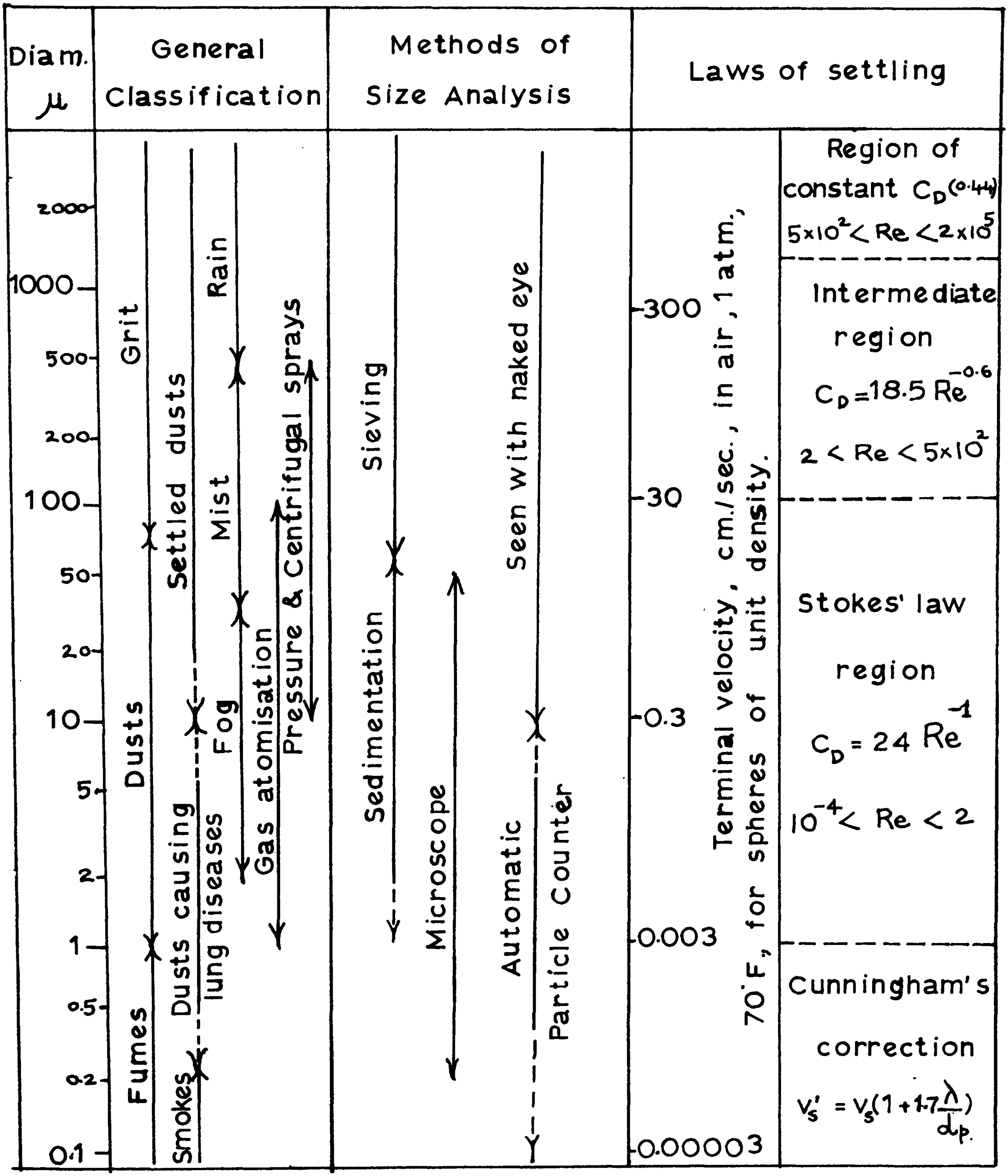

manganese dioxide, vegetable dusts such as cotton and bagasse, and other "organic" dusts such as graphite and coal.[4][10]

(3) The dust may be valuable, such as potash from the blast furnace gases, pulverised coal from flue gases of industrial boiler plants, cement from the cement kiln gases, and the catalysts from the cracking plants of oil refineries.

(4) The substance may have to be manufactured in powder form such as carbon black and high-grade zinc dust.

Supression systems relating only to the fine disease-producing coal dusts, as encountered in mining atmospheres, are discussed in the present work.

1.2 Pneumoconiosis

This pulmonary disease due to excessive dust inhalation has been known for centuries in the various dusty industries as mason's disease, potter's rot, miner's asthma, grinder's rot, Monday Morning fever, etc. Zenker[11] used the term "pneumonoconiosis" (compound of two Greek words 'pneumon' and 'conis', meaning 'lung' and 'dust' respectively) in 1866 to describe these dust-diseases and this was shortened to 'pneumoconiosis' by Proust[12] in 1874. Though the term denotes 'the disease of the lungs produced by the inhalation of dust', a more comprehensive definition of the term is being sought both to designate a pathological entity and to specify an occupational disease. Hamlin[13] describes the term as "an all-inclusive caption for a variety of pulmonary affections......Generically, it does not imply fibrosis, but simply 'dust' in the lung......therefore, pneumoconiosis must include any retention of dust in the lungs, whether of industrial origin or not, and whether of toxic, irritant, proliferative or inert dust."

Various forms of pneumoconiosis are distinguishable by radiological diagnosis of the chest, aided by a knowledge of the nature of dusty occupation and the history of exposure to dust. E.g. (a) Classical Silicosis due to the inhalation of Silica dust, is characterised by a large number of small, firm, grey, whorled nodules;[14] (b) Anthracosilicosis[15] among workers at the coal face and trimmers in the holds of ships is recognised by widespread extreme pigmentation in the lungs, where the Silica is masked by the coal; (c) Coal-miners' pneumoconiosis[16] is known by the condition of 'focal emphysema'; (d) Asbestosis[17] lesions take the form of diffuse fibrosis; (e) Siderosis[18] among haematite miners is characterised by diffuse-fibrosed areas of a bright brick-red colour; (f) Kaolinosis[17] has emphysema as a marked feature and the bluish colour of the lungs is distinctive; etc.

1.3 Incidence of Pneumoconiosis.

As long ago as 1556, Agricola[19] observed that many women in the Carpathian mining districts married seven husbands, "all of whom this dreadul disease has brought to an early grave". The magnitude of this problem can best be realised by the knowledge of the incidence of the disease. The incidence of raw cases of Silicosis in the mines of Witwatersrand was 9.53 per 1000 examined during 1941-'44, though it stood at 28.11 per 1000 during 1917-'20.[20] In the Kolar Gold Fields in India during 1940-'46, 7653 men with five years underground service or more were examined, out of whom 3351 (43.79%) were found to have abnormal radiological appearances of the lung fields.[21] The percentages of cases of pneumoconiosis in a foundry, fettling shop and core-shop are 5.2, 6.7 and 3.1 respectively.[22] In Britain, there were 22,000 men certified as disabled from coal-dust between 1931 and 1948[23] and in 1945 alone, 5224 cases of coal miner's pneumoconiosis were recorded in South Wales.[24] By 1960, 8080 men were receiving disablement benefits under the Pneumoconiosis and Byssinosis Benefit Scheme.[25] The incidence of the coal-miner's disease in Scotland is given in Fig. 1.1 for the year 1959,[26] and the average dust contents of coal-miner's lung is given in Fig.1.2.[27]

1.4 Harmful particle-size and concentration

Medical opinion is not conclusive on the physiological limits of dust particle-size retained in the deep lungs. It was first shown by McCrae[28] that 70 per cent of the particles in silicotic lungs were less than 1μ and

FIG. 1.1 PNEUMOCONIOSIS RATES IN SCOTLAND -1959

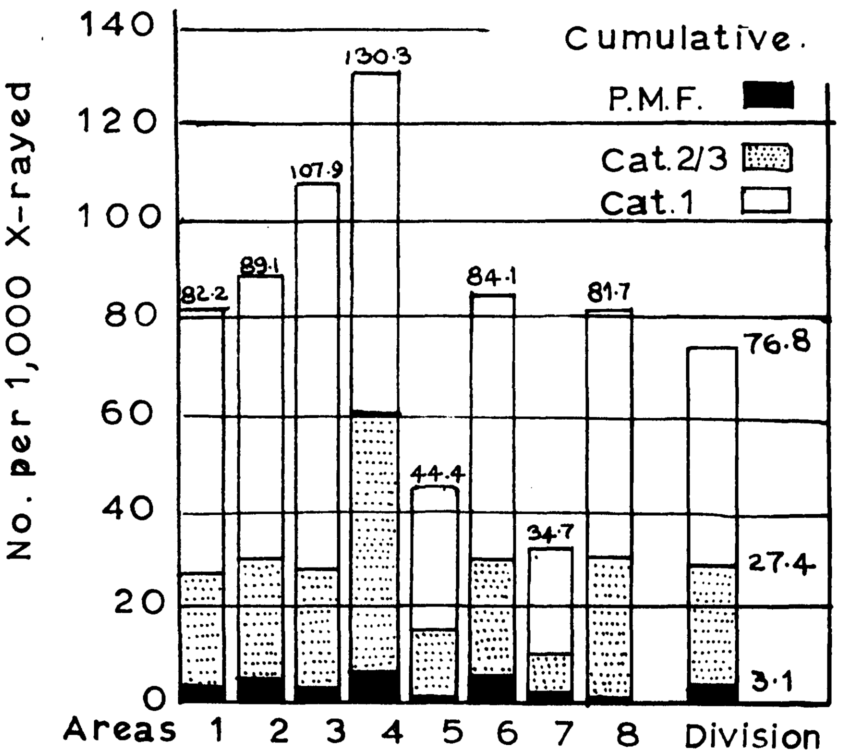

FIG. 1.2. DUST CONTENTS OF COAL-MINERS' LUNGS

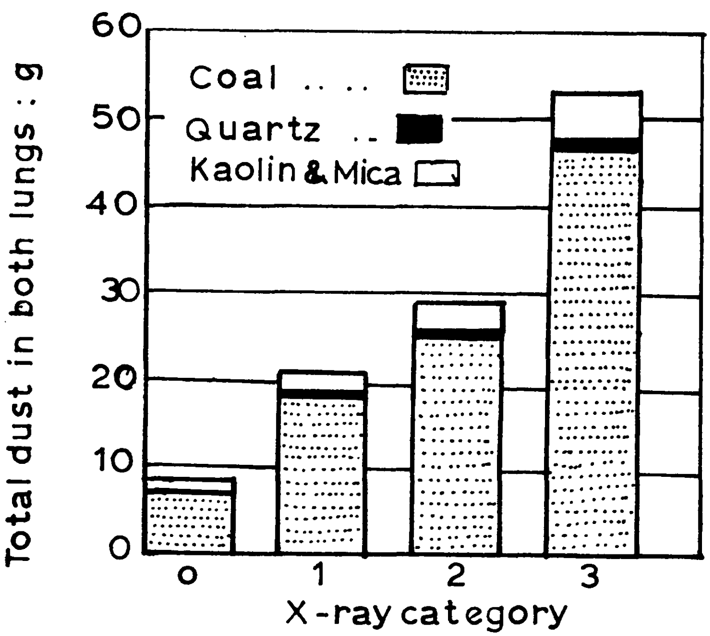

the largest particle did not exceed 10.5μ. On the basis of this work, Mavrogrodato[29] defined disease-producing dust as particles of 0.5 to 5μ in diameter. Gardner and Cummings[30] showed that a much more severe reaction resulted with a given weight of 1 to 3μ quartz particles, than with an equal weight of 6 to 12μ particles, the latter being comparatively inert. Tobbens, Schulz, and Drinker[31] found that the potency of quartz increased markedly as the particle size decreased from 3 to 0.6μ. The Committee on industrial pulmonary disease in Britain[32] has, as a result of extensive investigations during the years 1939-'43, concluded that, in the absence of knowledge to the contrary, all dust of a size less than 5μ should be considered as harmful. The National Coal Board has adopted the size range as 0.5 to 5μ for silica or rock and 1 - 5μ for coal.

Findeison[33] calculated the average air velocity at different points in the respiratory tract, by estimating the dimensions of various parts of the lung and assuming a constant air flow of 200 c.c./sec. during inhalation and exhalation. His velocities, which were later confirmed by Davies[34], are shown in Fig. 1.3. The precipitation of particles on to the lung surfaces is considered to take place by four distinct mechanisms, namely, inertia, sedimentation, wall effect and Brownian motion. Experiments on the retention of particles in the lungs have been carried out/

FIG.1.3. THE MAIN RESPIRATORY CHANNELS OF HUMAN LUNGS

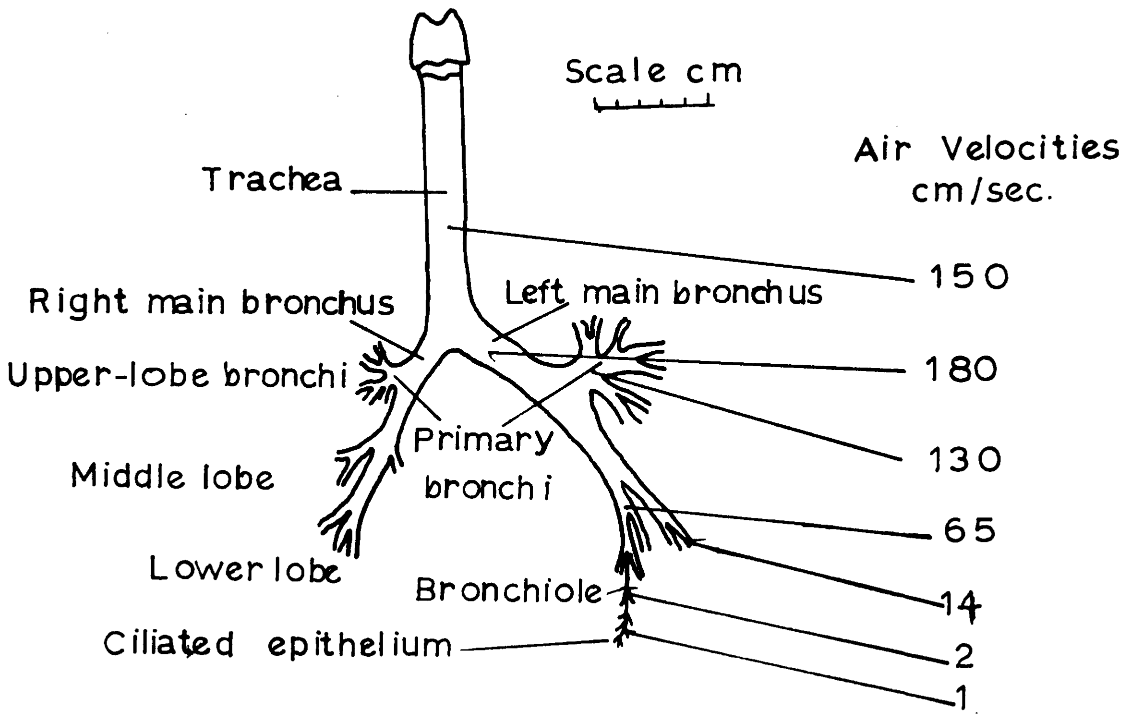

FIG.1.4. THE EFFECT OF PARTICLE SIZE ON ALVEOLAR DUST RETENTION

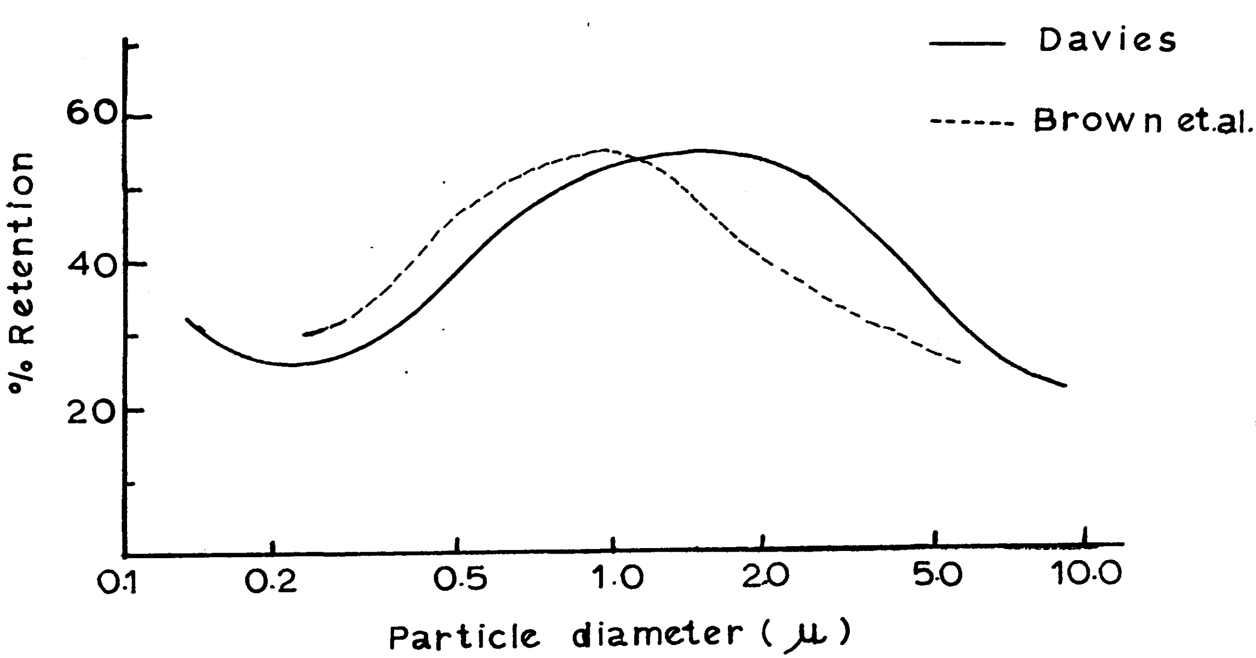

by Van Wijk and Patterson[35], by Landahl and Hermann[36] and by Wilson and La Mer.[37] The dusts used and the methods employed by these workers varied and the results were compared independently by Brown et.al.[38] and Davies[39], on the basis of spherical particles of unit density. Their curves are shown in Fig. 1.4. Brown et.al. showed that the optimum size particles for alveolar deposition is about 1μ and the probability of their being so deposited is the same for particles smaller and larger than 1μ, while Davies indicated that a peak deposition, ranging from 50 to 60 per cent of particles, occurs at 1.5 to 2μ in diameter, and about 30% of the 5μ particles are retained.

No absolute standard has yet been fixed for the maximum allowable concentration of air-borne dust and from the point of view of health, it is obvious that a gravimetric estimation of concentration of dust is of little value, unless it throws light on the quantity of dust in the size range which is of physiological significance. Arbitrary standards of 'approved conditions' do, however, exist. For example, in coal-mines, Bedford and Warner[40] suggested that particles <5μ should not exceed 660 particles per cubic centimetre of air (p.p.c.c.), out of which 600 p.p.c.c. should be coal and 60 stone. The standards laid down by the National Coal Board[41] are (1) 650 p.p.c.c. (1 - 5μ) for anthracite, (2) 850 p.p.c.c. (1 - 5μ) for bituminous coal, and (3) 450 p.p.c.c. (0.5 - 5μ) for stone dust. On a gravimetric basis, Briscoe et.al.[40] concluded that the mass concentration of dust should not exceed 10 mg. of coal dust and 1 mg. of 'stone' or inorganic dust per cu.m. of air and applies only to particles less than 5μ.

1.5 Methods of dust suppression in mines

Dust found in mines may be divided into two categories: inherent and mechanical.

Inherent dust, which is found lying along the cleavage planes or 'slips' in any coal seam, is the result of attrition, which occurred during formation of those cleavage planes.

'Mechanical' dust is produced by almost every operation in the working and transport of coal, such as coalcutting, loading, drilling, shot-firing and conveying and is also influenced by the standard of roof control. Since 1948, the introduction of organised dust-suppression has resulted in a progressive decrease of dustiness, as evidenced by the fact that the mean concentration in the working places has been reduced from 9500 p.p.c.c. in 1949 to 4000 p.p.c.c. in 1952 and to about 500 p.p.c.c.[42] by 1954.

The task of the engineer in maintaining the standards of dust-cleanliness divides itself into -

(i) control of dust at the dust-source, and

(ii) suppression of air-borne dusts.

(i) Control methods to prevent dust at source:

(a) pulsed-infusion shotfiring (water-blasting),

(b) water-infusion and wet-cutting,

(c) Dry drilling, with push-and-pull fan ventilation and various kinds of dust traps.

(ii) Measures to suppress air-borne dusts:

(d) water sprays,

(e) consolidation of roadways,

(f) use of steam,

(g) filters in airways, electrical precipitator or ultrasonic agglomerator.

Water is the principal agent used to suppress dust during coal-cutting, blasting, loading and transferring. At the coal-face, wet cutting and water infusion are the most widely used methods. The introduction of the "Whale" type jib in wet-cutting[8], where internal jets can spray in all directions inside the cut, has resulted in more effective suppression of dust. Water infusion is the process of injection of water under pressure into a coal-seam through bore-holes for the purposes of wetting preformed dust, softening the coal-seam and increasing its "ploughability". As the coal substance is impervious, water passes along the cleavage planes and hair structures, which join these cleavage planes. It is on these planes and fractures that the inherent dust is formed and it is wetted in situ, before the coal is worked. The success of infusion in any seam depends on a systematic study of the factors, which condition the penetration of water into the seam. The factors include[43] position, spacing and depth of infusion holes, pressure, quantity and rate of flow of water, position of the seal in the infusion hole, simultaneous or battery infusing and gas emission. Conditions in British mines have shown that the holes should cut the main cleavages or slips at an angle of from 60 to 90 degrees, the holes being between 4.5 and 5.5 cm. in diameter and 2.75 to 4.5 m. apart. The quantity of water is obviously influenced by the character of coal and the associated roof and floor beds, and an average value is about 7 litres per ton of coal. The rate of flow ranges from 7 to 11 litres per minute and the infusion pressure from 7 to 35 Kg/sq.cm. (100 - 500 p.s.i.). On faces where the pressure for infusion is high or evaporation losses due to slow rates of advance are considerable, the use of wetting agents and waste transformer oil in the form of an emulsion gave encouraging results, with reduced quantity of water, reduced pressure and reduced evaporation losses.

The technique of blasting, known as pulsed infusion, where the shot is fired under water pressure of about 28 Kg/sq.cm., has proved beneficial in reducing air-borne dust during the shotfiring shift. Here the shothole is charged with special explosives[44], which are capable of efficient detonation under water pressures up to 70 Kg/sq.cm. (1000 p.s.i.), the infusion tube is then placed in the mouth of the shot-hole, the water is turned on and the shot is fired while under water pressure.

Water sprays are used in wet-cutting and also at loading and transfer points. Sprays for wet-cutting issue from jets about 6.5 mm. diameter and a quantity of about 14 litres per metre of face cut is required at pressures around 5 Kg/sq.cm. The "fixed sprays" which are used to suppress dust at transfer and loading points, use specially designed nozzles 1.5 to 6 mm. in diameter with the pressure-range from 7 to 35 Kg/sq.cm. Three types of fixed sprays are classified, according to the feeding systems used:[45]

(i) Simple orifice nozzle, where the liquid is injected into the gas through a plain orifice (e.g. Morris Spray).

(ii) Hollow cone nozzle with tangential feed: The liquid is introduced tangentially into a cyclone chamber, in which it rotates as a whirlpool with the shape of a rotating hollow cone and is ejected from the orifice as a hollow cone (e.g. Porter sprays).

(iii) High capacity swirl nozzle with fixed screw. Here the rotation of the liquid is achieved by fixed screw or slanted channels. (e.g. Korting spray).

Under conditions where the use of water is precluded (e.g. high rock temperatures in the deeper levels of mines), the dry suppression methods consist of collection or damping of the cuttings, after extraction from the hole in an air stream induced by an ejector system. In some cases, the cuttings are extracted at the mouth of the hole by a dust hood; in others, they are extracted from the point of drilling through the drill rod. The Holman Dryductor and Hemborn Suction system, used in combination with the Huwood-Holman V bag filter, the Vokes dust trap and the Hemborn dust filter have been proved to suppress dangerous dust as efficiently as typical wet methods. Bit wear is also found to be less with dry drilling processes.[46]

The advent of a flameproof steam-raiser[47] based on the immersion-heater principle has now made steam available for underground dust suppression. Experiments with steam at surface mine tipplers have shown greater degree of dust suppression. Further, a very much smaller quantity of water is needed, if it is used in the form of steam.

Consolidation of roadways is effected by treating the floor first with a wetting agent and then with some hygroscopic salt, so that when trodden on, it becomes plastic. Flaked calcium chloride is normally used and if the relative humidity is greater than 75%, common salt can be used, with a good reduction in cost. In Germany, it is claimed that the salt-crust treatment[48] of the roadways is more effective, due to reduced redispersion of settled dust.

1.6. Liquid spray formation

A liquid spray is generally considered to be a zone of liquid droplets projected into a gaseous medium, and spraying is the process of atomisation of a liquid jet into a multitude of these droplets. The general purposes of spraying a liquid in air are to increase the surface area of a given mass of liquid and to distribute this liquid in air in such a way that the air volume swept by the liquid is large. Sprays in practice encompass a 10^6-fold range of drop sizes, a 10^{12}-fold range of drop areas and a 10^{18}-fold range of drop volumes.(49)

To break-up a liquid mass, it is first forced to assume an unstable free liquid configuration of large surface area. This is accomplished by imparting to it kinetic energy, which causes it to flow through some device which forms it into filaments or a liquid sheet. Because of surface tension, the configuration of large surface area is unstable, and on undergoing disturbances, e.g. the force of gaseous friction, it breaks up into a system of droplets. While the process of break-up is resisted by the viscosity of the liquid, the process of surface formation is resisted by surface tension and viscosity.

The break-up may happen in less than one-millionth of a second. Some kinetic energy imparted to the liquid mass appears as surface energy in the spray, but the major portion of the kinetic energy is retained by the spray drops, causing them to penetrate into the gaseous medium, into which the spray is directed.

Soon after its formation, a spray droplet takes up a terminal velocity with respect to the ambient gas, which is equal to its falling velocity under gravity. The terminal velocities of spheres falling freely in infinite gas volume are shown in Table 1.1. The falling velocity of drops of large size 500 - 5000 μ is likely to be lower than rigid spheres of the same diameter, since they are affected by deformation and internal circulation. It may also be noted from the Table that drops over 100 μ in diameter fall at terminal velocities greater than 30 cm/sec. and will rapidly disengage themselves from any spray moving horizontally.

The process of spray formation and the precise mechanism of atomisation of liquid jets at high injection velocities are complex and are generally known to be dependent on three factors -

(i) the disturbances set up in the liquid flowing through the atomiser;

(ii) the properties of the medium into which the jet is discharged;

(iii) the physical properties of the discharged liquid.

Each contributes to the process; but the difficulty of separating the factors has so far prevented an assessment of the exact contribution of each to the disintegration of the liquid jet.

Rayleigh[50] offered one of the first theories of liquid jet disintegration based upon a mathematical analysis of the stability of a non-viscous jet. He considered a laminar liquid flow with a velocity potential and with the jet only under the influence of surface tension forces, and found that a jet would be unstable and ready to disrupt, if its length were greater than its circumference, i.e. $\ell > 2\pi$. His conclusions were utilised in the later theories of Castleman,[51] Haenlein[52] and Weber.[53] Some authors have stressed the fact that turbulent flow in the atomiser aids the process of atomisation; thus Mehlig[54] and Schweitzer[55] indicated that this turbulence produced a radial component of liquid velocity, which enabled the disintegrating jet to overcome the forces of surface tension. Thieman[56] believed that disintegration was influenced by the relative velocity between the outside of the liquid jet and the air itself. While Strazheuski[57] concluded that air resistance and high jet velocity are the main factors causing and controlling spray formation, Oschatz[58] claimed that the final atomisation of the jet was mainly dependent on the resistance of the surrounding atmosphere.

Spray formation has been studied photographically[59] and three or even four stages of jet disruption were observed and attempts made to relate them to certain values of Reynolds Number[60]

Castleman[61] has put forward a theory of jet disruption, assuming that the most important factor is the effect of air friction, which causes the tearing of ligaments from the main jet core. It is claimed that the size of liquid droplets reaches a lower limit at high discharge velocities; when this condition is reached, the ligaments collapse, as soon as they are formed, and any further increase in the velocity (higher injection pressure) above 10,000 - 12,000 cm/sec., will not produce droplets of smaller size. This theory would seem to be justified in practice where it is found that at high atomisation pressures, the average droplet size is reduced by an increase in the number of small droplets rather than by a reduction in the size of the smallest droplets.[62][63]

The performance of an atomiser depends upon (1) the throughput of the spray nozzle, (2) the cone-angle of the spray, (3) the average droplet-size and (4) the droplet-size distribution. Utilising dimensional analysis, the relation between the properties of the liquid and the atomiser has been found to be[64] as follows :-

$$D_p \propto \left(\frac{\overline{FN}}{\Delta p . \Theta}\right)^{1/3} \left(\frac{PL}{\rho a}\right)^{1/6}$$

1.7 Capture of dust particles by spray droplets

To elucidate the principles involved, the analysis can be simplified to the consideration of the action of one water drop moving through a dust cloud. Best[65] has shown that droplets of water in air can be regarded as spherical when they are less than 1 m.m(1000μ) in diameter. When a water drop traverses such a cloud, it sweeps out a long cylindrical volume of space, but not all the dust particles contained in this volume are hit by the drop. Air is displaced sideways out of the track of the drop and some of the dust particles in this air are also carried out of the path. The fraction of the dust lying in the path of the drop which collides with it and is removed from the cloud is defined as the "collection efficiency" of the drop.

The problem of the collection efficiency of large spheres moving through a cloud of smaller particles has been studied theoretically by a number of workers, notably by Langmuir and Blodgett[66] and Fonda and Herne[67], and experimentally by Walton and Woolcock[68].

The theoretical investigations involve a number of simplifying assumptions and the theories are based on the physical model which comprises a sphere (the drop) of diameter D_p moving at a velocity v relative to a fluid (air) of density ρ_a and viscosity η_a. The fluid contains spherical dust particles of diameter dp and density ρ_s

initially at rest with respect to the fluid. As the sphere moves through the fluid, the latter is displaced out of its path and tends to drag the dust particles with it. The latter, however, because of their mass, are not immediately accelerated to the velocity of the fluid, but lag behind, so that a proportion collide with the sphere; these are the captured particles. Particles whose centres follow paths that pass within a particle radius of the sphere are assumed to make contact. The collection efficiency E is then the ratio of the number of particles hitting the sphere to the number whose centres initially lay within its track.

By the method of dimensional analysis, a theoretical relationship may be developed between the collection efficiency and the significant variables for the drop, for the fluid and for the dust thus:

$$E = f\left(\frac{v.\rho_a.D_p}{2\,\eta_a},\ \frac{v.\rho_s.d_p^2}{2\,\eta_a.D_p},\ \frac{d_p}{D_p}\right)$$

Studies of the trajectories of particles moving under the combined influence of inertia and viscous forces due to fluid flow round a sphere have been made by Langmuir and Blodgett(66), Das(69), Bosanquet(70), Vasseur(71) and Sell.(72) Fonda and Herne(67) gave an analytical treatment of the problem, by assuming that the flow pattern is that of a fluid around a sphere (water drop) and is undisturbed by the presence of the dust particles. If the particle is in the path of the sphere, the two may impact, but the flow of fluid round the moving sphere applies viscous forces to the particles, which tend to remove it from the swept path of the sphere. Whether impact occurs or not depends on the balance of viscous and inertial forces acting on the particle as the sphere approaches it.

On the assumption that the viscous drag force on the dust particle is directly proportional to the vector of the relative velocity of the particle in the fluid, the magnitude of the viscous drag on the particle, taken as a sphere, is $3\pi . d_p . v . \eta_a$ and therefore the particle behaviour can be completely characterised by the quantity

$$\frac{\text{Viscous drag force}}{\text{Inertial force}} \quad \text{or,} \quad \frac{3\pi . d_p . v . \eta_a}{\frac{\pi}{6} . d_p^3 . \rho_s} .$$

The dust particle trajectories within the fluid for purely viscous flow and for potential flow enable one to find which particles initially in the track of the drop ultimately collide with it. A laboratory investigation of the behaviour of methylene blue particles and water spheres[68] showed that all impacts lead to capture of the small particle by the larger sphere. On the other hand Brown[73] suggested that bouncing can occur with a probability depending on the relative velocity and the angle of incidence of each on the other.

A basic Parameter K has been defined, which is dimensionless and whose magnitude is a measure of the ratio of inertial to viscous effects.

$$K = \frac{\rho_s \cdot d_p^2 \cdot v}{9\,\eta_a \cdot D_p}$$

The curves showing the relationship of this parameter K to the collection efficiency of particles by droplets are given in Fig. 1.5.

1.8 Objects of research

Although a great deal of work has already been carried out in the mines on the suppression of fine dusts by sprays under widely varying conditions of wind velocity and dust concentration, it was felt that research should be initiated on the suppression of air-borne dusts by sprays under carefully controlled laboratory conditions. This project, thus, became a part of the Pneumoconiosis Research programme formerly supported by the Scottish Division of the National Coal Board.

Earlier workers in this programme had been engaged in the development of apparatus, for the examination of the air-settling characteristics of fine dust of a particle-size dangerous to health. Glen(62) used a dust chamber, into which the dust was injected and dispersed and which incorporated three pairs of photo-electric cells, connected in opposition

FIG.1.5 COLLECTION EFFICIENCY v PARAMETER

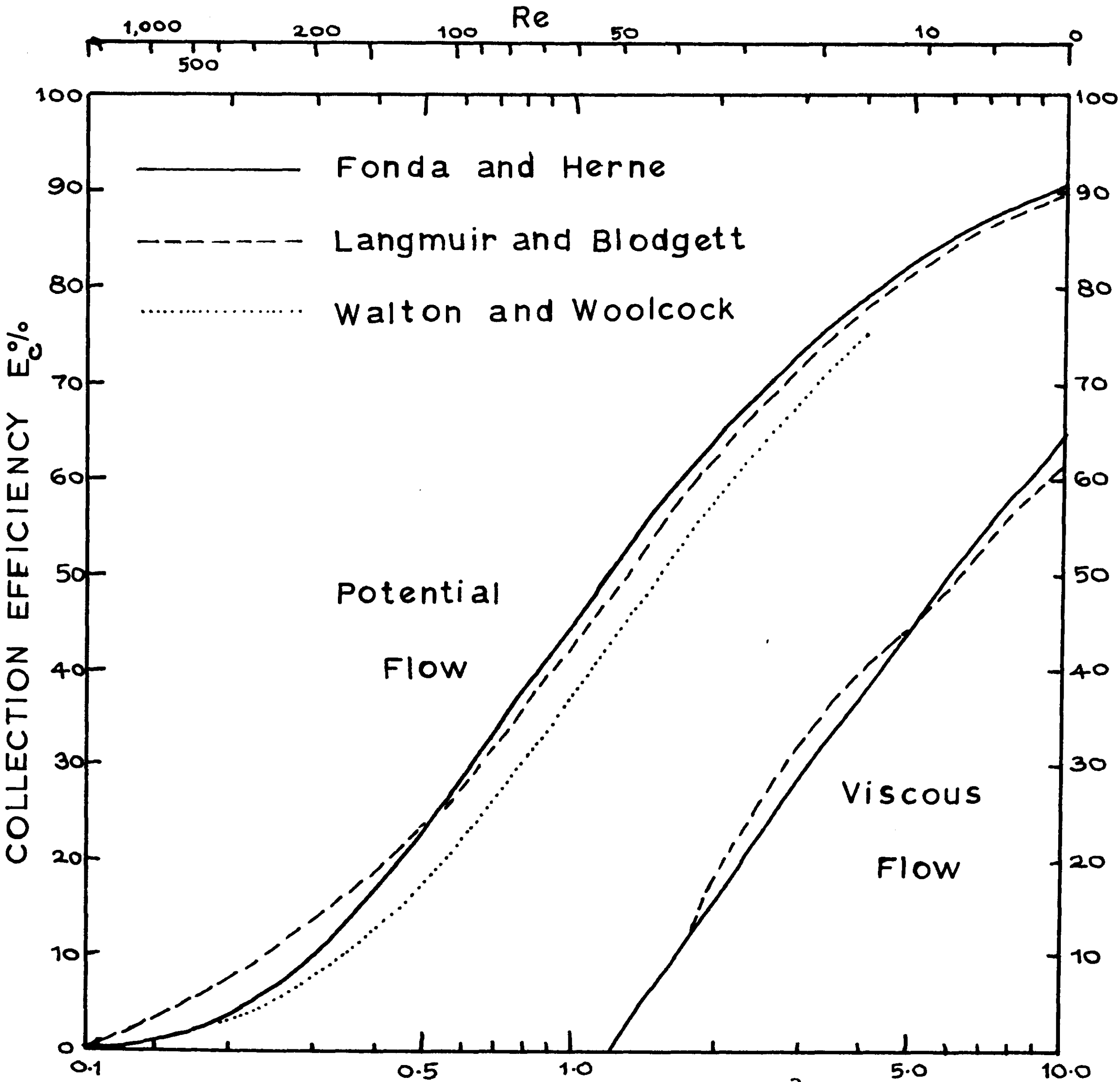

$$\text{PARAMETER } K = \frac{\rho_s \cdot d_p^2 \cdot v_r}{9\,\eta_a \cdot D_p}$$

and to a mirror galvanometer. The concentration of the dust cloud in the chamber was measured by the light extinction method. The effects of increased relative humidity and of mixing mineral dusts with silica were investigated by Massie.(74)

Hunter and others(63) measured the effectiveness of swirl atomisers on static dust clouds and studied the use of wetting agents for dust suppression. Their investigations were carried out in a dust chamber, with sprays not exceeding an atomisation pressure of 62 lbs/in^2 (4.36 Kg/sq.cm.). It was later envisaged that dust suppression systems should be studied in a dust tunnel, where reproducible dust concentrations and air velocities could be obtained over a wide range of values and the dust suppression efficiency could be evaluated quantitatively for a wide range of atomiser characteristics and spray-fluids, by means of thermal precipitator samples of the air-borne dust taken simultaneously before and after the dust suppression system.

Walton and Woolcock(68) showed that the mean efficiency of dust-suppression was as great as 55% for 2μ dust and 28% for 1μ dust for 100μ drops projected at 3000 cm/sec. and concluded that the high-velocity spray from a pressure nozzle might provide a practicable way of treating concentrated clouds near the source of production or ducted therefrom.

The object of the author's research was accordingly to study the effectiveness of such a laboratory flow system for carrying dust-laden air streams and to measure quantitatively the influence of high spray pressure and high wetting power of the fluid sprayed, on the efficiency of dust-suppression.

Earlier theoretical work has always assumed that droplet-particle impact results in particle capture. If the particle is difficult to wet with the droplet liquid a proportion of the impacts may not result in capture, the particle merely bouncing off into space. Thus the addition of a wetting agent may well be crucial for the effective suppression of some dusts.

To avoid personal error in particle size analysis an automatic particle counter utilising a wide-slit scanning technique and a photo-electric device was employed. It was necessary to ensure that the size of droplets produced at very high pressures (2750 p.s.i.) followed the same laws as those produced at low pressures (60 p.s.i.). Thus a method of droplet size measurements using the automatic particle counter was necessary and had to be evolved and droplets sized over a suitable pressure range.

The amount of water required to suppress a given quantity of air-borne dust had already been assessed[75]. It was necessary to extend this to higher spray pressures and to evaluate it for sprays of different wetting power.

It was also decided to study the effect of spraying dusty air with a number of high pressure hollow cone sprays arranged in series (tandem sprays) to find the maximum possible dust suppression in such a dust tunnel and the effect of increased water throughput at a specific pressure on the amount of water required to suppress a given quantity of dust.

2. INSTALLATION OF AN EXPERIMENTAL DUST TUNNEL AND ALLIED APPARATUS

2.1 The Wind Tunnel

Earlier experiments on dust suppression [62][63] were carried out in a dust chamber, using stationary dust clouds and though by themselves informative these experiments bore no direct correlation to the actual mining conditions. A dust tunnel was therefore designed, through which dust-laden air-streams similar to those actually encountered in mining practice could be passed and quantitative experiments on dust-suppression could be undertaken.

The experimental dust tunnel was originally constructed by Hutcheson and Sweetin[76] and was subsequently modified from time to time by the author. A drawing of the tunnel (not to scale), as it stands now, is shown in Fig. 2.1 and a view, looking from the fan end, is seen in Plate I.

The tunnel consists of seven lengths of 16-gauge mild-steel welded ducting, flanged at the ends and fitted with rubber gaskets. The overall length of the tunnel is about 20 metres and the outside diameter 45.72 cms.(18").

A 45.72 cm.(18") Keith-Blackman centrifugal fan, capable of producing an airflow of 1000 cm./sec. (about 2000 ft/min.) against a back pressure of 5 cm. water gauge (w.g.) was fitted to the higher end of the ducting by a flexible rubber tubing. The fan was driven at 1500 r.p.m. by a 2 H.P. fan-cooled squirrel-cage motor (400/440 volts, 3 phase, 50 cycle AC.). The airflow into the tunnel was made variable by

PLATE I

EXPERIMENTAL WIND-TUNNEL

FIG .2.1. THE EXPERIMENTAL WIND-TUNNEL

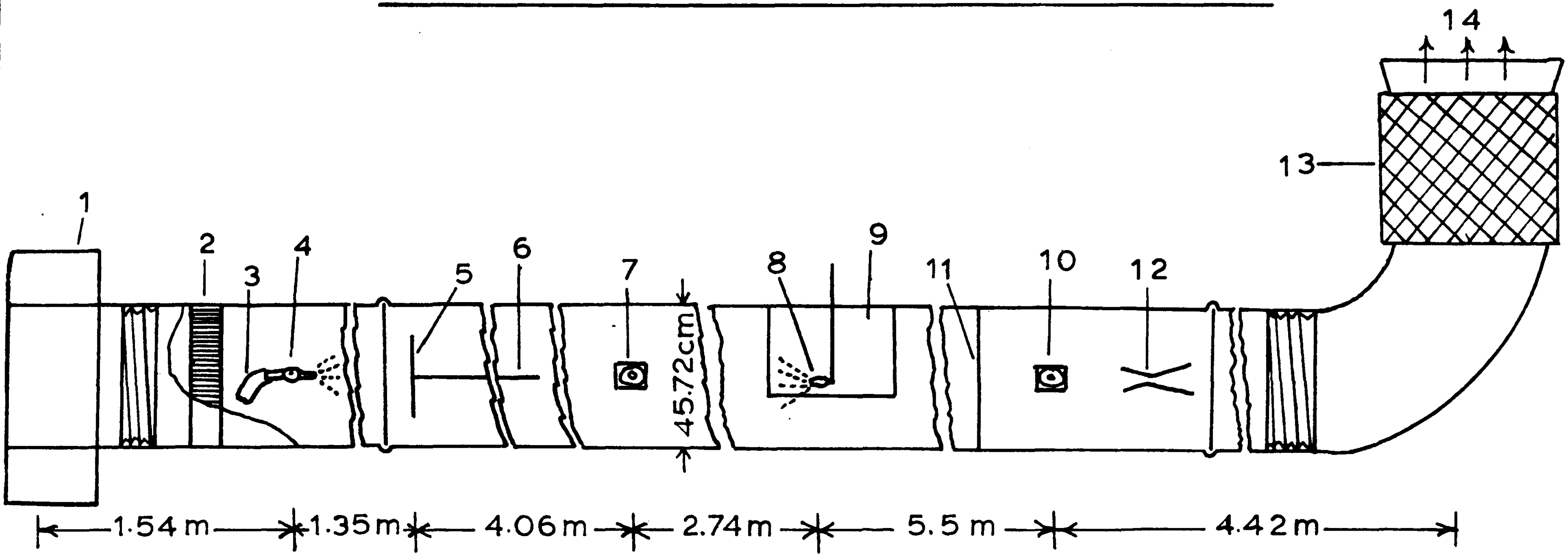

1, centrifugal fan; 2, honeycomb 10cm. wide; 3, connection from air blower; 4, dust injector; 5, $D/\sqrt{2}$ baffle plate; 6, anti-spin baffle 3D long; 7, thermal precipitator I; 8, spray nozzle; 9, window; 10, thermal precipitator II; 11, water trap; 12, venturi; 13, viscous oil filter unit; 14, effluent air fitting a Keith-Blackman Radial-leaf Damper to the fan inlet. This enabled the air velocity to be set to any desired value between 50 and 1000 cm./sec. (100 - 2000 ft/min.).

A 6.4 mm.(1/4 in.) mesh honeycomb structure, 10 cm. in depth, was fixed into the ducting immediately after the blower in an attempt to even out the air-flow pattern in the tunnel but this was later augmented by fitting a baffle plate of diameter $\frac{D}{\sqrt{2}}$ (32.35 cm.), concentric with the duct at a distance of about 3 metres from the fan and an 'anti-spin' baffle of length 3D (1.37 metres) along the axis of the duct, making contact with the back of the $\frac{D}{\sqrt{2}}$ baffle and of course perpendicular to it. The significance of the baffle plates with reference to the airflow pattern in the tunnel is more fully discussed in Chapter 3.

A perspex window was provided in the centre section of the tunnel, where the dust-suppression spray-systems could be watched and carefully controlled. Holes were cut for two thermal precipitator heads on either side of the spraying section. The 'top' thermal precipitator was about 7 metres distant from the fan on one side and is about 8.2 metres distant from the 'bottom' thermal precipitator on the other side.

The tunnel was mounted on angle-iron and wood supports, with the bottom end 15 cm. lower than the fan end, so that the water from the sprays would drain away easily. A 2.5 cm. high catchment dam was built across the lower end of the tunnel and a 1 cm. hole was drilled for water-drainage. This catchment dam was found inadequate and was subsequently replaced by a 7.6 cm. high catchment dam before the end of the fifth length of ducting and a 5 cm. diameter hole was drilled for draining water away.

A venturi tube was positioned within the tunnel near the downstream end and calibrated against a vane anemometer. A Keith-Blackman W-type viscous oil film filter battery, comprising four trays soaked with light lubricating oil and set at 45° to the horizontal, was fitted to the lower end of the dust tunnel by flexible rubber tubing. The dust-laden airstream was thus made to pass through the oil film, before escaping to the atmosphere.

The inside surface of the airduct was coated with hard gloss white paint. Angle-iron and wood supports, as also the flexible rubber tubing connecting the fan to the tunnel, kept vibrations due to the electric motor and fan to a minimum.

2.2 Allied Equipment for the dust tunnel

2.2.1 Dust-feeding Machine: A dust generator capable of producing a dust cloud with reasonably constant characteristics, was fixed at the top end of the tunnel at about 1.5 metres downstream from the fan. The outlet end of the injector nozzle was placed exactly at the centre of the tunnel cross-section, facing downstream. The unit is shown in Fig. 2.2 and a view of the dust feeding mechanism is seen in Plate II.

FIG. 2.2. THE DUST FEEDING MACHINE

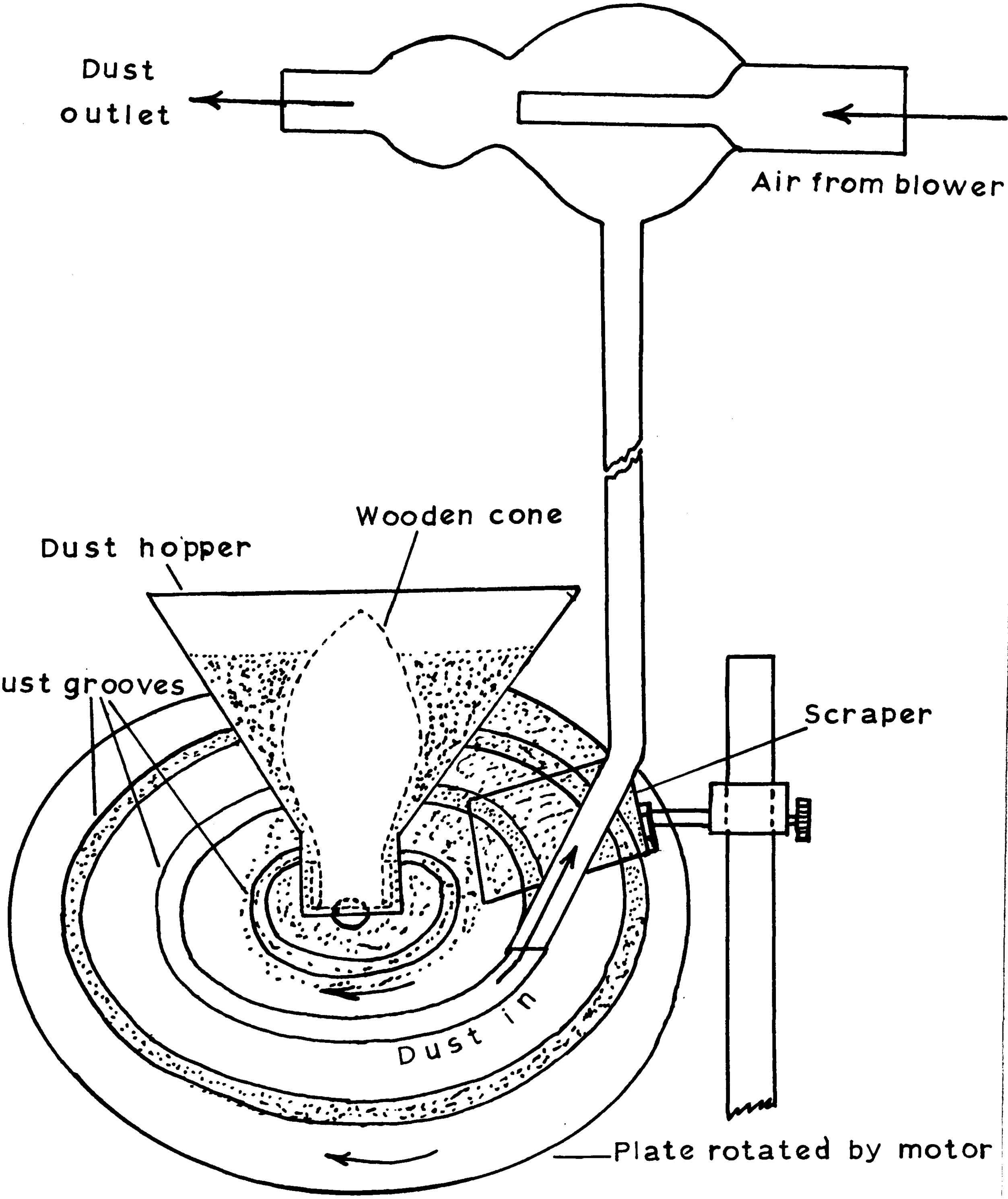

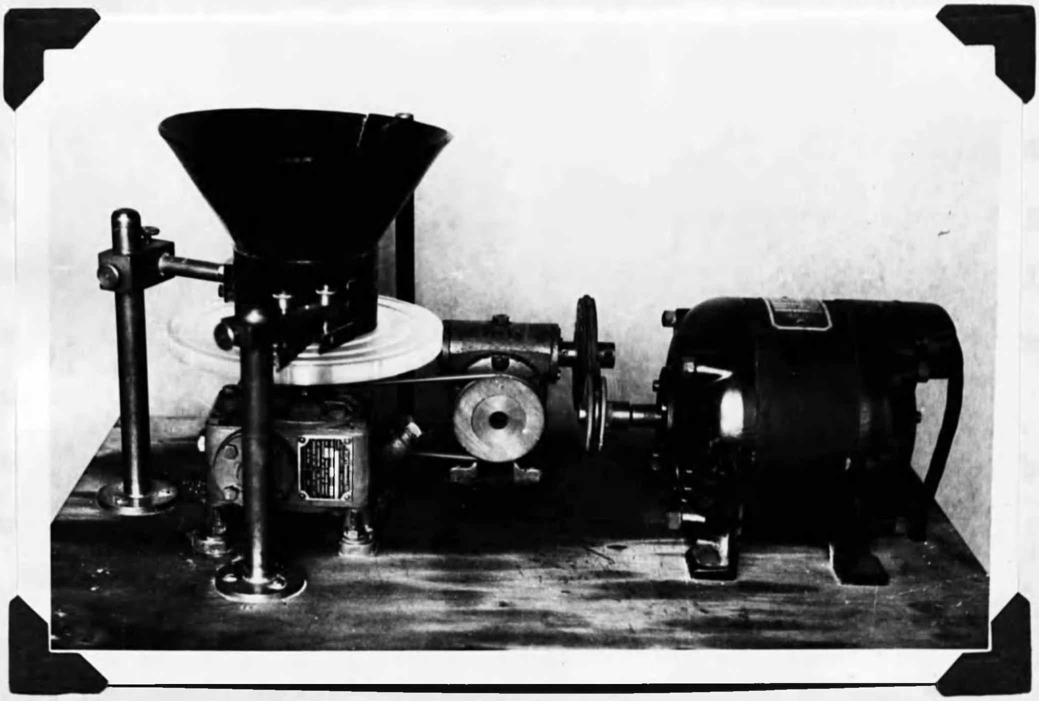

PLATE II

DUST-FEEDING MACHINE

The dust generator was a modified version of the apparatus described by Hattersley et.al.(77) and consisted essentially of a dust-metering device and a means of dispersing the dust into the air stream. The dust was placed in a truncated cone hopper, which was fastened to a vertical steel column and capable of being raised or lowered. Under this hopper, rotated a horizontal plate with three concentric grooves cut on its surface and as the plate rotated, dust flowed from the lower edge of the hopper and was swept across the plate by a scraper system, filling the grooves. The compressed-air ejector, with its bottom end placed on top of a particular dust-filled groove, sucked the dust out of the groove and blew it, mixed with air, into the tunnel.

Two circular 18 cm. perspex plates had three concentric grooves cut on each of their surfaces and one or the other could be arranged to rotate under the hopper. The groove sizes have been given below for the two plates:

TABLE 2.1 Dust Plate I

Outer Groove		Middle Groove		Inner Groove	
Width mm.	Depth mm.	Width mm.	Depth mm.	Width mm.	Depth mm.
9.15	1.59	12.2	1.59	12.2	1.59

TABLE 2.2 Dust Plate II

Outer Groove		Middle Groove		Inner Groove	
Width mm.	Depth mm.	Width mm.	Depth mm.	Width mm.	Depth mm.
5.08	1.59	4.32	1.27	4.57	1.27

These plates were driven by a small electric motor operating through a V-rope belt running on cone pulleys and a step-down gear box. With this system, it was possible to run the dust plates at 8 different speeds, viz. 0.420, 0.520, 0.568, 0.700, 0.705, 0.885, 0.940 and 1.185 r.p.m.

Theoretical dust concentrations could be calculated from the linear velocities, the dust-groove dimensions and the bulk density of dust, as shown in example given in 2.4.2.

Inside the hopper was placed a wooden cone of small diameter with four scraper blades attached to its base. These blades fed the dust out through the space between the hopper and the rotating plate. A secondary scraper in the form of thin brass strip of trapezium shape was fixed to a second vertical steel column to sweep the dust across the plate and to fill the grooves with dust. This scraper could be adjusted at any angle by pressing on to the rotating plate, so that the grooves were fully and evenly filled with dust. Reasonably good results were obtained by having a clearance of about 4 mm. between the hopper and the dust plate. This adjustment helped to fill the groove in the plate completely, with a small trickle of dust going to waste.

For dispersing the dust, the bottom end of the all-glass ejector could be set on any required groove of the dust plate, with the secondary scraper just behind it. The ejector was operated by an airblower, which provided compressed air at 4 cm.w.g. The suction developed at the top of the ejector was 5 mm.w.g.

The concentration of the dust cloud in the dust tunnel could thus be altered by:

(a) varying the air velocity at the centrifugal fan air-inlet,

(b) changing the size of the dust groove on either of the plates, and

(c) varying the speed of revolution of the plate used.

By using combinations of these three factors, particularly the first two, a wide range of dust concentrations from 350 p.p.c.c. to about 3000 p.p.c.c. was obtained. Theoretical dust concentrations based on dimensions of the rotating plate and size analysis of the coal dust appear elsewhere in this section.

2.2.2 The Dust Suppression System: The Spraying Unit

This unit was the outcome of much preliminary work. The liquid to be atomised was pumped by a three-throw reciprocating plunger pump manufactured by G. and J. Weir[78] through an air cushion cylinder to the spray nozzles. The pressure of spray could be as high as 210Kg./sq.cm. (3000 p.s.i.) depending upon the diameter of nozzle orifice and could be controlled easily to any desired value by varying the speed of the motor and the setting of a by-pass valve. The characteristics of the pump and the various swirl spray nozzles used are discussed in more detail in Chapters 6 and 7.

2.2.3 Instruments for dust-sampling: Standard thermal precipitators were employed to assess the air-borne dust concentration before and after the dust-suppression unit. A gravimetric dust sampler was also used for comparison purposes.

(a) Thermal Precipitator: The thermal precipitator[79] which is the reference instrument used in British coal mines to assess the concentration of respirable-size dust, was originally designed by Whytelaw-Gray and developed by Green and Watson[80], making use of the Aitken effect that the space surrounding a hot body is dust-free. (Fig.2.3).

Fine solid particles suspended in the gas in the immediate vicinity of a hot body, are repelled from it as a result of the differential bombardment set up by the thermal gradient in the gas. The hot body thus becomes surrounded by a region of dust-free gas. The dust particles are deposited in linear streaks on thin microscope cover glasses placed on either side of a hot wire.

The instrument consisted of two main parts, the head carrying the hot wire (Fig.2.4) and the aspirator, inducing air-flow through the head by water displacement. The total

FIG .2.3. DUST-FREE SPACE ROUND A HOT BODY

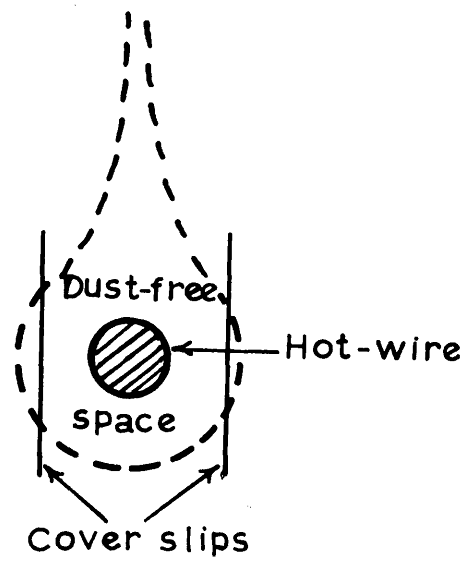

FIG .2.4. THERMAL PRECIPITATOR HEAD

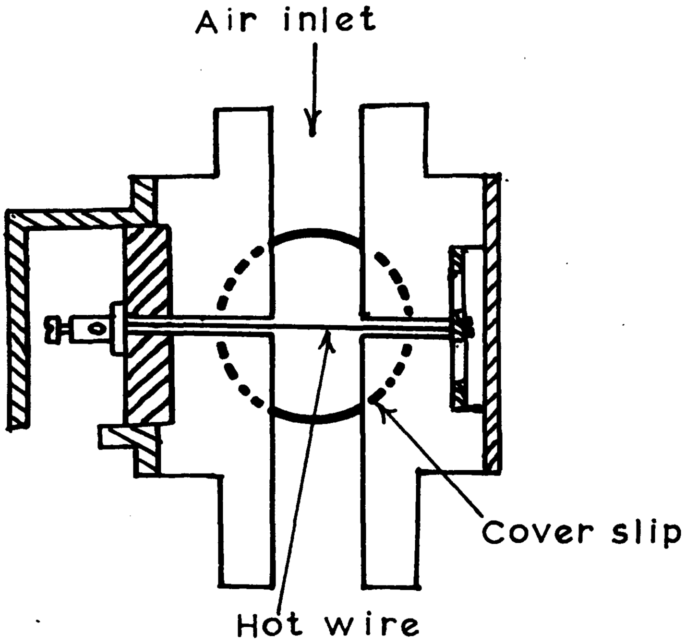

volume of water displaced is a direct measure of the volume of the air sample. The precipitator head takes the form of a cube. It comprises two brass blocks screwed together, and two sets of three strips of bakelite placed between to make a vertical slot.

A nichrome wire 0.025 cm. in diameter and 0.965 cm. long passes between these spacers and centrally across the slot. One end of the wire is connected to an insulated terminal, the other end to a spring, which keeps the wire taut when heated through the centre of each block. Cylindrical holes of 19 mm. diameter are cut and cover glasses are inserted through these holes so that they rest against the spacers on either side of the wire and are then held in position by closely fitting brass plugs. The wire is heated to about 100°C by passing a steady current of 1.3 amp from a 4.5 volt battery. At this temperature the diameter of the dust-free space is larger than the distance separating the cover-glasses.

In operation, dusty air is drawn through a slot 0.051 cm. by 0.95 cm. in cross section at a velocity of around 140 cm./min., the sampling rate thus being maintained between 6.5 and 7cc/min. The air passes between the cover glasses placed on opposite sides of the wire at a distance of 0.01 cm. from it. The brass plugs in contact with the cover-slips, conduct the heat away from the glass and maintain a sufficiently steep temperature gradient to ensure complete precipitation of particles.

Prewitt and Walton[81] found it reasonable to assume that the collecting efficiency of the instrument was 100 per cent in the size range 1.0 to 5.0 microns, provided that the temperature of the hot-wire is adequate and that the rate of flow of air through the precipitation zone is controlled within the limits 6.5 c.c./min. and 7 c.c./min.

The volume of air to be drawn through the instrument depends on the dust concentration. For instance, with 1000 p.p.c.c., a 50 c.c. sample would yield deposits adequate for accurate counting. The cover-glasses are subsequently removed from the instrument and mounted on a standard 7.6 cm. x 2.5 cm. microscope slide for particle counting and sizing.

(b) Gravimetric Sampling: Experiments using salicylic acid filters were also carried out and simultaneous samples from these two methods of sampling are compared in detail in Chapter 5.

2.2.4 Instruments to measure air velocity in the tunnel: Two instruments were installed to measure the velocity of air flowing in the tunnel -

(i) a Venturi meter

and (ii) a hot-wire anemometer.

(a) Venturi meter: A standard 15 cm. venturi tube was placed along the axis of the tunnel near the lower end of the duct at about 17 metres from the fan. (Fig.6). The pressure difference between the upstream end of the cone and the throat (Fig.2.5) was read on an inclined manometer. The venturi was calibrated against a vane anemometer and was principally used to measure air-velocities exceeding 500 cm./sec. (1000 ft./min.).

(b) Hot-wire anemometer: The instrumentation of the hot-wire anemometer, used to measure accurately low air velocities in the tunnel is shown in Fig. 2.6. It consisted of a copper-constanton thermocouple with one junction directly exposed to the air in the centre of the duct. The other junction had a heating coil of 60 ohms resistance wound round it. A steady current of 0.26 amperes was passed through this coil from an 18-volt accumulator. This accumulator was latterly replaced by a small rectifier unit, taking its supply from the A.C. mains. The heated junction caused a potential difference and this was read on a milli-voltmeter. When the air was flowing along the tunnel, the heat received by the junction was dependent on the cooling effect of the air on the coil and thus on the air velocity. The hot-wire anemometer was calibrated against an accurate vane anemometer.

Generally the routine maintenance of the tunnel consisted of -

(a) cleaning and resetting of the Keith-Black oil film filter,

(b) periodic recalibration of the hot-wire anemometer to allow for the effect of seasonal fluctuations of ambient air temperature,

FIG.2.5. VENTURIMETER

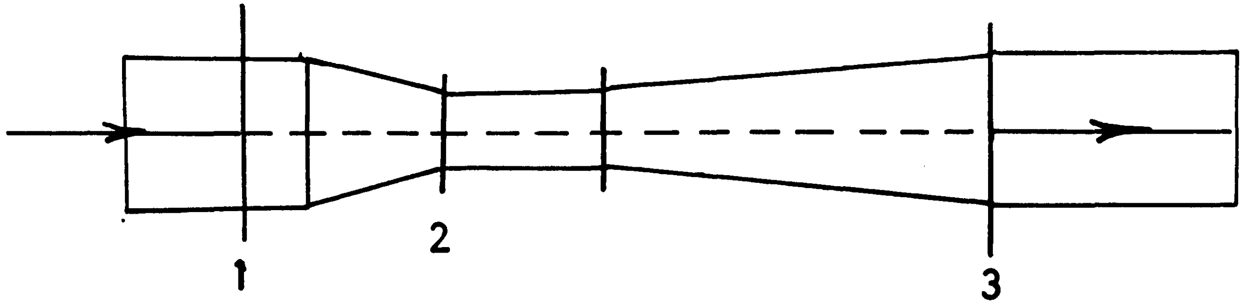

FIG.2.6. HOT-WIRE ANEMOMETER

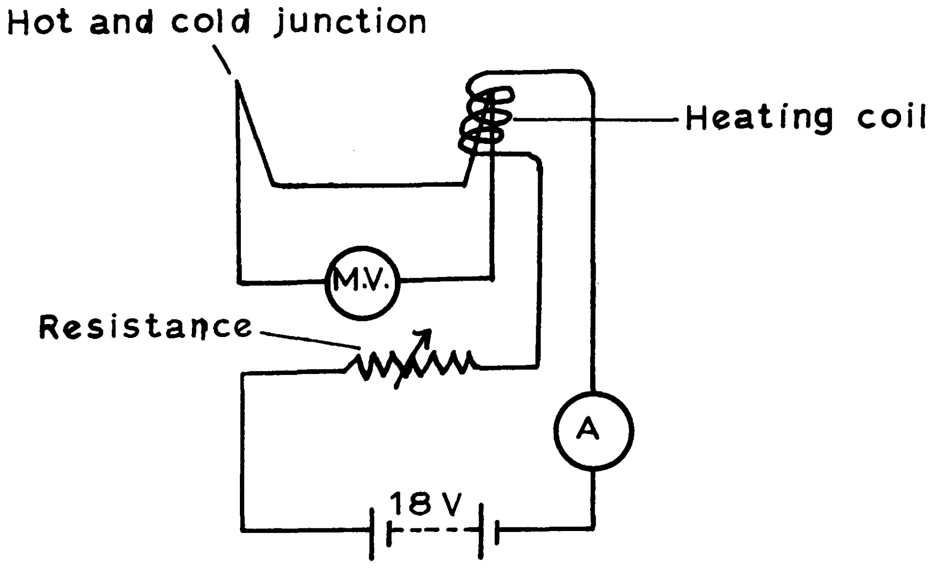

(c) cleaning the precipitator head and aspirator,

(d) cleaning the air cushion cylinder of the spraying unit and

(e) cleaning and resetting the dust injection unit.

2.3 Preparation of coal-dust for experiments

About 25 kg. of boiler house singles coal were first air dried overnight and then passed through jaw crusher and roller mill until the product obtained was about 3 mm. in size. This material was dried in small quantities for some hours at 110°C. The dry coal was passed through a high speed laboratory hammer mill, and subsequently ground further in batches of 40 - 50 g. in a mechanical agate mortar for one-hour periods. The product obtained from the agate mortar was sieved through 300 B.S. Sieve to ensure that the particle size of this experimental dust did not exceed 53 microns. The size-analysis of the dust described in Chapter 4, later proved that more than 90 per cent of the air-borne particles in the duct were below 5 micron in size.

2.4 Some theoretical considerations

2.4.1 Critical velocity for turbulent air-flow in the tunnel:

For flow in a tunnel of circular cross-section, the condition for turbulent flow is

$$Re > 2300$$

where $$Re = \frac{\rho_1 . u . D}{\eta_a}$$

For a tunnel of diameter 18 inches, the critical velocity of flow for turbulence

$$U_c = \frac{Re_{(c)} \times \eta_a}{\rho_L \cdot D} = \frac{2300 \times 0.14}{18 \times 2.54}$$

$$= 7.04 \text{ cm./sec. } (13.82 \text{ ft./min.})$$

i.e. at speeds above 13.8 ft./min. at ambient temperatures, the air flow in the tunnel is turbulent.

In turbulent flow, the transfer of momentum takes place as a result of the movement of comparatively large groups of molecules or eddies across the section of the duct and the velocity distribution law, as formulated by Prandtl[82] is illustrated in Fig. 2.7. For a range of air velocity in the duct 14 ft./min. (7 cm./sec.) to 3×10^4 ft./min. (1.5×10^4 cm./sec.) (when $Re = 10^7$) the velocity profile over the cross-section will be between curves II and III. The experimental velocity measurements and the effect of baffle plates on velocity profile are discussed in Chapter 3.

2.4.2 Theoretical dust concentration in the tunnel:

Dust concentrations in the tunnel could be calculated theoretically for different air velocities, from a knowledge of the dimensions of the dust-plate groove employed and also velocity of approach of groove and average particle size of the dust. This also provided a rough guide for choosing the right combination of dust-groove and air velocity for a desired dust concentration in the tunnel.

FIG. 2.7. VELOCITY PROFILES FOR FLOW IN PIPE

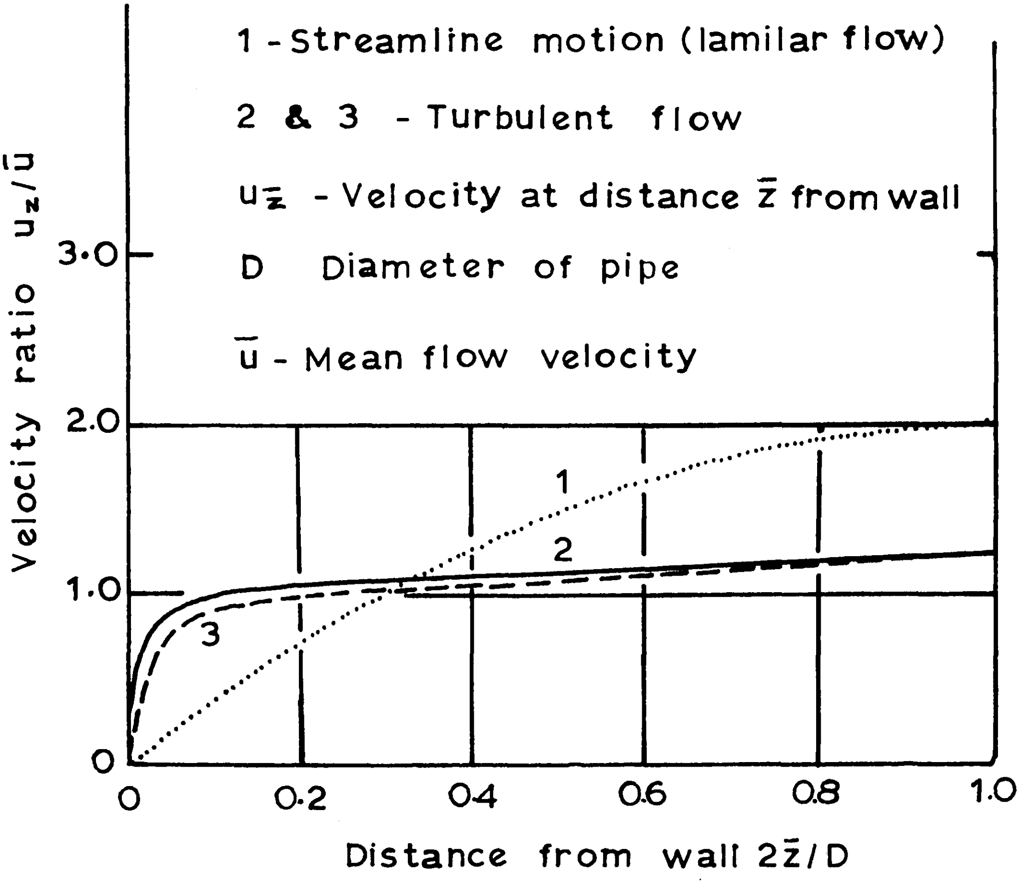

Application of laws for turbulent flow :

1. $(u_z/\bar{u}) = 1\ 24\ (2\bar{z}/D)^{1/7}$:- From onset of turbulence $Re \doteq 2\ 3 \times 10^3$ up to $Re \simeq 10^5$

2. $(u_z/\bar{u}) = 1\ 24\ (2\bar{z}/D)^{1/10}$:- Circa $Re = 10^7$

An example for the theoretical calculation of dust ejected from the dust machine on the basis of 100 per cent efficiency, is given below:

Specification of groove: Groove No.2, Plate I.

Inner diameter of groove	... 13.08 cm.
Outer diameter of groove	... 14.28 cm.
Depth of groove	... 0.1589 cm.

∴ Volume of groove $= \frac{\pi}{4}(14.28^2 - 13.08)^2 \times 0.1589$

$= 3.86$ c.c/revolution of groove

Weight of dust ejected, assuming 100% efficiency,

= volume x bulk density x Rev./min.

$= 3.86 \times 0.0196 \times 27.68 \times 1.191$

= 2.465 g./min.

No. of particles < 6.59µ = wt. of dust/min.x particles <6.5µ/gm.

$= 2.465 \times 8760 \times 10^6$ (experimental)

$= 21.62 \times 10^9$ particles/min.

At an air velocity of 150 ft/min. in the wind tunnel, volume of air in the tunnel

$$= \frac{150 \times 60}{1.987} \times \frac{\pi}{4}(18 \times 2.54)^2 = 7.505 \times 10^6 \text{ c.c. per min.}$$

∴ Number of particles < 6.59µ present in the tunnel

$$= \frac{21.62 \times 10^9}{7.505 \times 10^6}$$

= 2880 p.p.c.c.

Thus the theoretical dust-concentration was calculated at different velocities, as shown in Table 2.3.

TABLE 2.3

Theoretical dust-concentration in the tunnel

p.p.c.c. (< 6.59 μ)

Speed of plate ... 1.191 R.P.M.

No.	Tunnel mean Air Velocity		Dust-concentration in p.p.c.c.
	cm./sec.	ft./min.	Plate I. Groove 2
1	75	150	2880
2	125	250	1810
3	200	400	1130
4	450	900	502

2.4.3 Iso-kinetic sampling for the thermal precipitator: In order to obtain a sample of dust truly representative of its concentration and size distribution in the air that carries it, the velocity of the dusty air entering the sampling instrument should be exactly equal to that in the main stream. If the velocity of sampling be lower than the air velocity, the greater inertia of the larger particles causes them to be collected preferentially. On the other hand, too high velocity of sample intake results in the rejection of some of the larger particles. It appears, however, that this equalization of sampling and stream velocities can never be truly attained in mining practice, not only because air velocities in the mine vary greatly from instant to instant and from place to place, but also because sampling instruments like the thermal precipitators are designed to be most efficient within a closely-controlled rate of sampling. For instance, a thermal precipitator head sucking in dusty air through a slot 0.051 by 0.95 cm. in cross-section at a controlled rate of around 7 c.c./min. assumes a sampling velocity of only 2.35 cm./sec. (4.7 ft/min.).

Withers[83], however, was unable to find any appreciable change in size selection when the ratio of ambient air-velocity to sampling velocity varied from 0.6 to 2.2.

If one assumes an air velocity of 100 cm./sec. (200 ft./min.), which is quite a normal figure in mines, and control the rate of sampling for maximum thermal precipitator efficiency at 7 c.c./minute, to obtain an isokinetic sampling, the area of thermal precipitator inlet mouthpiece must be

$$\frac{7 \times 100}{60 \times 100} = 0.117 \text{ sq.mm.}$$

Thus if the inlet had a circular cross-section, the diameter of the mouthpiece should be

$$\sqrt{\frac{0.117 \times 4}{\pi}} = 0.386 \text{ mm.}$$

or 386 microns.

This is much too small for practical operation.

From these figures, it is quite apparent that under mining conditions isokinetic sampling cannot be effectively carried out, and so it has become necessary almost completely to ignore the effect of differential velocities in sampling procedures for thermal precipitators.

3. DISTRIBUTION OF AIR-VELOCITY AND DUST-CONCENTRATION IN THE TUNNEL.

3.1 Distribution of air velocity

3.1.1 Introduction: Since the air flow in the tunnel was created by a centrifugal fan, capable of producing flow-rates in the range 50 - 1000 cm./sec., it was decided that a knowledge of the air-velocity distribution at various cross-sections of the tunnel would be necessary. Non-uniform velocity distribution would then be corrected by suitable baffles placed in the tunnel. An N.P.L. hemispherical head pitot tube was employed to measure air velocities, since it produced no appreciable pressure loss and it could be inserted through a comparatively small hole into the tunnel wall. The pitot-tube head of N.P.L. hemispherical end type is shown in Fig. 3.1. The two concentric tubes of the pitot tube were connected to the two ends of a micromanometer which measured accurately pressure differences to 0.0005 inch. or 0.00127 cm. water gauge.

3.1.2 Pitot-tube traverses: Since this device measured the instantaneous velocity at one point, it was necessary to take a number of readings at different points to get a clear picture of velocity distribution across any section of the tunnel.

A circular tunnel such as this was best considered to have its cross section divided into a number of concentric rings of equal areas, as shown in Fig. 3.2. The intersection

FIG.3.1 PITOT TUBE : N.P.L. HEMISPHERICAL HEAD

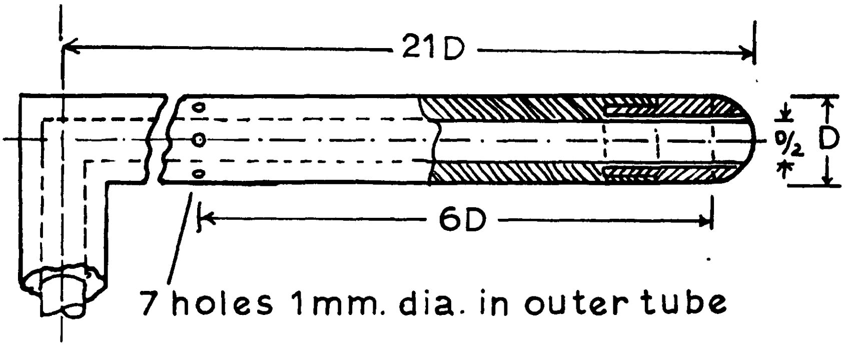

FIG.3.2 PITOT TUBE TRAVERSING POINTS IN TUNNEL

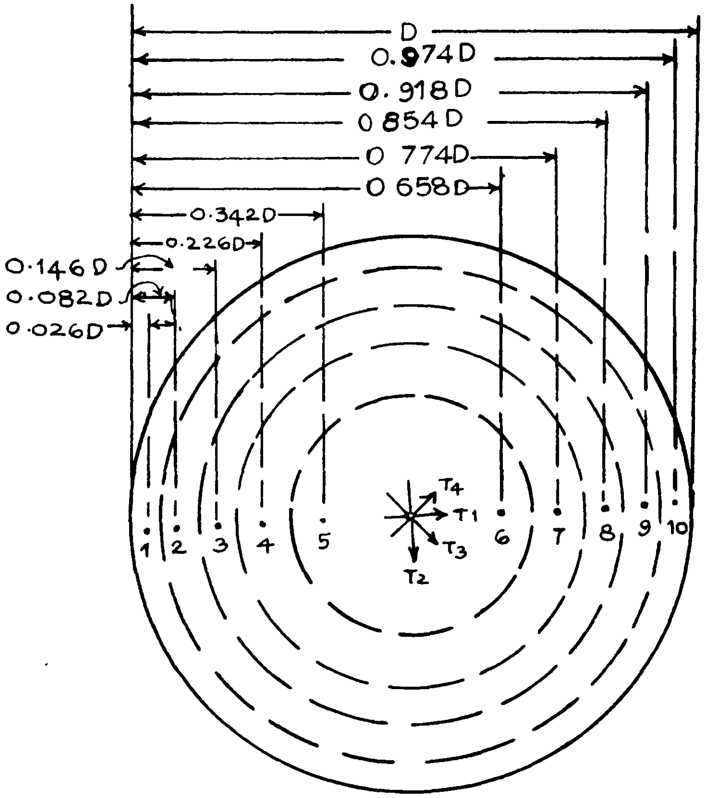

of the circle which divided each of these areas into two equal parts with a diameter determined the points at which the pitot-tube head was to be placed. Thus 10 traversing points were obtained together with the centre for any one diameter. Across any section of the duct, four diameters - vertical, horizontal and two others at 45° to those, were selected for traversing. For the five concentric rings of equal area into which the tunnel cross-section was considered to be divided, the required distances to the centres of the areas - viz. the traversing points for the pitot-tube - from the wall of the tunnel are given in the table below.

TABLE 3.1

Diameter of duct ... 45.72 cms.(18 inches)

Establishment of Traversing Points

Point No.	Distance from the wall.cms.	Point No.	Distance from the wall.cms.
1	1.19	6	30.08
2	3.75	7	35.39
3	6.68	8	39.05
4	10.33	9	41.97
5	15.64	10	44.53

A hole of about 1.5 cm. diameter was made for the insertion of the pitot-tube into the duct and it was carefully plugged with a rubber bung when measurements were being made. Care was taken to ensure that the Pitot-tube was placed accurately pointing upstream, since it has been shown that inaccuracies to the extent of $2^1/2\%$ in velocity could be obtained, if the tip of the tube was inclined at an angle of 20° to the air stream.[84] The readings of the micromanometer were taken at each of the traversing points along each of the four diameters across any section. The temperature of the air in the tunnel during the experiment was also noted. Taking the pressure of the air in the tunnel to be practically that of the atmosphere and assuming the air to be dry, the air velocity was calculated from the formula [85]

$$V_{ft/min.} = 174.24\sqrt{t + 459.6} \cdot \sqrt{H}$$

$$= K_t \cdot \sqrt{H}$$

For the temperature of 65°F, this reduces to

$$V_{ft/min.} = 3990.\sqrt{H}$$

$$\text{or} \quad V_{cm/sec.} = 2027.\sqrt{H}$$

Having determined the velocity of air at different points across any section, iso-velocity curves were drawn to represent the velocity distribution.

3.1.3 Effect of honeycomb on velocity distribution:
Preliminary experiments indicated a most uneven distribution of air. Accordingly, a 6.4 mm. ($^1/4$") mesh honeycomb structure, 45.72 cm. in diameter and 10.6 cms. deep, was inserted in the tunnel immediately after the fan in an attempt to even out the air flow.(86)

The fan was set to give a velocity of about 250 cm./sec. and pitot-tube traverses were carried out at the section of the tunnel in line with the mouth of the dust-injector nozzle.

The velocity distribution curves showed that the honeycomb device did not make a significant contribution towards even distribution of air, since it could not exert sufficient back pressure for the purpose. The air velocity remained higher in the upper left quadrant of the tunnel (as looking downstream) and lower in the bottom right quadrant. For example, the velocity at the near end of the tunnel was more than double that at the far end. (300 cm./sec. as against 142 cm./sec.).

The effect of overall air rate on the velocity distribution in the tunnel through the honeycomb was also investigated. Pitot-tube traverses were carried out at the same section, opening the damper of fan each time to change the air velocity in gradual increments from 250 cm./sec. to 750 cm./sec. It was found that the velocity distribution was more non-uniform at speeds higher than 400 cm./sec., and as the speed increased the high-velocity air in the upper left quadrant of the tunnel spun itself more into the bottom right quadrant.

With a view to investigate the nature of the velocity distribution along the tunnel with the honeycomb in position, the fan was set for 150 cm./sec. and velocity measurements at various points on four traverses were made at five sections as follows :- (see Fig. 2.1)

(a) at the mouth of the dust nozzle,

(b) just in front of the thermal precipitator I,

(c) just beyond the thermal precipitator I,

(d) just in front of the thermal precipitator II,

and (e) just beyond the thermal precipitator II.

This was repeated at speeds of 300 and 500 cm./sec. and the results were plotted as iso-velocity curves for each section. It was seen, as suspected, that the velocity distribution was by no means uniform and varied with the traverse selected at any one section. The air fan seemed to concentrate the maximum velocity in one quadrant of the tunnel section.

The air flow at the tunnel cross-section corresponding to the mouth of the dust nozzle was found to be very uneven. For example, for the fan set at a nominal 150 cm./sec., the upper half of this section recorded a velocity as great as 325 cm./sec., whereas the centre of the right half was recording one as low as 40 cm./sec. As the fan-damper was opened more, it was found at this section that the maximum velocity streams slowly spun around clockwise (as looking downstream), so much so that at the fan set for 500 cm./sec., the centre of the right half of the tunnel had an air-velocity of 650 cm./sec., while the centre of the left half of the tunnel recorded a lower velocity of 300 cm./sec., as may be seen in Fig. 3.5(a).

The air flow pattern, however, became more uniform, as it passed along the tunnel. At sections near the thermal precipitators, the velocity ranged, for three damper positions corresponding to 150, 300, 500 cm./sec. from 125 to 185 cm./sec., from 200 to 320 cm./sec., and from 425 to 600 cm./sec. respectively. It was interesting to note that while at high velocity (500 cm./sec.) the point of maximum velocity was siuated near the centre of the right half of the tunnel, at lower velocities (150 cm./sec.), it moved to the left half of the tunnel, but nearer to its axis. It seemed that standing waves were being set up in the tunnel at the higher velocities.

<u>3.1.4 Effect of Half-area mixing baffle on velocity distribution</u>: To reduce this non-uniformity of air flow in the tunnel, a half-area "mixing" baffle - a steel disc of diameter $D/\sqrt{2}$, viz. 32.4 cms.(12.75") - was fitted concentric with the tunnel at about 3.7 metres from the fan. This had the additional advantage in that the dust sample extracted from such a system would be more representative.[87]

Even when dust sampling was carried out isokinetically as was done with a salicylic acid filter in later experiments, the sample extracted might only be representative of the material at the point of sampling and would not therefore be representative of the whole of the material in the duct, unless the dust had been adequately mixed by means of a suitable device. This mixing baffle could be expected to ensure this effect.

With the honeycomb and the mixing baffle in their positions, and the damper of the fan set for an air velocity of about 500 cm./sec., iso-velocity curves were obtained for five sections of the tunnel as given below:

(i) Section distant 1 D (45.72 cms.) beyond the baffle.
(ii) Section distant 2 D beyond the baffle.
(iii) Section distant 3 D beyond the baffle.
(iv) Section just in front of thermal precipitator I.
(v) Section just in front of thermal precipitator II.

The results for sections (i), (ii) and (iii) are shown in Fig. 3.3.

On comparison of these with the iso-velocity curves at the section corresponding to the position of the dust nozzle (Fig. 3.5(a)), it was easily seen that the point of high velocity was still at the top right quadrant of the tunnel, even at 3 tunnel-diameters beyond the mixing baffle. There had been only a small increase in uniformity, but at the sections near thermal precipitators, the points of maximum velocity were nearer the axis of the tunnel, though not on the axis. The mixing baffle was thus not causing sufficient obstruction to ensure even velocity distribution. Even at sections in front of the thermal precipitators, the velocity ranged from 400 to 550 cm./sec. and the maximum velocity was not along the axis.

3.1.5 Effect of anti-spin baffle on the velocity distribution: Obstruction of a greater cross-sectional area of the tunnel by a larger mixing baffle might have resulted in a better distribution of velocity; but it was not attempted since it would have had greater impact on the dust distribution in the tunnel, during the later experiments. Also, since the velocity distribution pattern at the mouth of the dust nozzle was found to have a spin with increasing air velocities, drifting the high velocity streams from the top left quadrant at slow speed to the bottom right quadrant at higher speeds, it was felt that some device should be sought which could arrest the spin.

Accordingly, an "anti-spin" baffle of length 3 D (1.37 metres) and breadth D (45.72 cms.), was fitted along the axis of the tunnel, making contact with the back of the Half Area Mixing Baffle and, of course, perpendicular to it. The effect of this arrangement was studied by means of iso-velocity curves at the same five sections and at the same speed as was done for the $D/\sqrt{2}$ baffle alone and the results for sections (i), (ii) and (iii) are shown in Fig. 3.4, and for sections (iv) and (v) in Fig. 3.5(b) and (c).

FIG.3.3 THE EFFECT OF D/√2 BAFFLE PLATE MOUNTED CONCENTRIC WITH THE AIR DUCT

LOOKING DOWNSTREAM

Units.. cm/sec x 1.97

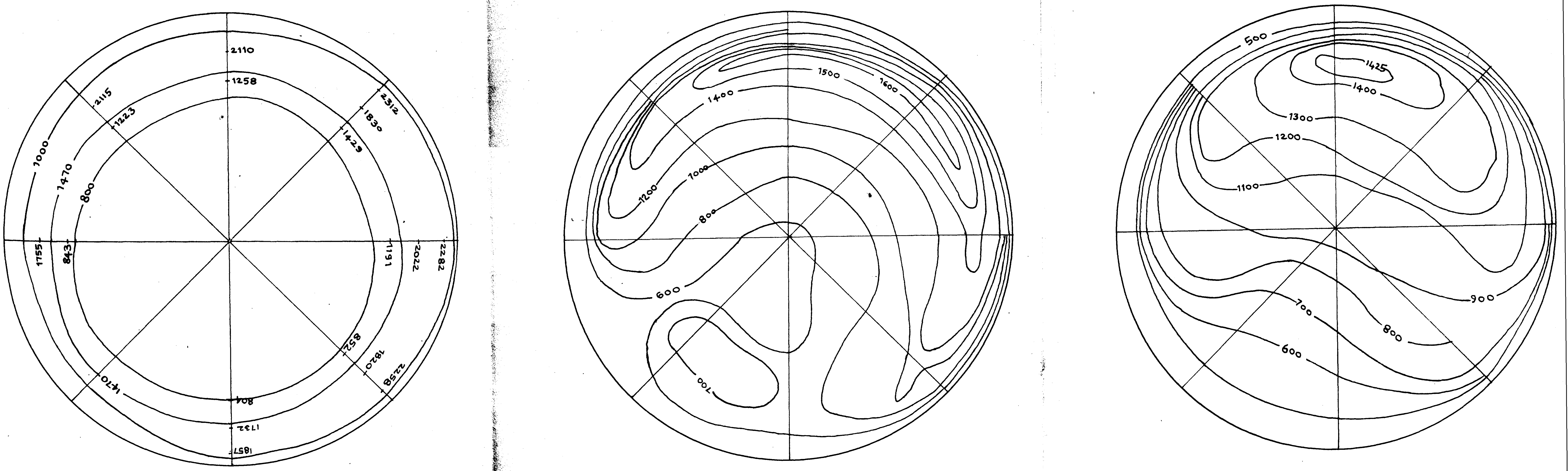

(a) 1D behind the baffle

(b) 2D behind the baffle

(c) 3D behind the baffle

FIG.3.4 THE EFFECT OF ADDITION OF ANTI-SPIN BAFFLE ON VELOCITY DISTRIBUTION IN THE DUCT

LOOKING DOWNSTREAM

Units.. cm/sec x 1.97

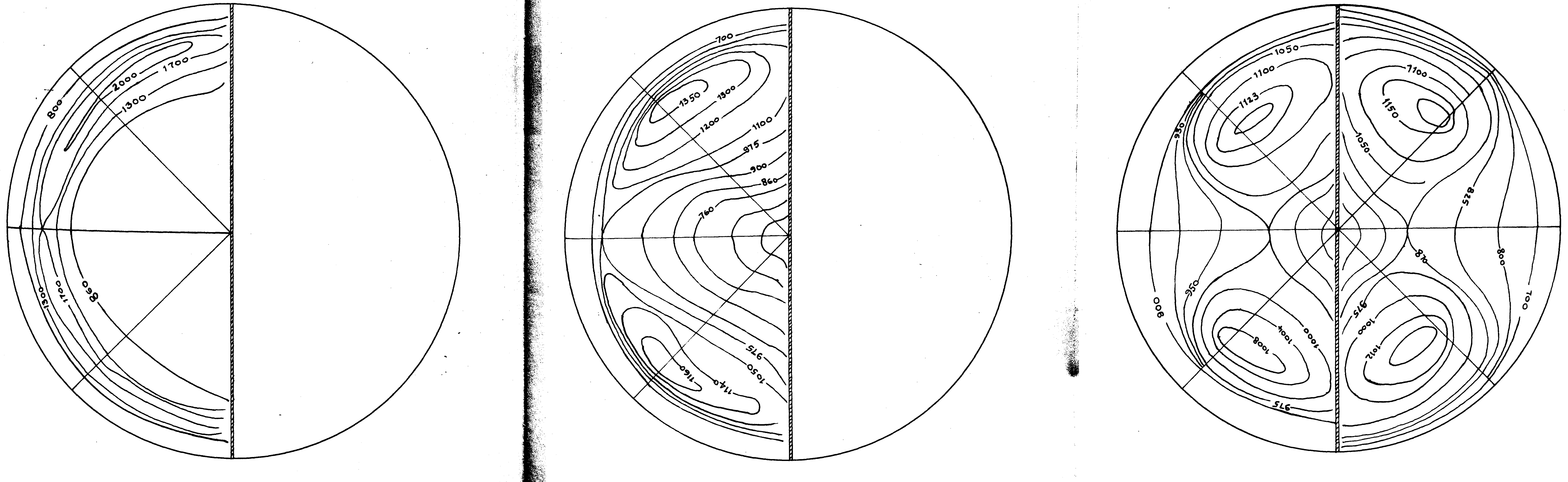

(a) 1D behind $D/\sqrt{2}$ baffle

(b) 2D behind $D/\sqrt{2}$ baffle

(c) 3D behind $D/\sqrt{2}$ baffle

FIG.3.5 ISO-VELOCITY CURVES SHOWING THE EFFECT OF BAFFLES ON VELOCITY DISTRIBUTION IN THE DUCT

LOOKING DOWNSTREAM

Units.. cm/sec x 1.97

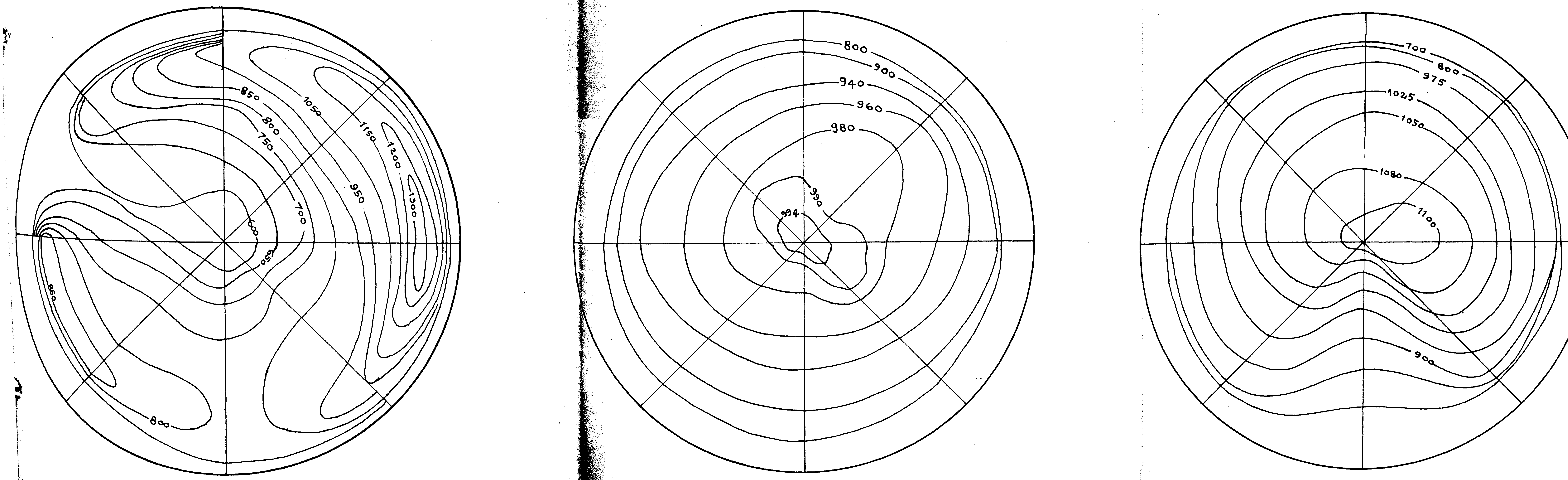

(a) At dust-feeding nozzle

(b) At thermal precipitator I

(c) At thermal precipitator II

The movement of air and its progressive distribution along the length of the anti-spin baffle plate made an interesting study and justified the use of the baffle, for the purpose.

Comparing with the velocity distribution patterns at the mouth of the dust nozzle (Fig. 3.5(a)), and at 1D beyond the $D/\sqrt{2}$ baffle when there was no anti-spin baffle (Fig. 3.3(a)), it was easily seen that even at a distance of one ~~tunnel-diameter~~ beyond the $D/\sqrt{2}$ baffle, the anti-spin baffle had achieved a fair measure of air-flow straightening which the $D/\sqrt{2}$ baffle by itself failed to achieve. The high velocity streams seen at the top left quadrant of Fig. 3.3(a) were found to have distributed more uniformly into the bottom left quadrant as well in Fig. 3.4(a). It was also clear from Fig. 3.4(c) that a minimum length of three tunnel diameters was necessary to arrest the spin of air streams and distribute them more evenly across the tunnel.

At the section, in front of the thermal precipitator I (Fig. 3.5(b)), the whole effective section of the tunnel records a velocity of 475 ± 25 cm./sec. Obstructions like the thermal precipitator and the spray nozzle seemed to disturb the air flow significantly, which resulted in a less satisfactory, though well-balanced uniform distribution of air in front of thermal precipitator II (500 ± cm./sec.). In both the sections, the maximum velocity occurred at the axis of the tunnel and with this arrangement therefore, it was now possible to produce better velocity distribution in the tunnel simulating standard turbulent flow of fluid in pipes. Velocities of about 500 cms./sec., at which the effects of the baffles were found, corresponded to Reynolds Number of the order of 1.6×10^5. The Prandtl velocity distribution law[82],

$$U_z = 1.24\,\bar{U}\,\left(\frac{2\bar{z}}{D}\right)^n$$

was found to apply. For velocity measurements for turbulent flow around $Re = 1.6 \times 10^5$ (mean velocity .. 500 cms./sec.), a value of $^1/6.18$ was obtained for n.

$$U_z = 1.24\,\bar{U}\,\left(\frac{2\bar{z}}{D}\right)^{1/6.18}$$

This is consistent with Prandtl's values of n. i.e. $n = {}^1/7$ for $R_e = 10^5$ and $n \simeq {}^1/10$ at $R = 10^7$

The ratio of mean velocity to the velocity at the centre was also calculated and found to vary between 0.82 and 0.93. The average ratio $\frac{V\ mean}{V\ centre}$ was 0.88, for Reynolds Number of the turbulent airflow around 1.6×10^5.

<u>3.1.6 The effect of obstruction of tunnel outlet on the static pressure and air-velocity:</u> If the viscous oil filter at the outlet end of the tunnel was kept in service for a long period, it soon became choked with the dust, which it was filtering from the air. The result was that the filter which had passed down the tunnel, exerted a continually increasing back pressure and reduced the air velocity in the tunnel corresponding to a given setting of the damper. E.g. At one time, with the filter connected

and the damper adjusted to its maximum 'open' position a maximum velocity of only 750 cm./sec. was recorded. With the filter disconnected, a velocity of 1250 cm./sec. was obtained. In view of the difference, it was decided to investigate the effect of this obstruction of tunnel outlet on the air velocity, since it would also enable periodic assessment of the condition of the filter to be made.

The viscous oil filter was disconnected and arrangements were made, at least 6D in front of the tunnel outlet, to measure the static pressure by means of an inclined water manometer, and also to make a four-diameter-traverse with the Pitot-tube at a section near thermal Precipitator II. For different settings of the damper from 'fully open' to 'fully closed', obstruction of the tunnel-outlet was effected by means of a large sheet of board. The board was arranged to obstruct in turn one-sixth, one-third, one-half, two-thirds, five-sixths and finally the entire cross-sectional area of the tunnel. A pitot-tube traverse was carried out at each setting of the board and damper to determine the mean velocity of air in the tunnel. The static pressure difference was simultaneously read on the inclined manometer. The effect of the percentage obstruction of cross-sectional area of tunnel outlet on the static pressure and mean air velocity are shown for each damper setting in Figs. 3.6 and 3.7.

FIG.3.6 CHANGE OF STATIC PRESSURE DIFFERENCE WITH OBSTRUCTION OF DUCT OUTLET

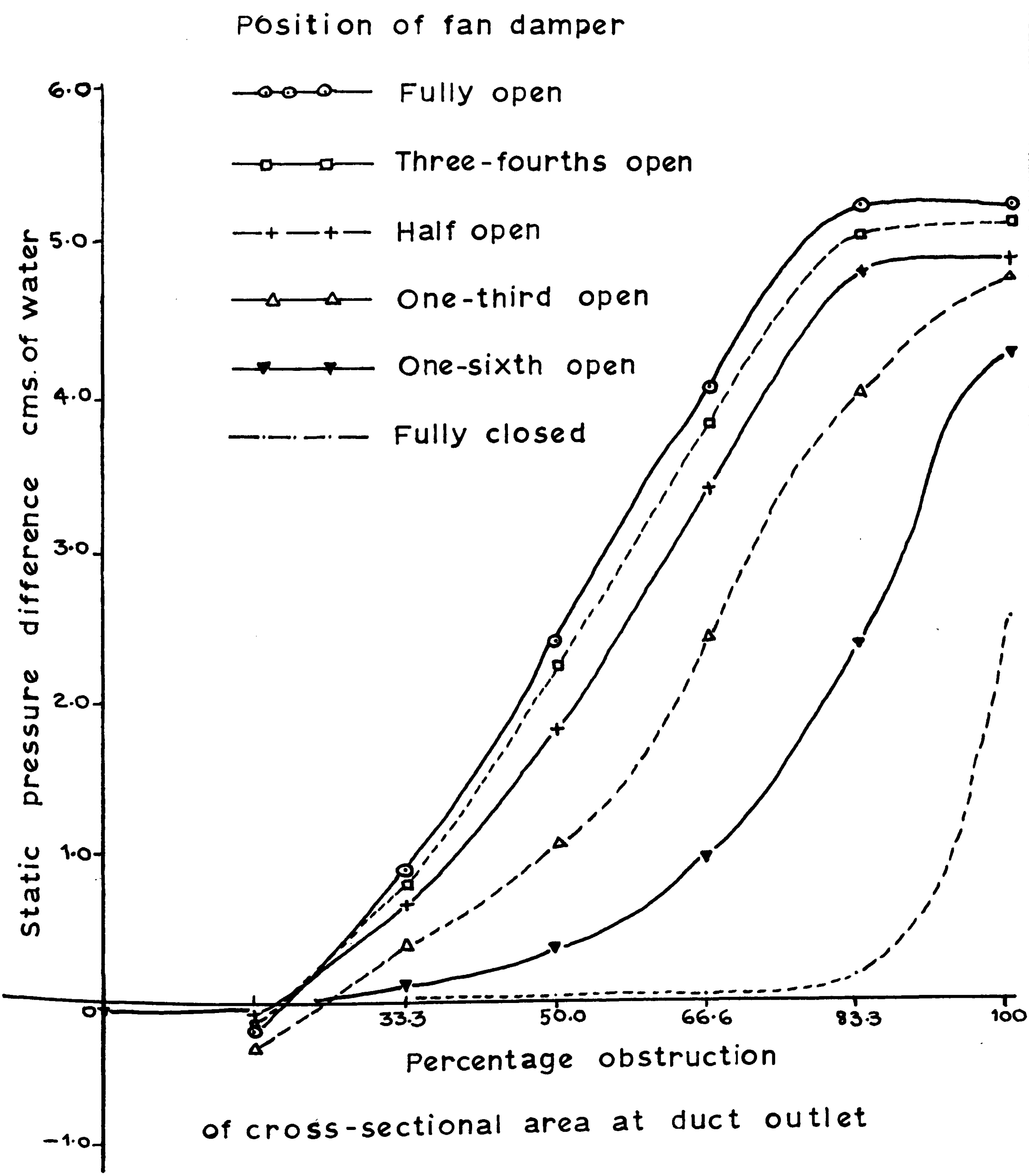

FIG.3.7 THE CHANGE OF VELOCITY WITH BACK-PRESSURE

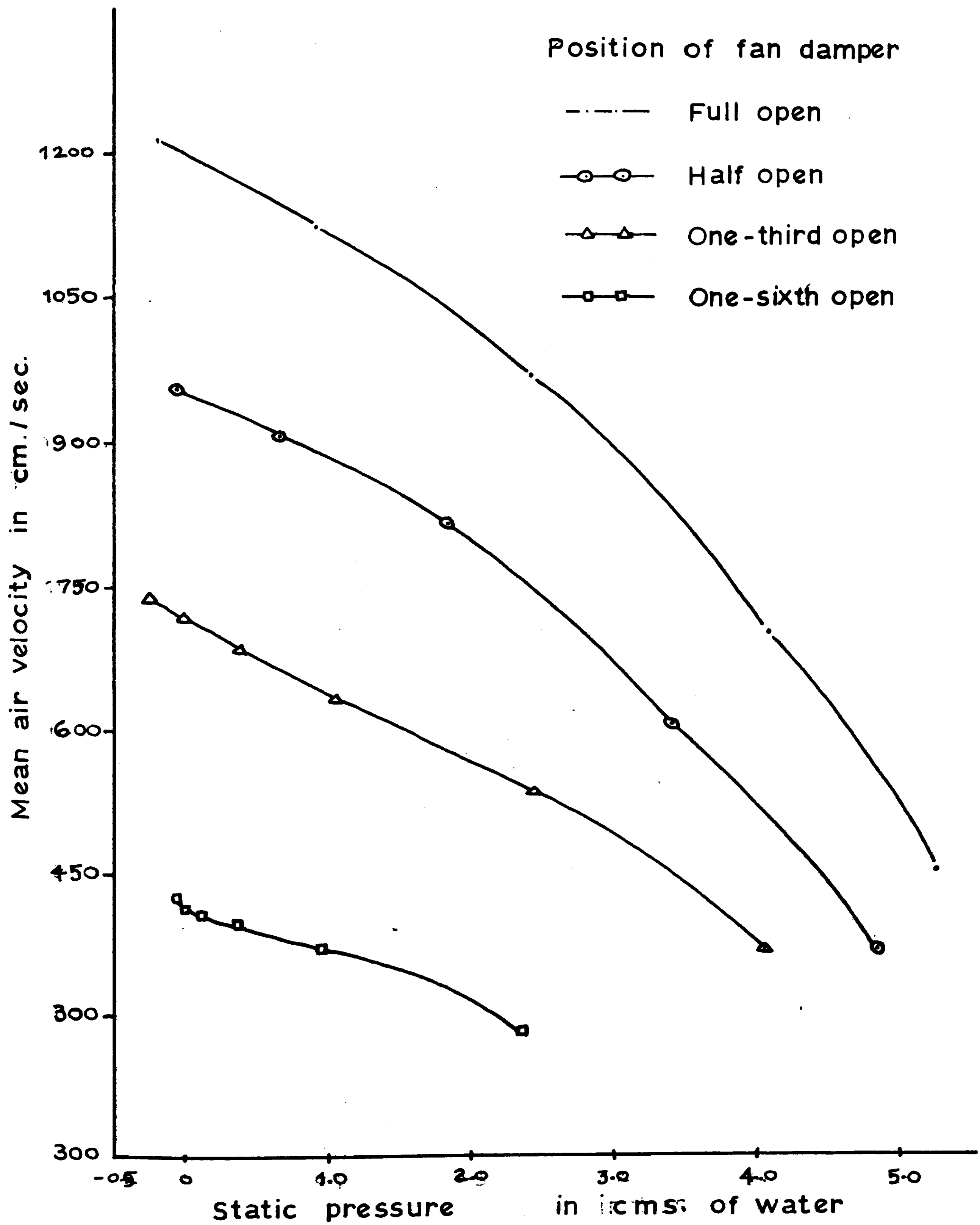

It could be seen from Fig.3.6 that any obstruction to the extent of about 20% of the cross-sectional area of tunnel-outlet did not cause any significant change in the mean velocity of air flowing through it, and also that with the damper fully closed (normal mean velocity about 60 cm./sec.), obstruction as much as 80% did not produce appreciable change in velocity.

From Fig. 3.7, it is clear that the rate of change of velocity with increasing obstruction of outlet is proportional to the opening of the fan-damper, i.e. the greater the intake of air the greater is the reduction of air velocity by a given obstruction. The results showed that for air velocities from about 700 to 1200 cm./sec. there was a static pressure increase of about 0.8 cm. head of water for every 10% area obstruction at the outlet.

These results were found to be most useful in maintaining the tunnel system in order, since it made it possible to check from time to time the obstruction being produced by the filter.

<u>3.2. Distribution of dust concentration</u>

<u>3.2.1 Introduction:</u> Having obtained an even velocity distribution in the tunnel, it was now necessary to assess the uniformity of dust-concentration within it. This required dust samples to be withdrawn at various points. It was important that the method of dust sampling should not cause a large disturbance to the air-flow velocity distribution and the

samples collected should be representative of all the dust passing through the tunnel.

3.2.2 Gravimetric Sampling: The gravimetric dust sampler assembly used for the experiments is shown in Fig. 3.8. A vacuum pump was employed to draw the dust-laden air into the sampling nozzle, iso-kinetic sampling being maintained by the use of a calibrated flow meter. The dust-laden air passed through a "soluble" filter-bed, consisting of pure salicylic acid crystals, which retained the dust particles. Salicylic acid was selected as the filter medium, due to the fact that its needle-shaped crystals could be packed into a bed which removed satisfactorily dust particles down to sub-micron sizes. It was also important to use a sharp-edge sampling nozzle and a "slow" smooth bend to cause change of direction of the dust-laden air.

The salicylic acid crystals for use in sampling filters were prepared by making a saturated solution of salicylic acid in boiling water. The liquid was filtered hot and allowed to cool to about 50°C., the supernatant liquor was then poured off and the crystals retained. If allowed to cool much below 50°C, the crystals have been found to be too large for use.(88)

With the fan set for an air velocity of 100 cm./sec., and the dust-injector set to eject into the centre of the duct, the tunnel filling the middle groove of the dust-plate I,

FIG. 3.8 THE GRAVIMETRIC DUST SAMPLER ASSEMBLY

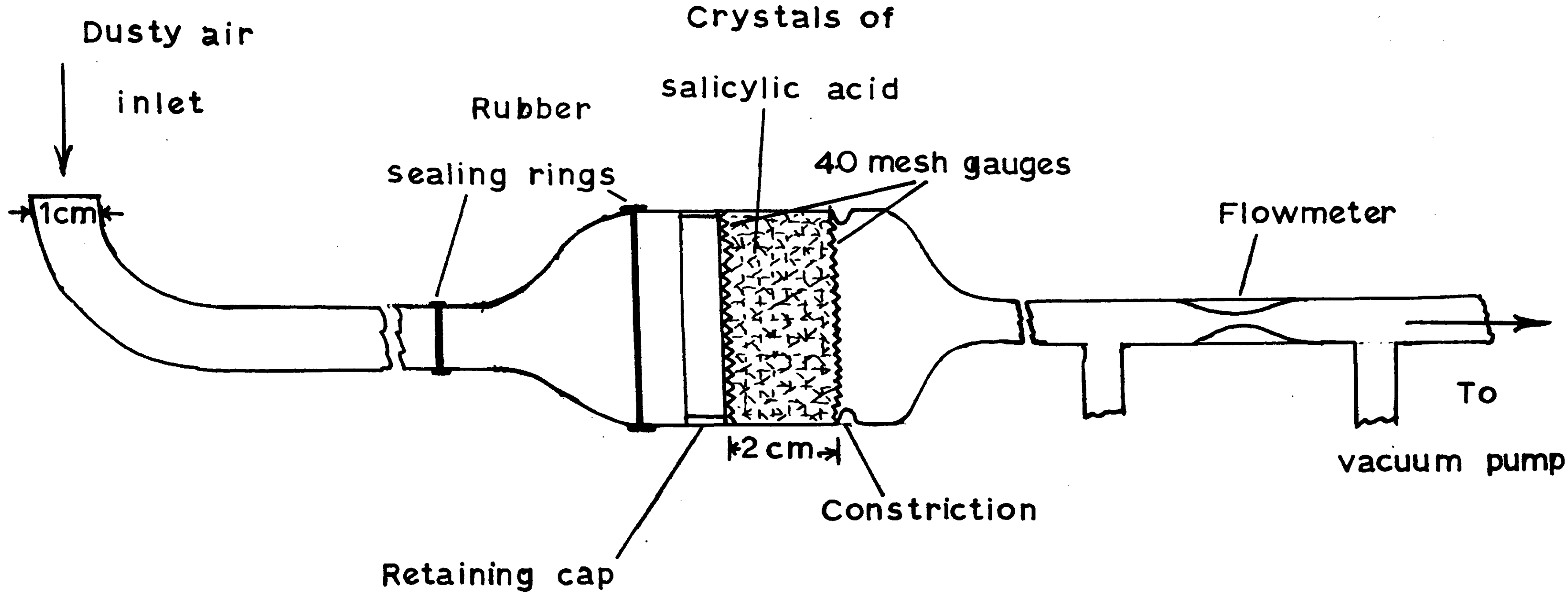

and allowing a few minutes for conditions to become steady, the dust was sampled at five sections.

The sampling sections were :-

(i) Just in front of the half-area mixing baffle;

(ii) Just in front of Thermal Precipitator I;

(iii) 1 metre beyond the spray nozzle;

(iv) 3 metres beyond the spray nozzle;

(v) Just in front of Thermal Precipitator II.

At each of these sections, simultaneous sampling of dust was carried out for an hour at each of the corresponding five positions at each section, viz. at the centre, 7.62 cms. either way and 15.24 cms. either way from the centre (dividing the horizontal diameter into six equal parts). The filter was weighed before and after the experiment.

The results are shown in Table 3.2 and are represented graphically in Fig. 3.9.

TABLE 3.2

Section No.	Sampling section in the duct	Dust Concentration mgm/cu.m. Distance of sampling point from the tunnel wall.				
		$^1/_6$D	$^1/_3$D	$^1/_2$D	$^2/_3$D	$^5/_6$D
1	Just before $D/\sqrt{2}$ baffle	116.2	154.0	133.0	122.8	131.6
2	Just before T.P.1	62.9	62.5	69.2	58.8	61.0
3	1 m. beyond spray nozzle	49.8	55.5	64.6	53.1	49.2
4	3 m. beyond spray nozzle	48.5	55.4	61.6	49.5	48.9
5	Just before T.P.2	45.5	50.8	58.9	44.4	44.8

FIG.3.9. DUST DISTRIBUTION IN THE TUNNEL

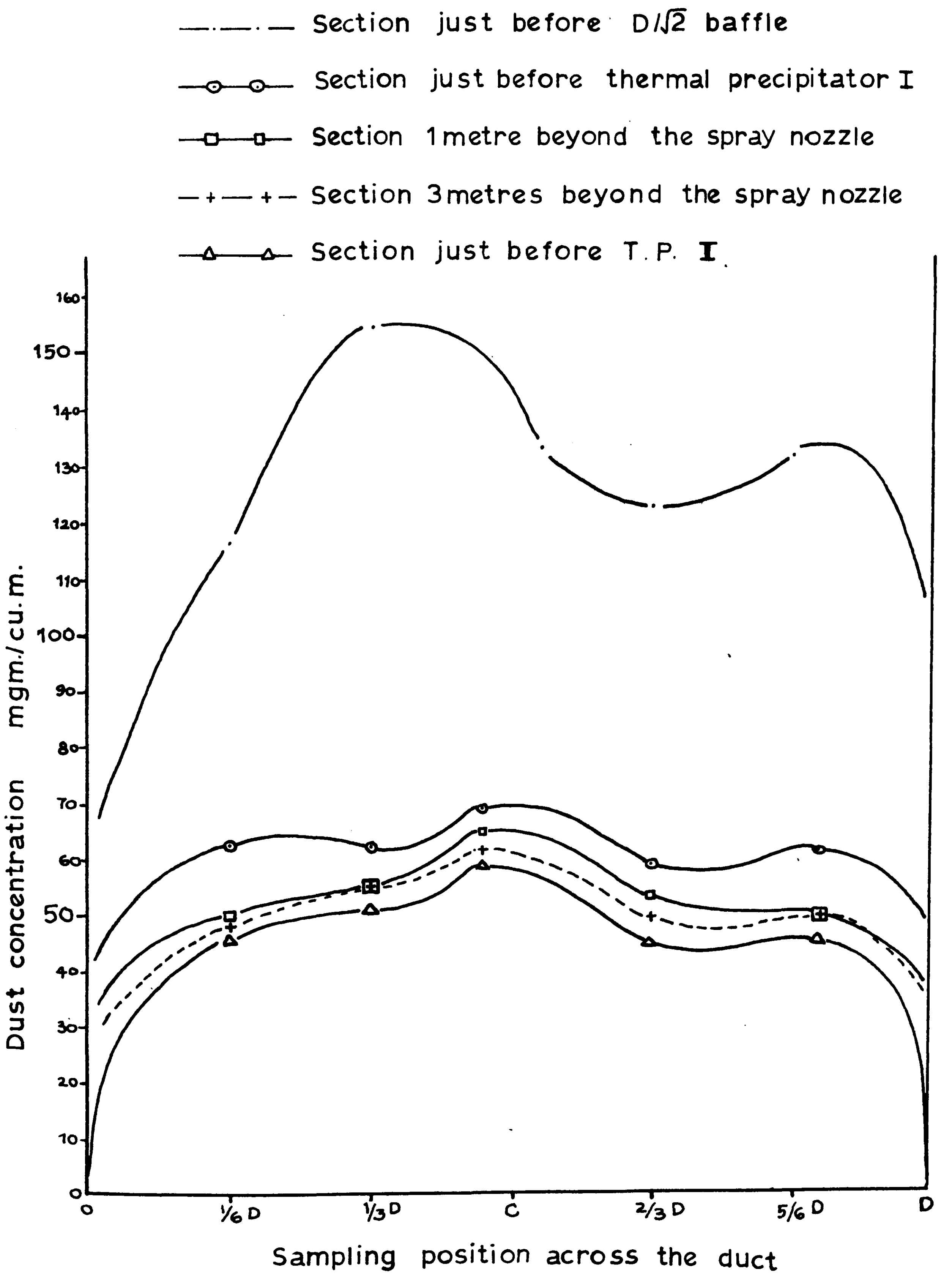

The results showed relatively uniform concentration of dust across the tunnel-sections beyond the baffle plates, although there was some decrease in the concentration of dust, as it passed along the tunnel towards the outlet end. The dust-distribution pattern in the tunnel after the baffle plate was in keeping with the velocity distribution pattern, since in all the sections beyond the baffle plates, the maximum concentration of dust appears to be at the axis of the tunnel.

The large diminution in dust concentration between section 1 and section 2, i.e. in crossing the baffles, could be attributed to the impaction of large dust particles on the baffle and their subsequent fall-out. On average the results of Table 2 show that the extent of the removal of dust by these baffles was about 52% of the material injected. The particle size of the material removed at this point was found to lie between 15μ and 53μ. This was consistent with results on the efficiency of impaction on discs, shown by Stairmand(89).

Considering only dust concentration changes beyond the baffle plates (Sections 2 - 5) it can be seen that the dust concentration decreased by about 14 mg/cu.m. as the dust cloud travelled from Section 2 to Section 5 along the tunnel. This rate of decay of concentration of air-borne dust with distance along the tunnel is shown in Fig. 3.10 and the fall-out amounts on an average to about 3.2 per cent

FIG.3.10 DECAY OF CONCENTRATION OF AIR-BORNE DUST WITH DISTANCE ALONG THE TUNNEL

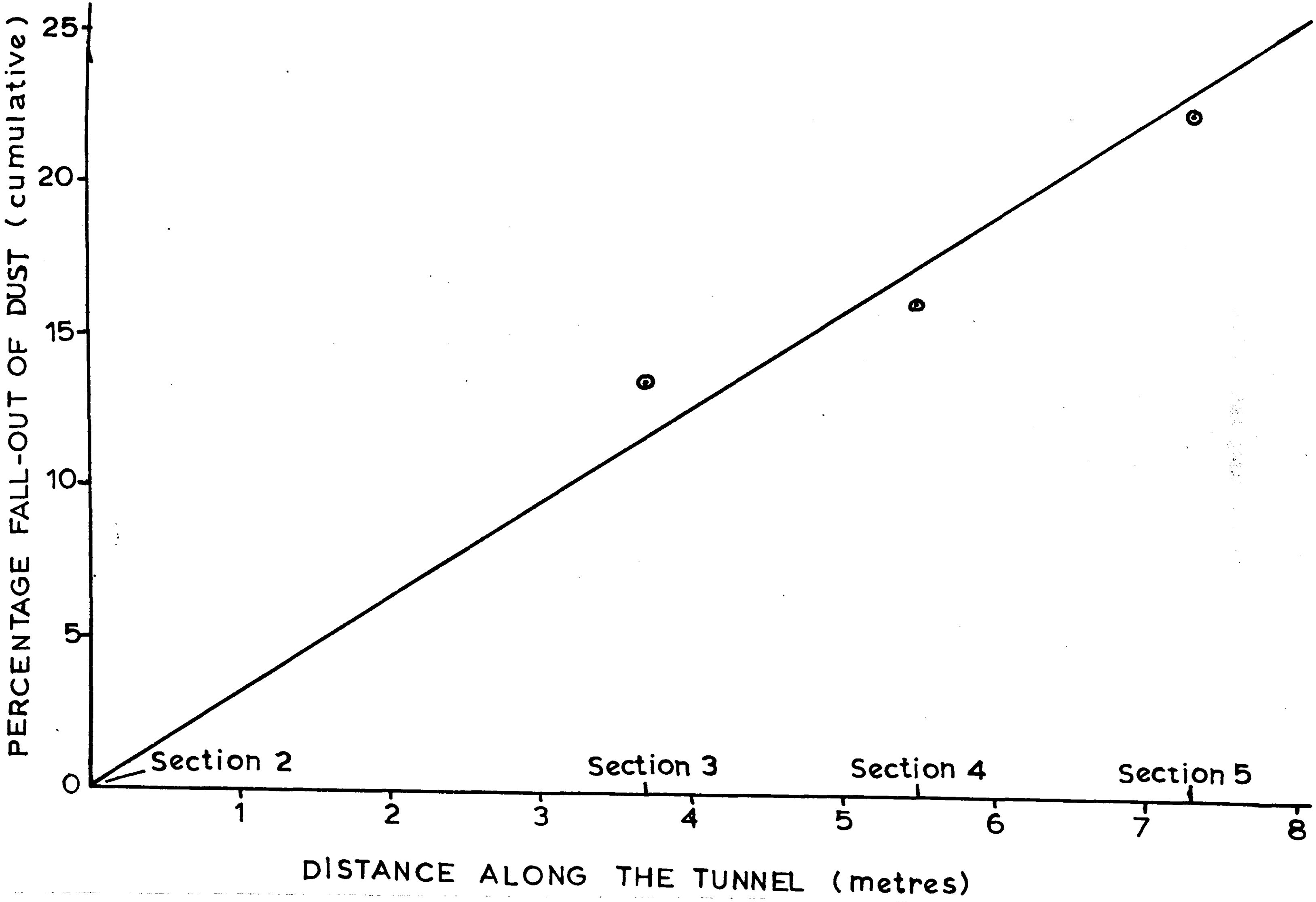

of the original dust concentration per metre length of travel along the tunnel.

At any one section, the distribution of dust concentration across the tunnel at the turbulent velocity of 100 cm./sec. is found to be uniform, with a standard deviation of about 5, as shown in Table 3.3.

TABLE 3.3

Fall-out of dust along Tunnel

Section No.	Mean dust concn.mg/cu.m.	Standard Deviation of dust concn.	Percentage removal of dust (cumulative)
2	62.9	3.48	-
3	54.4	5.57	13.5
4	52.8	5.06	16.05
5	48.9	5.51	22.25

3.2.3 Mechanisms of dust fall-out: There are at least six transport mechanisms which could account for the removal of air-borne dust as it flows in air suspension along the tunnel. These are :-

1. A thermal gradient force produced by friction at the tunnel wall. This can be neglected here as Pereles[90] has shown that such deposition in turbulent flow at 100 cm./sec. is less than a factor of 10^{-5} of the total deposition.

2. Deposition due to electrical charges on the dust particles. This also can be neglected since Dawes and Slack[91] have shown that such electrical forces need only be considered when the particles have already been brought to within a few particle diameters of the wall by some more widespread mechanism.

3. Deposition by the action of gravity in a turbulent airstream. Any particle travelling along the centre of the tunnel is liable to be deposited by the gravity force in turbulent stream within the length of the tunnel and this must be one of the major deposition processes, accounting for the diminution in dust concentration along the tunnel.

4. Deposition by eddy impaction. If a laminar sublayer is postulated next to the wall, only particles greater than 35 microns in diameter are found to be deposited by eddy impaction at an airstream velocity of 100 cm/sec. Since the particles in the experiments were up to 53 micron in diameter, it is suggested that this mechanism may have accounted for a considerable proportion of dust deposition along the tunnel.

5. Brownian deposition. This may be disregarded, since it is known to be not more than $^{1}/1000^{th}$ of the total deposition for particles above 1 micron.

6. Turbulent Diffusion. This is probably the main transport mechanism causing the deposition of dust.

The theory of dust deposition by eddy impaction on the basis of a conventional laminar sublayer fails to explain fully the fall-out mechanism, since turbulent motion of dust particles within this laminar sublayer has been observed by Fage and Townend(92) within 0.5μ from the wall. Hence it is possible that the transport of dust particles across the laminar sublayer (which is of the order of 1 mm. thickness in the case of air at a mean air speed of 100 cm./sec.) to the wall takes place by turbulent diffusion.

On average, the dust deposition rate beyond the baffle plates was of the order of 1 mgm/mm. of air/metre length of tunnel, viz. 3.2% fall out/metre length of tunnel.

<u>3.2.4 Thermal Precipitator Sampling:</u>

Simultaneous air-borne dust samples were drawn into the two thermal precipitators set in the tunnel. This experiment was carried out at three air velocities with the dust machine adjusted to give a suitable dust concentration. The number concentration of dust particles was evaluated on the automatic particle counter described later, and the results shown in Table 3.4.

TABLE 3.4

Simultaneous dust concentration at two points in tunnel as determined by Thermal Precipitator.

Air Velocity cm./sec.	Dust conc. at T.P.1. p.p.c.c.	Dust conc. at T.P.2. p.p.c.c.	Difference in dust conc. p.p.c.c.	Removal of dust %
75	1447	1420	27	1.87
200	1030	1020	10	0.97
450	640	628	12	1.87

It is apparent that the number concentration of dust particles as sampled by T.P. has not decreased to any great extent, unlike the weight concentration as measured by the filter. This suggests that material which has fallen-out of the air stream constitutes a relatively small number of large (and heavy) particles, and agrees with the postulated mechanism of gravity settling for this dust removal. There is also the point that the T.P. has a very low efficiency for dust particles outside the range 0 - 20μ, and that, although there is settlement of large dust particles down the length of the tunnel, from the point of view of the T.P. which only collects particles in the size range that concerns us, there is no significant change in dust concentration between the T.P. points. Since the same T.P's were used in the dust suppression work described later, changes in dust concentration recorded by them refer only to changes in the size range which they sample.

4. A METHOD OF MEASUREMENT OF PARTICLE SIZE

4.1. Introduction

A recently developed automatic method of microscopic size analysis based on mechanical scanning together with photoelectric detection and high-speed-pulse counting, was adopted the measure the particle sizes and to count the number of dust particles in the samples taken by thermal precipitator.

Visual counting of particles has always been a slow and tedious process in which the observer has continually to make judgments about individual particles, correct for focus, allow for edge effects and variations in opacity, and systematically evaluate the population, remembering each particle as it is counted. Even when the operator has been trained for visual counting, and the size and shape of particles are comparatively uniform, subjective errors are involved.[93]

In visual counting, moreover, measurements are carried out on a series of randomly selected fields, taken to be representative of the whole sample.

In the automatic counting method, the principle is to use as the sole parameter, variation in light intensity falling on a photocell, in such a way that the discriminations about particle sizes can be made without ambiguity. In this way the potentially high counting rate of an electronic system can be exploited.

Various methods of automatic size analysis are known,[94,95] and the work of Hawksley et.al.[96] has resulted in the commercial manufacture of an "Automatic Particle Counter and Sizer" by Casella (Electronics) Ltd., London.[97]

The Casella machine utilises the technique of wide track scanning, which is said to have the following advantages:-

(i) No critical timing circuits are required to measure "intercept lengths". The particle produces a voltage pulse, whose measured amplitude is proportional to the amount entering the scanning slit.

(ii) The instrument can be set to suit the optical characteristics of the material to be analysed.

4.2 Theory of Particle Sizing and Counting by track scanning.

In this sizing technique the number, length and height of pulses from intercepted particles are found and the number of particles per unit area and their size distributions are obtained therefrom.

The significance of particle interception by a track is shown in Fig. 4.1, where it may be observed that there are three types of intercepts:

(a) particles, of size x less than the track width w and projection h equal to x, lying wholly within the track;

(b) particles, of any size x and projection h, falling partially within the track;

(c) particles, of projected size x greater than w and projection h equal to w, lying wholly across the track.

Suppose that an illuminated field of well-separated circular particles, of constant optical density, is scanned by a slit-shaped aperture of length w and negligible breadth. A photo-cell behind the aperture is set to record changes in light flux as the slit intercepts particles in the scanning track. The peak heights of the pulses are then proportional to the projections h, while their durations are proportional to the intercept lengths y. The total number of pulses is equal to the total number of particles intercepted. If the pulses are fed to a pulse amplitude discriminator that records only those pulses exceeding some preset height, the recorded number of pulses is equal to the number of projections h exceeding a value $h = s$, corresponding to the setting of the amplitude discriminator.

In counting, the number N of particles per unit area is to be found from observation of the number ϕ of pulses per unit length of scan. The number of intercepts $\phi(w)$, obtained by scanning a length L of the specimen with a slit of width w and of sensitivity z is given by

$$\phi(w) = N(w - 2z + \bar{d})L \qquad \ldots\ldots \quad (1)$$

where N is the number of particles oversize z and $\bar{d}$ is the mean size oversize z. By sensitivity z, is meant that a particle must enter a slit by an amount $h > z$ to be recovered (see Fig. 4.1).

FIG.4.1. INTERCEPTION OF PARTICLES BY A TRACK SCAN

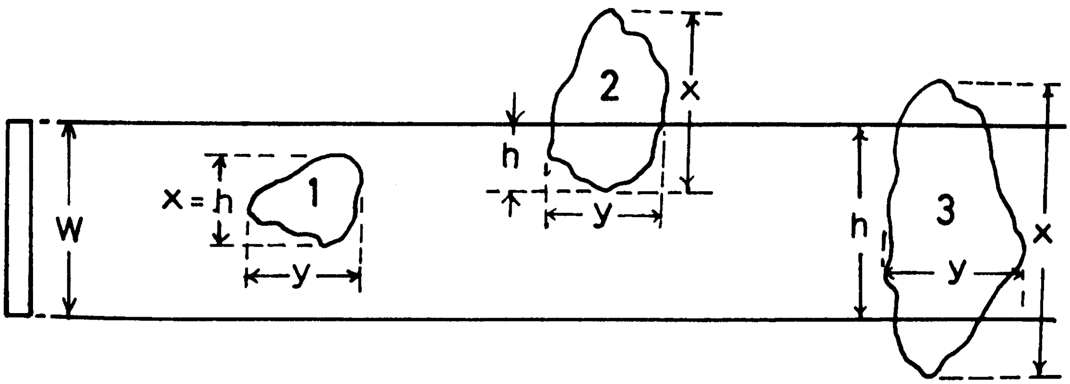

w, track width; x, projected size of particle; y, intercept length; h, projection of particle within track; 1, particles (x<w) wholly intercepted; 2, particles intercepted by one edge; 3, particles (x>w) intercepted by both edges.

FIG.4.2. GRAPHIC REPRESENTATION OF RESULTS

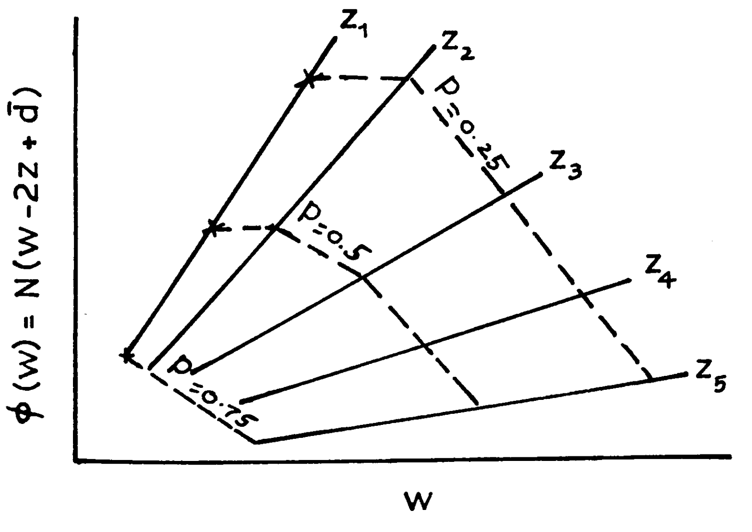

The number N of particles per unit area is obtained by scanning the specimen rtwice with two slits of different widths w, keeping z constant. The equation becomes,

$$N = \frac{\phi(w2) - \phi(w1)}{(w2 - w1)\ L} \qquad .... \qquad (2)$$

A straight line graph with slope equal to NxL, is obtained, $\phi(w)$ is plotted against w for a constant value of z. The graphs are shown in Fig. 4.2.

In the instrument, intercepts greater than z are not directly recorded, but instead pulses proportional to fractions of w per unit length of scan. The maximum pulse occurs when the slit w is completely obscured. An amplitude discriminator, which can be set at any desired fraction p, is used to select the pulse heights. Where $\phi(w)$ is a count of all pulses greater than the fraction p which has been set, p x w = z. Therefore equation (1) can be written as

$$\phi(w) = N\ [\ w(1 - 2\ p) + \bar{d})\ L \qquad .... \qquad (3)$$

The size distribution of particles in respect to their projected sizes is f(x), so that

$$\int_a^b f(x)\ dx = 1 \qquad .... \qquad (4)$$

the limits a and b are the smallest and largest particles respectively. The sum of all the particles between the limits $a < x < b$ is N per unit of area.

The procedure is to obtain a number of z lines, each such that $z1 < z2 < z3 \ldots < zN$. The classification into n size grades requires n z-lines, as shown in Fig.4.2.

4.3. Description and operation of the Counter

The 5-channel Automatic Particle Counter is shown in Plate III along with the schematic diagram of the instrument in Fig. 4.3. The console unit can be considered to be comprised of 5 blocks: (1) Left Bottom block, having the main power supplies for the amplifier and amplitude discriminators. (2) Left top block, having in the bottom panel the main amplifier and Amplitude Discriminator control unit, tuning indicator and Amplitude Discriminator Dial No.1 and in the other two panels, four other amplitude discriminators and their tuning indicators. (3) Top right block consists of five dekatron registers for their corresponding Amplitude discriminators situated in the top left block. (4) Bottom right block has a writing table and also houses the supply unit for the microscope lamp, and (5) Central block, which is the microscope and stage unit and stage control unit.

The filament lamp type of illumination gives a high light intensity when using Kohler's system of illumination and also uniform illumination over the field of the object. The light intensity is such that good signal to noise relationship is obtained for slit sizes below a micron in width.

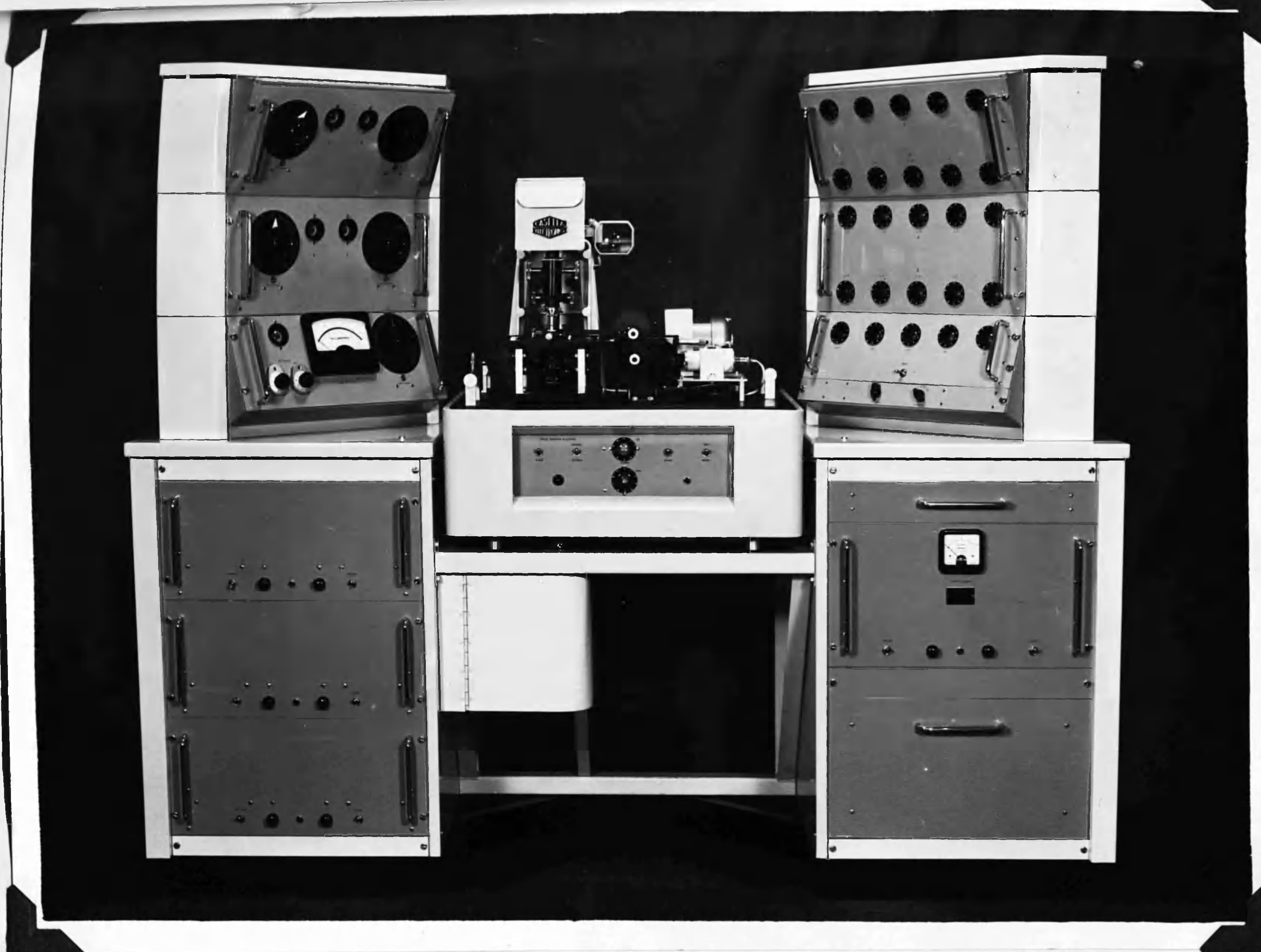

PLATE III
AUTOMATIC PARTICLE COUNTER AND SIZER

FIG. 4.3. SCHEMATIC LAYOUT OF AUTOMATIC PARTICLE COUNTER

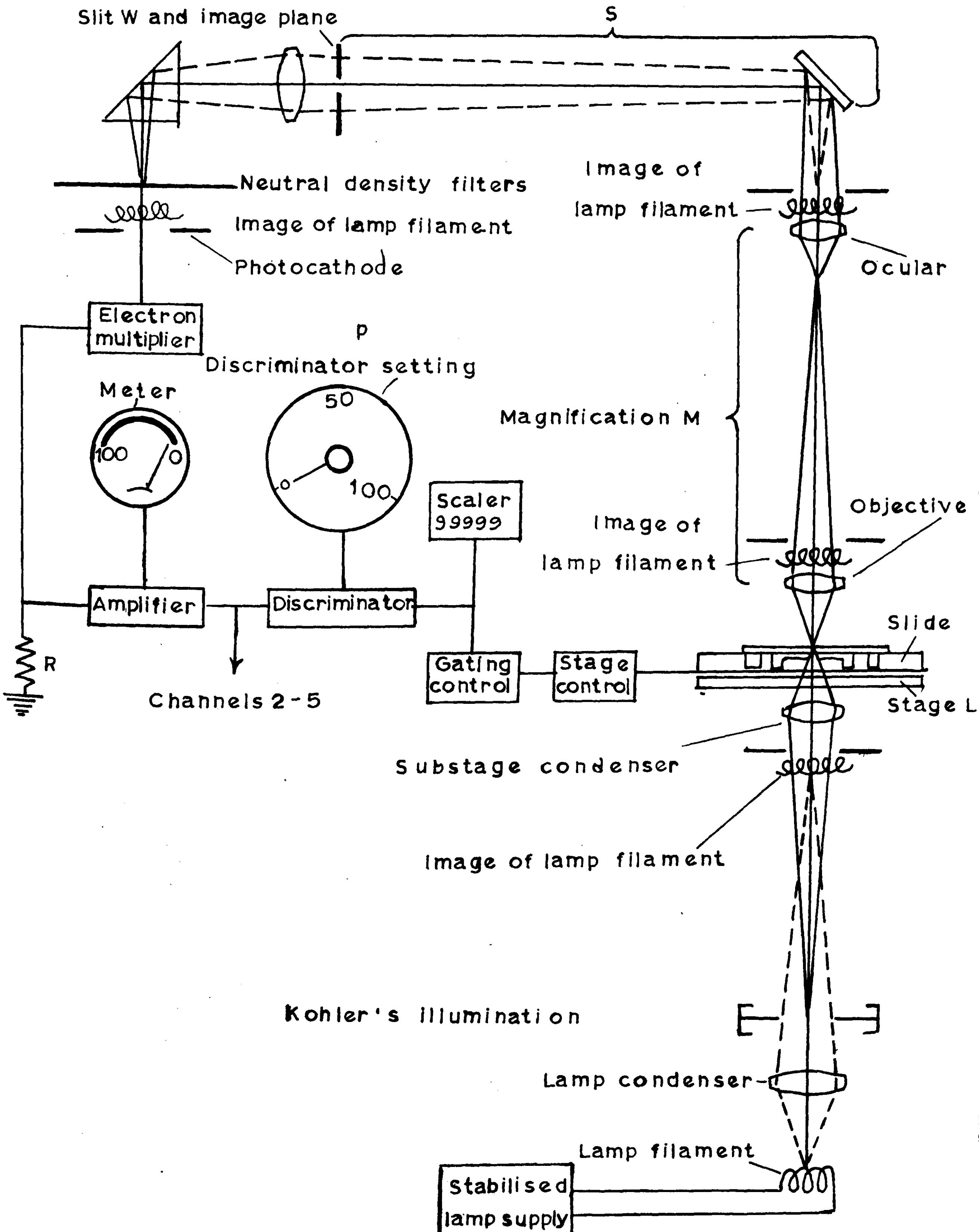

As a first step, a programme data sheet is drawn up, by selecting size levels (z), track widths (w) and discriminator dial settings (p) over the size distribution in question. A specimen programme sheet for counting and sizing of particles in the size range 0.5 - 4.0 μ is shown in Table 4.1.

If the size levels (z) chosen stand in no particular relationship to each other and if the same is true of the discriminator settings, then it is clear that a different setting of the track is necessary for each z, p combination. The efficiency of operation can therefore be increased, by achieving a minimum number of slit resettings, combined with a fixed series of discriminator dial settings. This is done by choosing a series of size levels (z) standing in a geometric progression and discriminator dial settings (p) also standing in the same progression. Thus the track width necessary for each z stands in the sample progression. In the example given, it can be seen that, about 32 different dekatron readings pertaining to size levels 0.5, 1.0, 1.4, 2.0, 2.8, 4.0 and 5.7 microns can be obtained, with only 10 different slit settings and therefore the time consumed in scanning is highly reduced.

Operation:- The machine is switched on and allowed to warm up for a few minutes. Then the lamp is switched on and the current for Koher's system of illumination adjusted

TABLE 4.1

$\sqrt{2}$ Programme sheet for 5 channel-unit APC

Objective. .2 mm. Oil immersion; Ocular x 6 ; Mag. x 540

z_μ	p1	p2	p3	p4	p5	Slit Width $w = z/p$	Microm. Setting $10 - \frac{wxM}{1000}$	Dekatron Reading $\phi(w)$
0.5	0.8					0.625	9.663	687
		0.5656				0.884	9.523	1200
			0.4			1.250	9.325	1990
				0.2828		1.768	9.046	2995
					0.2	2.500	8.650	4475
1.0	0.8					1.250	9.325	498
		0.5656				1.768	9.046	949
			0.4			2.500	8.650	1667
				0.2828		3.536	8.091	2701
					0.2	5.000	7.300	4180
2.0	0.8					2.500	8.650	414
		0.5656				3.536	8.091	1140
			0.4			5.000	7.300	2162
				0.2828		7.070	6.183	3534
					0.2	10.000	4.600	5545
2.83	0.8					3.536	8.091	387
		0.5656				5.000	7.300	790
			0.4			7.070	6.183	1304
				0.2828		10.000	4.600	2085
					0.2	14.140	2.365	3162
4.0	0.8					5.000	7.300	250
		0.5656				7.070	6.183	437
			0.4			10.000	4.600	740
				0.2828		14.140	2.365	1105

Slide Reference:- TP2A

to 7.8 amperes. The slide is now mounted on the reciprocating stage, which allows the scanning slit to be located on the optical axis of the microscope. The slide is fixed in position by means of two slips, and the dust-particles in the slide are brought to focus on a small screen, just in front of the gate and the slit, with the help of the microscope, utilising a 2 mm. oil immersion objective. The slit width and length can be set to the desired value by operating the two micrometers which are fixed in the system. The pulse meter in the top left block is adjusted to read 0 with clear filter and 100 with opaque filter, by the use of "Set min." and "Set max." controls located adjacent to it. Keeping the meter reading zero, and using clear filter No.1, the optical density of a few particles in the slide-sample is determined by bringing each of them in turn before the slit to produce a pulse on the meter and the amplitude discrimination unit is corrected for the average optical density of the sample by adjusting the "set" controls.

When the stage motor is switched on, the stage travels away from the operator, reverses automatically after 20 scans, takes a track differing by 50 microns from the original to come forward to the starting position after 20 scans. The length of scanning is 10 mm. The slit is instantaneously obscured by particles and if they produce a pulse greater than the discriminator set value, it is recorded on the dekatron unit. The procedure is repeated for different slit settings.

The overall magnification M of the optical system is always measured using a stage micrometer.

4.4 Mounting of slides for counting In microscopy the visual observer repeatedly adjusts the focus of his microscope to keep the particle field in sharp focus, a procedure which cannot be carried out during automatic scanning. Therefore it is very important that all the particles over the dust strip are uniformly in good focus, to obtain a correct count. That means that the cover glass, on which the dust strip is deposited in thermal precipitators, must be laid exactly parallel to the micro-slide, which is mounted on the reciprocating stage. A method of ensuring this has now been developed(98) and was used in all work reported here. Green's tissue papers are cut to 2.5 cm. square with 1.6 cm. diameter circle in the centre. A thin strip of the paper is laid flat on the microslide, using a dilute glue solution. When it is dry, the dusty cover-slip is glued on to the tissue paper, making sure that the dust strip is at the centre of the circle. This paper insert effectively holds the glass surface parallel.

In order to evaluate the dust on the thermal precipitator slides, various size-distribution programmes and different arrangements of objective and ocular were tried. It was finally decided to utilise a magnification of 540, produced by a 2 m.m. oil immersion objective and a x6 ocular, together with a $\sqrt{2}$ programme in the range 0.5 to 5.67 microns. To prevent the oil[99], used for immersion of the objective, penetrating through the tissue paper into the dust strip, cellulose lacquer was applied to the circumference of the cover-slip to seal the edge.

4.5 Specimen calculation of size distribution.

A dust-strip obtained from thermal precipitator II with the dust-machine and the air velocity adjusted to give a dust-concentration of about 1000 p.p.c.c. in the tunnel, is used in the illustration which follows. The size distribution is evaluated in the size ranges 0.5 - 1.0μ, 1 - 2μ, 2 - 2.83μ and 2.83μ - 4μ.

From the recordings of dekatrons, graphs of w against $\phi(w)$ are plotted, for the $\sqrt{2}$ programme of Table 4.1 as shown in Fig. 4.4 and the size distribution shown in Table 4.2.

Particles oversize z = 0.5 micron

No. of particles per unit area of dust strip on cover glass above 0.5 micron $= \dfrac{\phi(w_2) - \phi(w_1)}{(w_2 - w_1).L}$

where L is the total length scanned (800 mm.)

Substituting, the no. of particles per unit area

$$= \frac{44}{11} \times \frac{1000}{2} \times \frac{1000}{800} = 2{,}500$$

FIG. 4.4 GRAPH FOR SIZE - DISTRIBUTION OF SPECIMEN

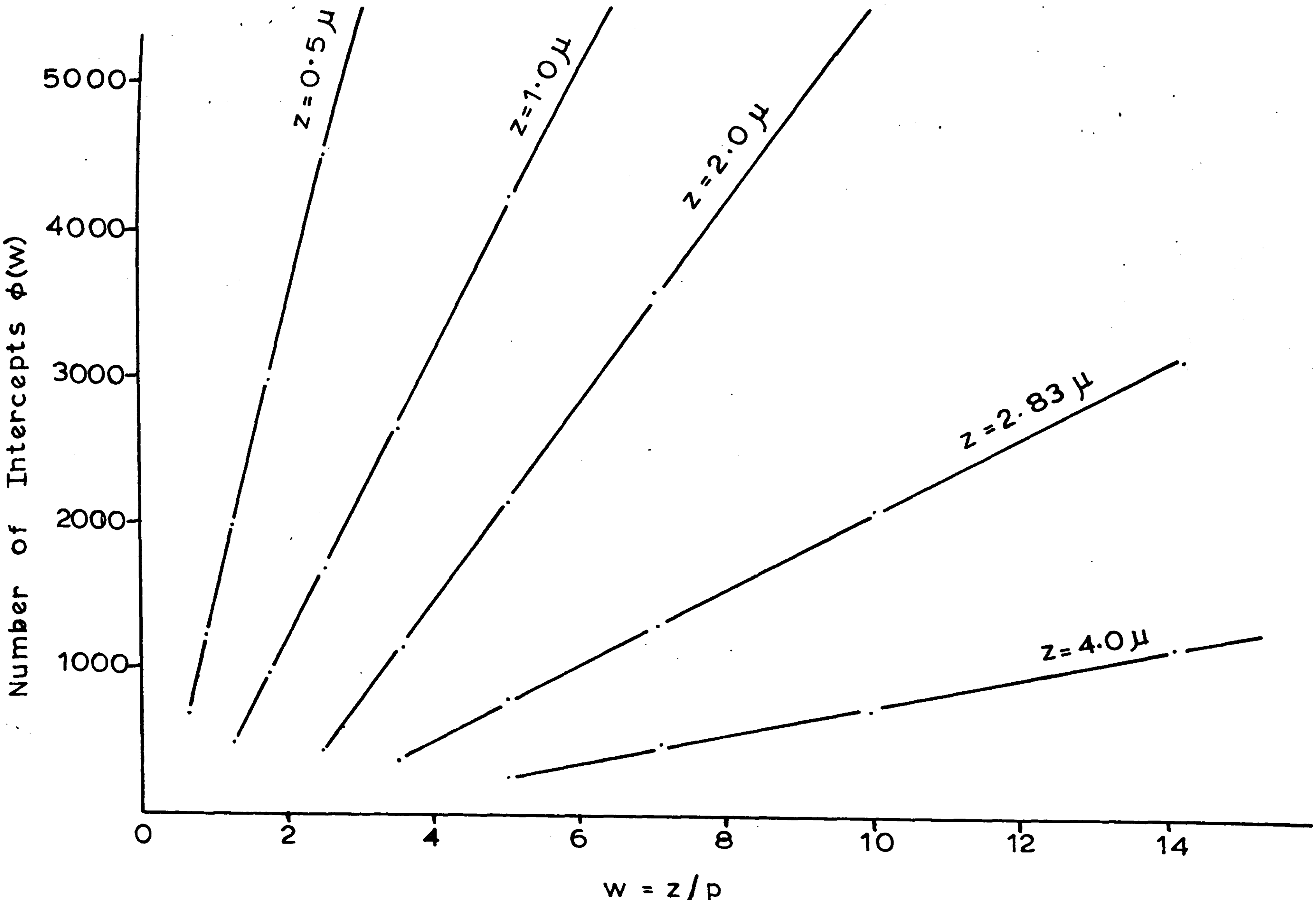

The photomultiplier counts particles only within 10 x 2 = 20 sq.m.m. area on the dust-strip of the cover glass.

∴ Total No. of particles above 0.5µ = 2,500 x 20 = 50,000

Hence, dust concentration in particles /cu.cm. of air

$$= \frac{\text{No. of particles}}{\text{Vol. of air sampled}}$$

$$= \frac{50,000}{45} = 1112 \text{ p.p.c.c.}$$

The size-distribution of particles is given in Table 4.2.

TABLE 4.2

Size-Distribution of Dust

s	>0.5µ	>1.0µ	>2.0µ	>2.8µ	>4.0µ
Gradient	2500	1180	857	341	123
Particle No.	1112	524	381	152	55
Size range	0.5-1.0µ	1-2µ	2-2.8µ	2.8-4µ	>4µ
Particle No.	588	143	229	97	55
Number Percentage	52.8	12.87	20.6	8.7	4.95

4.6 Size Frequency of experimental coal-dust injected into the tunnel.

Several representative samples of the dust were withdrawn iso-kinetically, through salicylic acid filter, from the air at different sections of the tunnel, mixed, and a representative sample prepared for counting under the automatic particle counter, as described in Chapter 5. An average size frequency representative of the experimental coal-dust, is given in Table 4.3.

TABLE 4.3

Average Size Frequency in the experimental Coal-Dust

Size Range	0.5-1.0μ	1.0-2.5μ	2.5-5.0μ	>5μ	Total
Number Percentage	42.96	31.46	9.40	16.15	100.0

and the cumulative Size Frequency is shown in Fig. 5.1.

4.7 The effect of change of opacity on dust-count

To investigate the effect of change of opacity on the dust-count, several dust strips with dust concentrations of about 1000, 1500, 2000, 2500 and 3000 particles per cu.cm. of air were prepared and counted at different particle counter "filter numbers", i.e. for different values of opacity.

If the dust-strip was exactly parallel to the stage, all the particles over the dust strip would be in sharp focus and the selection of opacity value could be easily and correctly made. On the other hand, if all the particles could not be brought to sharp focus at the one setting, the smaller particles were preferentially brought to focus, since the correct counting of smaller particles mattered more. In such cases, the opacity of the material might well vary over a range, which could make necessary the random selection of one of three filters.

In the specimen chosen, the opacity of the material as measured ranged from 72 to 84% and therefore necessitated the use of one of the filters numbered 6, 7, or 8.

The effect of variation in opacity from 65% to 100% was studied for different dust-strips and the results for one cover glass are shown in Fig. 4.5. It is apparent that the error introduced in counting by altering the filter number by one either way from the correct one, i.e. No.7, is not significant. In this case, the average error is only about 30 p.p.c.c. for a concentration of about 1100 p.p.c.c. The dust counts, however, diverge from the truth more rapidly, if the error in percentage opacity exceeds ± 6% i.e. by more than one filter number either way from the correct opacity. This is well illustrated in Fig. 4.5. It

FIG.4.5 THE EFFECT OF OPACITY ON DUST-COUNT

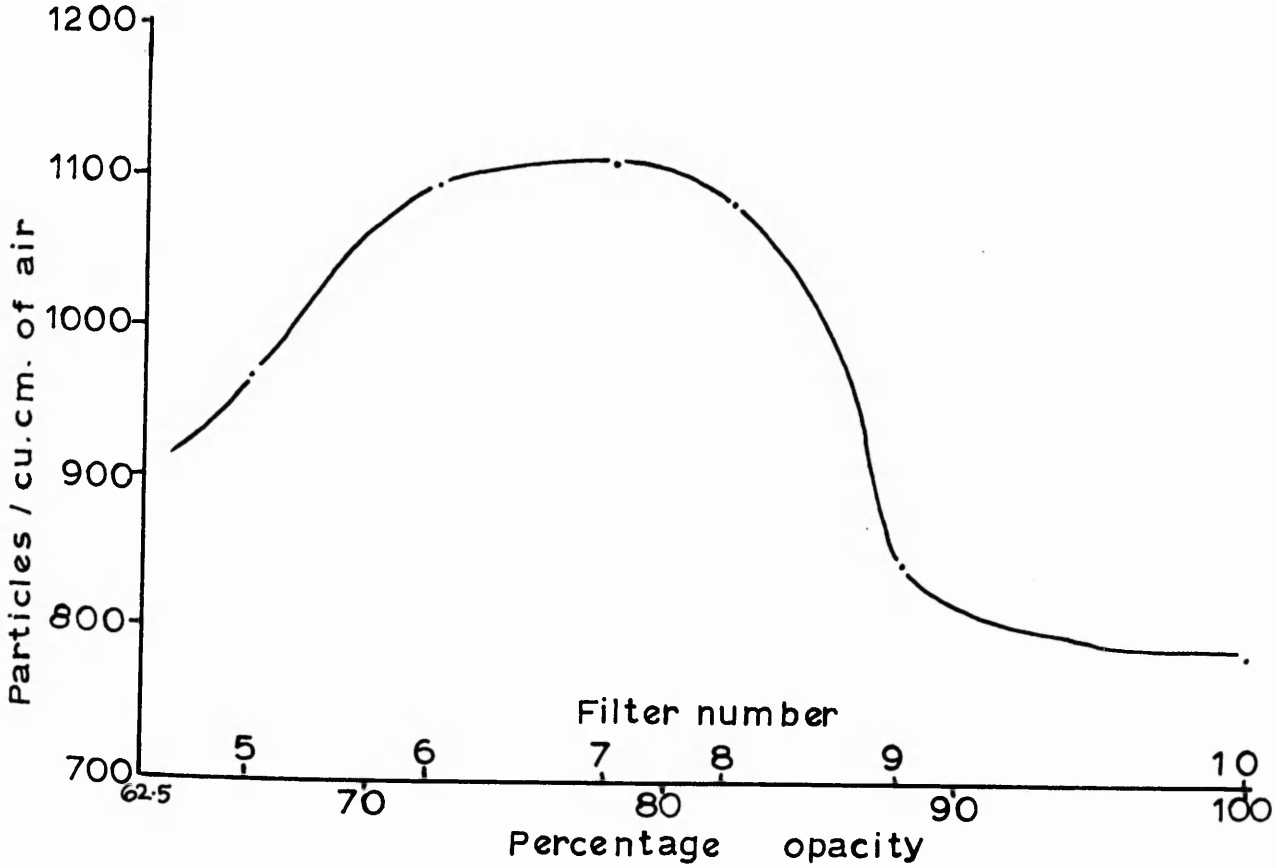

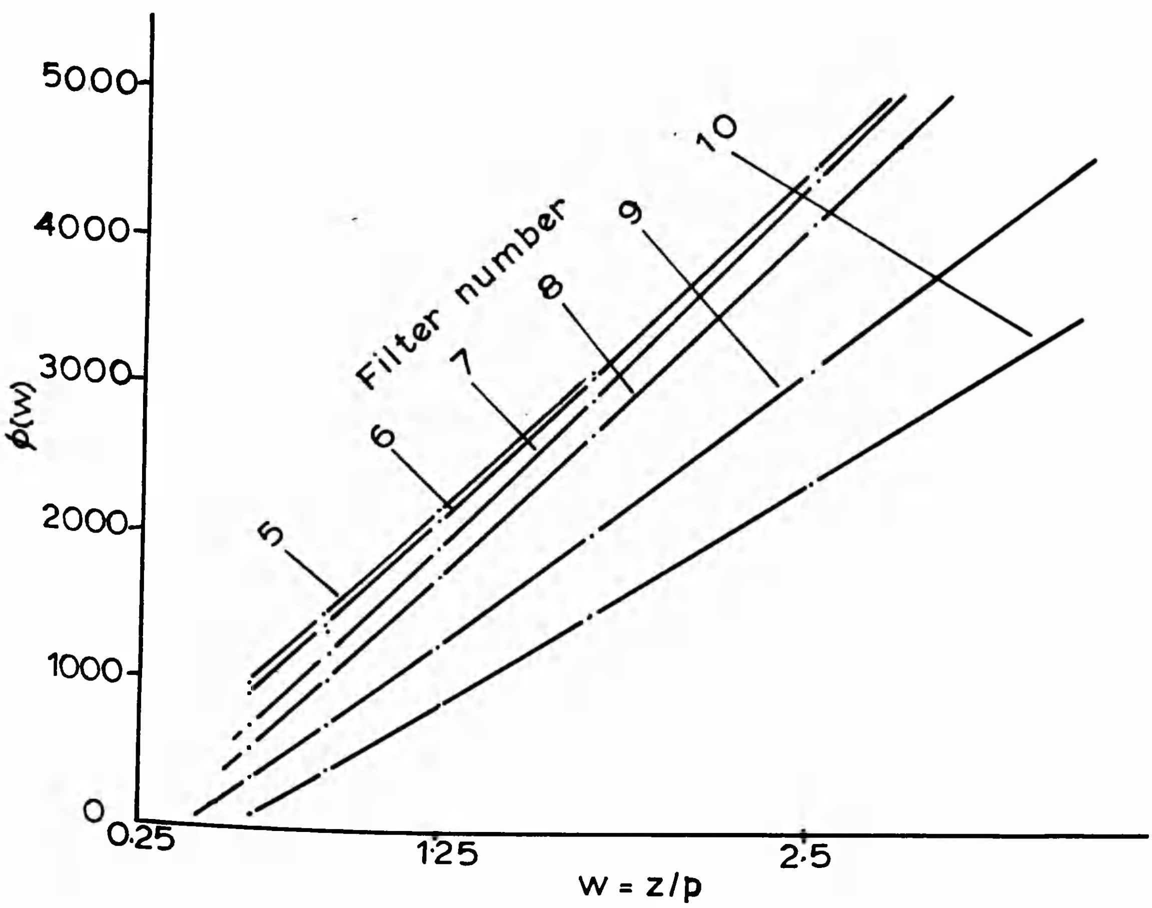

is therefore obvious that care should be taken in selection of the proper filter to suit the opacity of the material counted.

4.8 Analysis of Variance for the Automatic Particle Counter.

Four factors could be envisaged, which might contribute to significantly erroneous dust-counts made by the Automatic Particle counter:

(a) The dust-strip not being exactly parallel to the stage, (b) errors due to the changing of amplitude discriminator settings, (c) errors in the placing of the slide under the microscope and (d) errors due to the change in opacity.

Since the dust-strip is set parallel to the stage and the amplitude discriminators are set at the same values each time, factors (a) and (b) do not normally arise.

To study the interaction of factors (c) and (d) and their effect on dust-counts, a specimen slide was counted at three different opacities (one normal and one on either side of it). The placing of the slide was then disturbed, placed again in position and again counted. This was repeated at four more placings and the results obtained shown in Table 4.4.

TABLE 4.4

Dust Counts p.p.c.c.

Filter No.	Percentage opacity	Dust Counts p.p.c.c. For Random Placings of Slide						Total
		S_1	S_2	S_3	S_4	S_5	S_6	
8	84 (O_1)	1087	1082	1097	1112	1162	1017	6557
7	78 (O_2)	1112	1110	1123	1152	1234	1038	6769
6	72 (O_3)	1097	1087	1105	1123	1180	1021	6613
							Total ...	19,939

<u>Variance Calculation</u>:

To calculate the variance between opacities and within samples:

(i) Total sum of squares (crude)

$$= 1087^2 + 1112^2 + 1097^2 \ldots\ldots + 1021^2$$

$$= 22,135,829$$

(ii) Crude sum of squares between opacities

$$= \frac{(6557)^2 + (6769)^2 + (6613)^2}{6}$$

$$= \frac{132,545,379}{6} = 22,090,896$$

(iii) Correction due to mean $= \frac{(19939)^2}{18} = 22,086,873$

(iv) Total sum of squares = (i) − (iii) = 48,956

(v) Sum of squares between opacities = (ii)−(iii) = 4023.

TABLE 4.5

Analysis of Variance Table

Source of variance	Degrees of Freedom	Sum of Squares	Variance
Between opacities	2	4023	2012
Within samples	15	44,933	2996
Total	17	48,956	-

Since the variance of the "between opacities" is less than the variance of the "within samples", the opacity change is insignificant. Hence all the data can be regarded as random samples from a universe with mean and standard deviation estimated respectively by

$$\frac{19,939}{18} = 1108 \quad \text{and} \quad \sqrt{\frac{48,956}{17}} = \sqrt{2880} = \pm 53.7.$$

It would appear therefore that the error introduced in counting is ± 0.5%.

4.9 Conclusion

The Automatic Particle Counter is thus found to offer many advantages over visual counting:

(a) It covers all the particles on the thermal precipitator-dust-strip and so it is more reliable and more representative of the dust-concentration at the sampling point.

(b) Human error involved in counting is insignificant. Even with the change of opacity amounting to ± 6% of the correct one, the error introduced in counting is found to be the order of ± 0.5%.

(c) Counting is done more quickly, and

(d) Heavier concentrations of the order of 4000 p.p.c.c. do not present any problems. (2,0 - 6.5 x 10^4 particle density).

5. A METHOD OF CORRELATING THERMAL PRECIPITATOR DUST-SAMPLES WITH SALICYLIC-ACID-FILTER DUST-SAMPLES.

5.1 Introduction

In British mining practice, the standard procedure for assessing the concentration of air-borne dust at any point involves dust sampling by thermal precipitator and expression of the dust concentration as a number of particles per c.c. of air. The efficiency of the thermal precipitator is claimed to be 100% for particles below 10 μ in diameter and somewhat less for particles above that size. Hence it was felt that an independent gravimetric sampling filter should be employed to sample the dust and the dust concentration by weight in the usual size ranges should be compared with that of the thermal precipitator dust strip for the same experimental conditions. This assessment by weight, calculated on the basis of the density of the dust particles, would also give a correlation factor, which might take into account the eccentricity of the particles in the thermal precipitator dust strip. The method of gravimetric sampling employed for these experiments was discussed in more detail in Chapter 3.

5.2 The Effect of direction of Sampling Nozzle on dust collection in gravimetric sampling.

To obtain a representative sample on the bed of salicylic acid crystals, it was essential to maintain iso-kinetic sampling of the dust-laden air-stream, by the use of a calibrated flow-meter. With dusty air flowing down the tunnel at an average velocity of 100 cm./sec., sampling of dust was carried out simultaneously over a period of one hour on the axis of the tunnel at two sections - viz. at 1 metre beyond the spray nozzle and at 3 metres beyond the spray nozzle. At the first section, the sampling nozzle was placed facing downstream and at the second section, it was placed facing upstream and the dust concentration was determined from the collected samples. A second test was carried out under identical conditions, with the sampling nozzle placed perpendicular to the air-flow, at 2 metres beyond the spray nozzle. The dust concentrations, calculated on the basis of amount of dust sampled, are shown in Table 5.1.

TABLE 5.1

The effect of direction of sampling nozzle on dust collection.

Position of sampling nozzle	Concentration of dust. mg./cu.m.
Facing upstream	68.0
Perpendicular to the airflow	61.8
Facing downstream	34.4

From the figures in Table 5.1, it would appear that to collect the maximum sample and thus perhaps the most representative sample, the sampling nozzle should be facing upstream. It is thus enabled to collect all the dust that might be flowing into it iso-kinetically. The nozzle placed perpendicular to the air-flow is fairly successful in drawing the dust into the filter; only about 9% by weight of the particles miss the opening of the sampling tube. The nozzle facing downstream has a very low sampling efficiency, only collecting 50% of the dust drawn into the tube, when facing upstream.

In the remainder of the tests, therefore, the sampling nozzle was always placed pointing upstream on the axis of the tunnel. Three runs, each lasting for an hour, were carried out, during which gravimetric and thermal precipitator sampling were simultaneously carried out. The salicylic acid filter was weighed carefully before and after the experiments and the increase in weight was taken to be equivalent to the dust sampled.

5.3 Recovery of sampled dust from the gravimetric filter

After a dust sample had been collected, the salicylic acid filter bed (see Fig. 2.8) was removed from the container and placed in a small beaker. The crystals were dissolved in ethanol and the suspension of dust particles centrifuged in an electrical centrifuge at 4,800 r.p.m. for 17 minutes. This interval was calculated from Svedberg's modified

Stokes' equation[100] to be suitable for the sedimentation of a 0.4 micron dust particle in the centrifuge tube. After centrifuging, the supernatant liquid was decanted, the tube again filled with ethanol and centrifuged a second time. The process of centrifuging, decanting and adding more ethanol was repeated six times in all, to make sure that all particles bigger than 0.4 μ had been retained in the centrifuge tubes. The collected dust was finally suspended in a small volume of ethanol, the liquid washed into a small basin and evaporated to dryness in an oven.

5.4 Preparation of slide for counting under A.P.C.

A fresh suspension of the dust particles was made in ethanol and a few representative drops of it were transferred to a microscope slide by means of a pipette. Four slides were made with one, two, three and four drops on them[101]. The solution was allowed to evaporate for some hours and when dry, the slides were mounted in the usual manner and the particles sized by means of the Automatic Particle Counter.

The counts at various sections of the four slides proved a nearly uniform distribution of the particles on the slides and the number percentage size frequency of the dust sampled by the gravimetric filter is given in Table 5.2. From the size frequency data and the total weight of dust collected, the proportionate weight of the particles in the size ranges was calculated, assuming that the particles were spherical, that the density of the coal was 1.279 g./c.c. and taking a mean size for each size range and a maximum of 10 μ for the range > 5 μ (Table 5.3).

TABLE 5.2

Number Percentage Size Frequency of dust samples

Size Range	0.5-1.0μ	1.0-2.5μ	2.5-5.0μ	>5μ	Total
Salicylic acid filter Dust sample	42.96	31.48	9.40	16.15	100.00
T.P. Dust sample	61.12	26.62	7.45	4.81	100.00

For the same experimental conditions, the T.P. slide was counted and sized under the Automatic Particle Counter. The average number percentage size frequency of the thermal precipitator dust sample is also shown in Table 5.2, and again knowing the total number of particles in each size range and their density, the weight of dust in each size range was calculated within the same limits. The resulting weight distribution is shown in Table 5.4.

The cumulative number size distributions corresponding to Table 5.2 are given in Fig. 5.1.

TABLE 5.3

Salicylic Acid Filter Sampling

Dust concentration by weight (experimental) and proportional weights in various size ranges (calculated).

Size Range μ	Number % Size Frequency	Wt.%	Dust concentrations mg./cu.m.			
			Run 1	Run 2	Run 3	Mean
Total	100	100.0	62.3	61.7	53.9	59.3
0.5-1.0μ	42.96	0.24	0.1498	0.1481	0.1292	0.1422
1.0-2.5μ	31.48	1.93	1.202	1.19	1.04	1.144
2.5-5.0μ	9.40	7.18	4.47	4.435	3.87	4.255
< 5.0 μ	83.85	9.35	5.84	5.78	5.05	5.56
> 5.0 μ	16.15	90.65	56.46	55.92	48.85	53.74

TABLE 5.4

Thermal Precipitator Sampling

Calculated weight concentration of dust in T.P. slide based on the density of coal particles (1.279 g./c.c.)

Size Range μ	Number % Size Frequency	Wt.%	Dust concentrations mg./cu.m.			
			Run 1	Run 2	Run 3	Mean
Total p.p.c.c. :-			876	1153	1315	1114
0.5-1.0μ	61.12	0.79	0.1532	0.1856	0.2818	0.2065
1.0-2.5μ	26.62	4.35	0.694	1.265	0.785	0.915
2.5-5.0μ	7.45	12.06	3.262	3.538	2.098	2.966
< 5.0 μ	95.19	17.20	4.09	4.985	3.215	4.09
> 5.0 μ	4.81	82.80	18.25	16.095	14.15	16.165
Total	100.00	100.00	22.34	21.08	17.365	20.26

TABLE 5.5

Dust concentration of the 'hypothetical T.P.' sample, calculated from that of the salicylic acid filter sample on the basis of the ratio of the number percentage size frequency of the dust samples in T.P. and gravimetric filter.

Size Range μ	Ratio of size frequencies (No. %) T.P. slide / SAF slide	Dust concentration in mg./cu.m.						
		Run 1		Run 2		Run 3		Mean Hypothetical T.P. sample Wt.
		S.A.F. Sample Wt. (Table 5.4)	Hypoth. T.P. Sample Wt.	S.A.F. Sample Wt. (Table 5.4)	Hypoth. T.P. Sample Wt.	S.A.F. Sample Wt. (Table 5.4)	Hypoth. T.P. Sample Wt.	
0.5-1.0μ	$\frac{61.12}{42.96}$	0.1498	0.2138	0.1481	0.2118	0.1292	0.185	0.1422
1.0-2.5μ	$\frac{26.62}{31.48}$	1.202	1.019	1.19	1.05	1.04	0.881	0.969
2.5-5.0μ	$\frac{7.45}{9.4}$	4.47	3.545	4.435	3.518	3.87	3.076	3.378
< 5.0μ			4.79		4.745		4.14	4.55
> 5.0μ	$\frac{4.81}{16.15}$	56.46	16.8	55.92	16.68	48.85	14.58	16.02
Total			21.59		21.425		18.72	20.578
Calculated weight of dust in actual TP slide		22.34		21.08		17.365		20.26
Correction factor		0.9672		1.016		1.081		1.0214

5.5 Discussion and method of arriving at the correlation factor 'k'

As can be seen from Table 5.2 and Fig. 5.1, the thermal precipitator would appear to be more efficient in collecting particles less than 5μ in diameter. The number percentage of dust > 5 μ retained by the gravimetric filter is 16.15, while the T.P. had collected only 4.81% of similar dust under identical experimental conditions.

Table 5.5 is drawn up by correcting the weight percentages in the salicylic acid filter sample to a "hypothetical T.P." weight percentage, by multiplying each weight by the ratio of the appropriate number percentage of the T.P. sample to that of the gravimetric sample. Thus the weight concentration of dust > 5 μ is seen to be reduced from 53.74 mg./cu.m. in the actual salicylic acid sample (Table 5.3) to 16.02 mg./cu.m. in the "hypothetical T.P." sample. (Table 5.5), viz. in the ratio 16.15 : 4.81 .

This anticipated proportional weight concentration of dust in the T.P. dust sample, (Table 5.5), calculated from the salicylic - acid - filter dust sample on the basis of the ratio of size frequencies, compares well with the weight of dust in the actual T.P. slide, calculated on the basis of the number of particles in each size range and the density of the dust (Table 5.4). It can be seen that the proportional weight of dust < 5 μ in the 'hypothetical T.P.' slide, as extrapolated from the weight concentration of actual

FIG.51.SIZE FREQUENCY OF SAMPLED DUST

(Number Percentage)

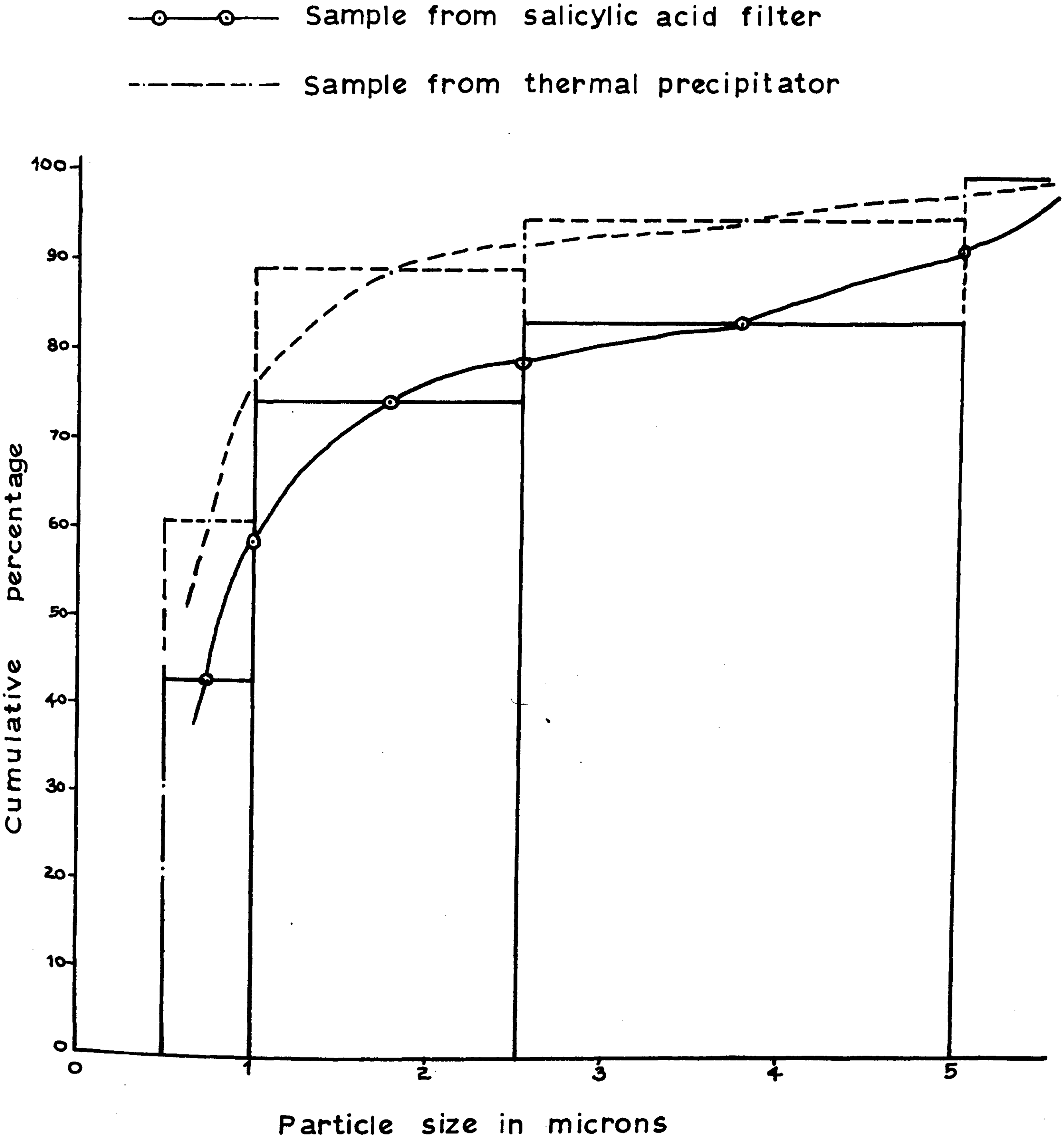

gravimetric sample was 4.55 mg./cu.m., whereas the calculated weight of dust in the actual T.P. slide was 4.09 mg./cu.m. The anticipated value for the weight of actual T.P. dust samples agreed quite well, even in the range > 5 μ, i.e. 16.02 mg./cu.m. as against the actual 16.165 mg./cu.m.

The total weight of dust anticipated in the thermal precipitator, which was based on the actual weight of dust sampled in the gravimetric filter and the proportionate size-frequencies, was 20.578 mg./cu.m., while the calculated weight of dust from the actual T.P. slide was 20.26 mg./cu.m.

The figures in Tables 5.4 and 5.5 suggest that there is not much eccentricity in the particles sampled by the thermal precipitator, since the figures, calculated on their assumption of spherical particles, agree very well with the anticipated weight. The correlation factor is worked out in Table 5.5 to be 1.0214.

There thus appears to be a very good correlation between the dust samples obtained from salicylic acid filter and from the thermal precipitator and by the above method, it is possible to predict the results that will be given by one sampling method, through the use of another.

6. MEASUREMENT OF DROPLET SIZE IN HIGH PRESSURE SPRAYS.

6.1 Introduction.

The purpose of spraying in dust-suppression systems is to disintegrate a continuous jet of liquid into a multitude of small droplets, so that the volume of air swept by the liquid is greatly increased. Generally, sprays drops travelling at high velocity from pressure-atomisers are known to have a higher collection efficiency for dust particles, than when falling at a lower speed under gravity.

A liquid can be atomised merely by discharging it into the atmosphere under high pressure through a small orifice. Such a device is known as a plain atomiser and has quite a small cone angle subtended by the spray cone, since little tangential velocity is imparted to the liquid. In the swirl atomiser type, turbulence is created by forcing the liquid through tangential slots or along helical grooves into a small vortex chamber from which it is discharged into the atmosphere. The spray produced in this way has a larger cone angle and consequently a lower penetrating power. It is usually hollow in the centre, but it may be 'drowned' or converted into a solid - cone spray, by having a small hole drilled through the plug of the swirl - nozzle. The following work was done with such a 'solid - cone' spray nozzle.

Various workers[102] have studied the mechanism which determines droplet size in atomisation, in an attempt to derive a relationship between spray performance and the variables of an injection system. The variables can be considered in terms of : (a) the type of atomiser and the nature of the flow at the orifice; (b) the physical properties of the liquid atomised; and (c) the physical properties of the atmosphere into which the liquid is discharged.

The first group of variables include (i) the diameter of the orifice, which controls the area of jet surface for a given volume of liquid, (ii) the spray cone-angle, which is a measure of the ratio of the tangential and axial components of the jet velocity, and (iii) the discharge velocity of the liquid. The second group of variables include (a) the density, (b) viscosity, and (c) surface tension of the liquid, and the third group, (a) the density and (b) the viscosity of the gaseous medium into which the liquid is discharged.

In the present work the degree of atomisation of water caused by a "solid - cone" nozzle was determined in the pressure range 35.2 - 210.9 Kg./sq.cm. (500 - 3000 p.s.i.g.). All the variables of the injection system except the discharge velocity of the jet were kept constant and the effect of injection pressure on droplet size and spray uniformity was studied.

6.2 The Spraying Unit

A three-throw reciprocating pump was used to obtain high pressure atomisation. An air cushion cylinder was installed in the delivery line of the pump to even out the piston pulses and enable projection of spray into the atmosphere at a constant discharge velocity. The injection pressure was controlled by manipulating the speed of the pump motor and a water by-pass valve. All the connections were made in heavy gauge 3.2 mm. ($^1/8"$) I.D. copper tubing and all joints were welded or brazed.

A detailed drawing of the 'solid-cone spray' nozzle used in the experiments is shown in Fig. 6.1. It was similar to those used in domestic swirl atomisers for spraying insecticides. The nozzle consisted of two parts, a grooved plug screwing into the nozzle cup. Water was discharged through the annular space between them, along the helical groove of the plug and out through the orifice drilled in the outer cup. In the case of the solid cone spray, the liquid was also discharged through a 0.5 mm. diameter hole, which was drilled through the centre of the plug and this prevented the formation of an air-core in the spray.

The diameter of the cup, the depth and the width of the helical groove were measured by means of a travelling microscope. The characteristics of the nozzle are shown in Table 6.1 and the throughput curve for the nozzle is shown in Fig. 6.2.

FIG. 6·1. THE SOLID-CONE SPRAY NOZZLE

(a) The Nozzle Cup

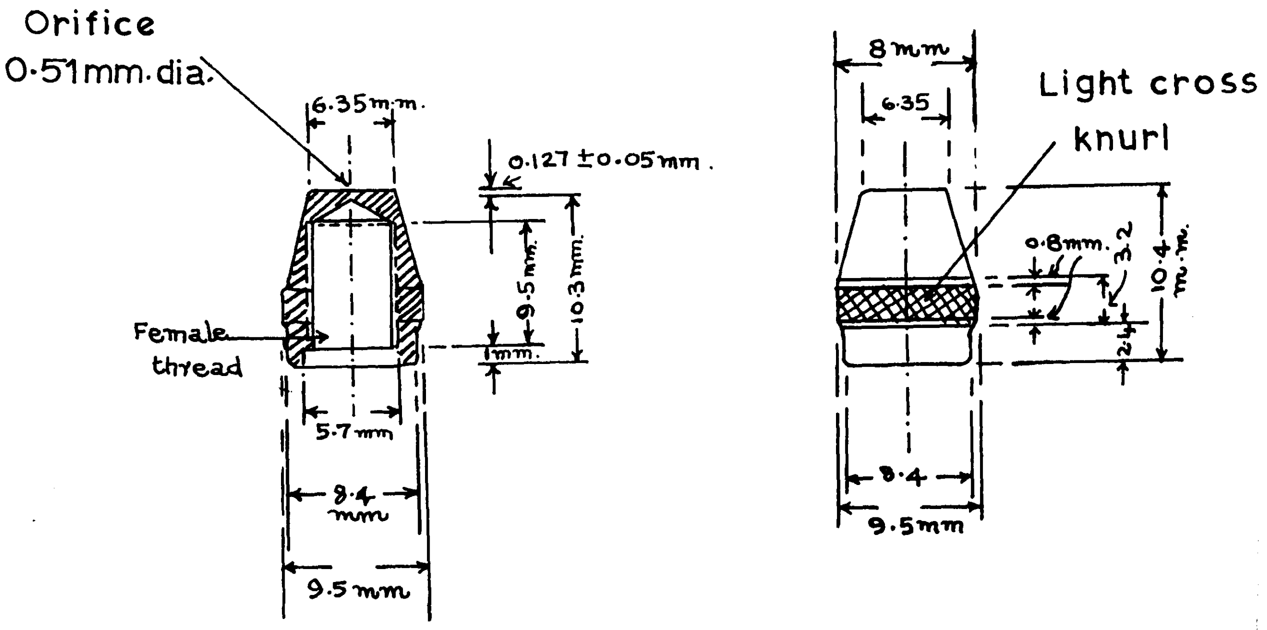

(b) The Grooved Plug

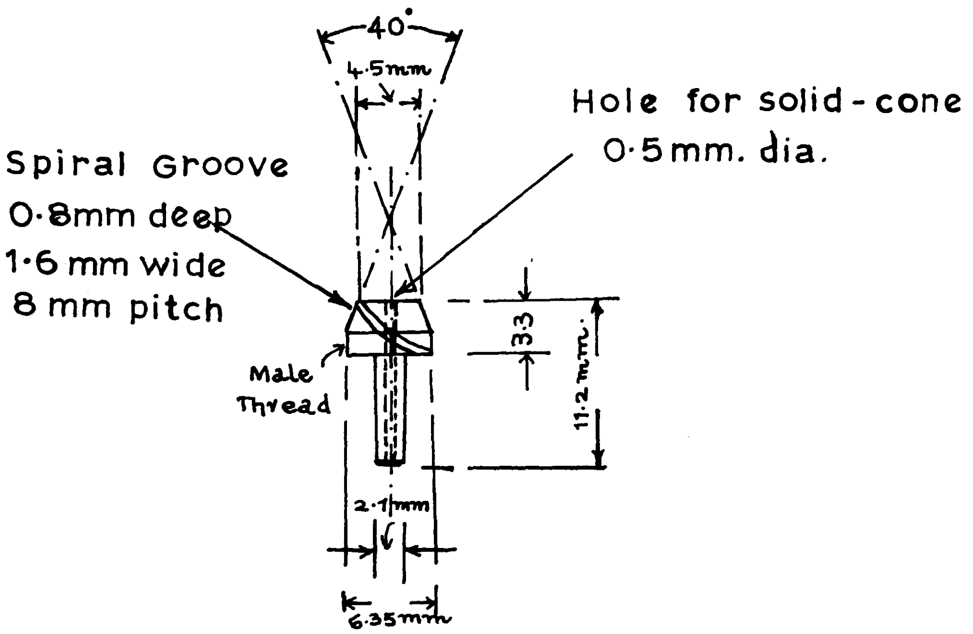

FIG. 6·2. THROUGHPUT CURVE FOR NOZZLE 1

Solid cone spray

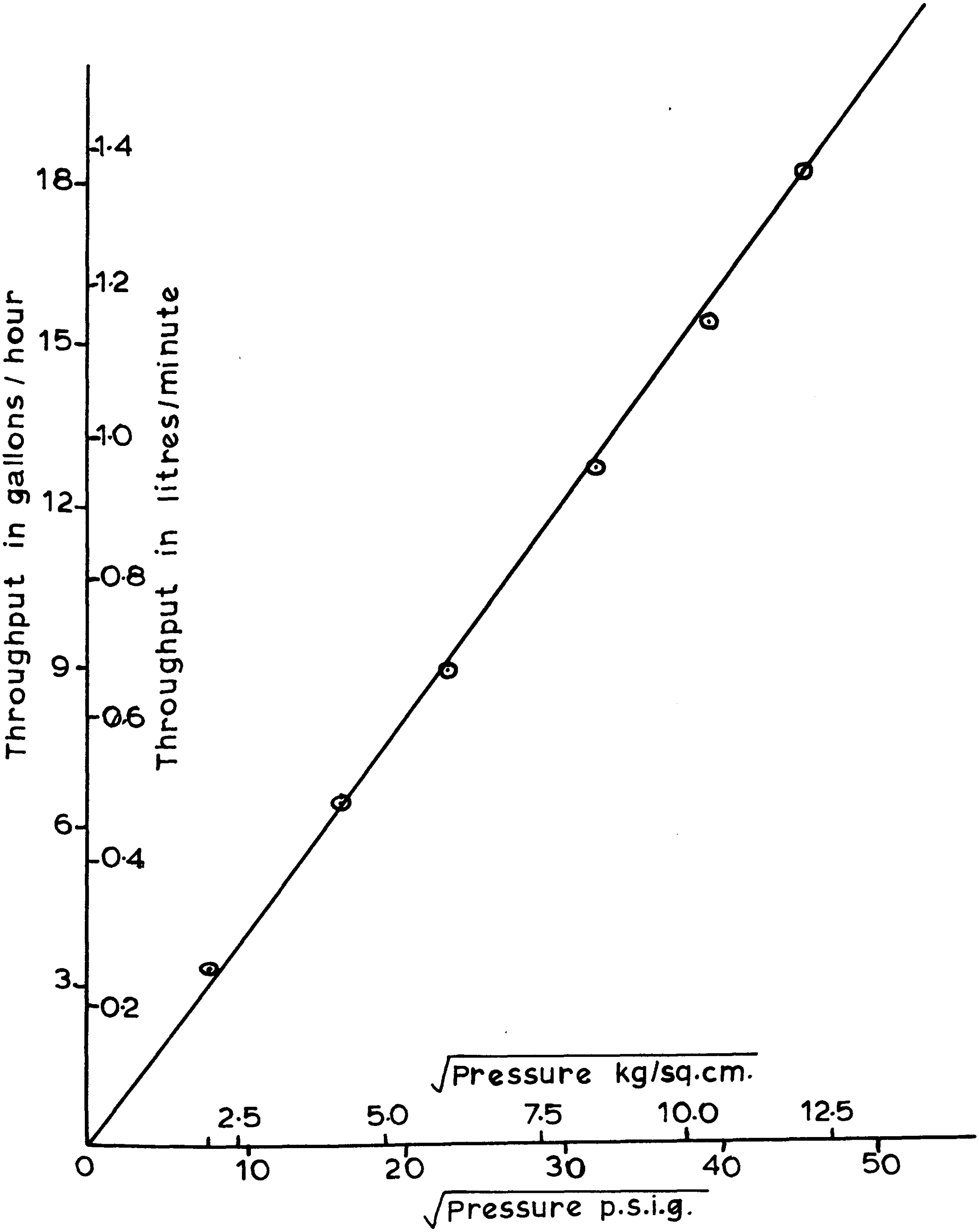

TABLE 6.1

Characteristics of 'solid-cone' spray nozzle.
Diameter of the hole in the plug .. 0.5 mm.

Nozzle Ref. No.	Orifice Diameter Do cms.	Orifice length / Orifice diam.	Flow Number FN	Mean Coefficient of Discharge Cd	Cone Angle
1	0.0510	0.360	0.408	0.68	40°

6.3 Methods of sampling air-borne droplets

The following difficulties are inherent in any attempt to obtain a representative sample of airborne spray droplets

(a) The high discharge velocity of the liquid yet. The curve relating the injection pressure to the discharge velocity of spray is shown in Fig. 6.3 and it can be seen that the discharge velocity is of the order of 5,000 cm./sec., even for an injection pressure of 35.2 Kg./sq.cm. (500 p.s.i.g.).

(b) The large range of sizes involved. The droplet size may vary from < 20 microns to > 200 microns.

(c) The changes in droplet size with time and distance travel due to droplet impact, rupture, and evaporation.

A number of so-called "direct" methods for the determination of the size of spray droplets were investigated at a spray pressure of 8.5 Kg./sq.cm.

The methods considered were :-

(i) Immersion method

(ii) Gravimetric method

(iii) Impression method using:

(a) Magnesium Oxide layer, and

(b) Carbon layer.

In all cases it was found necessary to restrict the number of spray droplets falling on the target in order to prevent overlapping and aggregation. This was achieved by restricting the time of spraying at the target by means of a shield, incorporating a shutter capable of a speed of 0.005 seconds. The spray had a penetration of about 4 metres and was therefore placed horizontally, while the targets were placed horizontally below the nozzle at suitable positions.

(i) Immersion Method:

In this method as described by Hunter[63] the samples were collected in a shallow petri dish (about 5 cm.dia.) containing the immersion liquid. To prevent the droplets falling to the bottom, flattening out and losing their spherical shape, the bottom of the dish was coated with a smooth layer of vaseline free from air bubbles.

Light kerosene (density .. 0.79 gm./ml; viscosity .. 1.32 centipoise) was chosen as the immersion liquid.

About 80 droplets were collected in each sample and they were then measured using an optical microscope with a calibrated eyepiece.

This method has the advantage that the true droplet sizes are observed and measured directly. Its several disadvantages, however, include the fact that there is a time limit imposed on measuring and counting of droplets due to coalescence and evaporation. Moreover, the technique cannot be applied successfully to coarse sprays, because large droplets hitting the liquid surface even at small distances, still possess relatively high momentum, which may cause them to split. On the whole it is a tedious and time consuming process and errors in the judgement of droplet size tend to creep in.

(ii) Gravimetric Method:

The target in this case was a piece of paper of suitable texture, which had previously been weighed. After spraying, it was re-weighed to find the total weight of droplets which had landed on it. The droplets were then counted by means of a microscope in order to find the average droplet weight, from which the average droplet size was calculated.

In practice the best paper was found to be graph paper (quadrille ruled medium cream wove - 24 lb.), as the squares in it facilitated the counting. Addition of a little of Potassium Permanganate to colour the water droplets was also found to facilitate counting. An allowance was made for loss in weight due to evaporation of water from the paper. A series of weighings were carried out to find out the rate of evaporation of water from the drops on the paper and then the plot of weight versus time was extrapolated back to zero time.

The gravimetric method had the advantage that it was not necessary to measure the size of each droplet. Also, after the initial weighing had been done, the actual counting did not need to be hurried. The disadvantage, however, resulting from possible failure to count all the droplets in the sample could not be disregarded.

(iii) Impression Method:

In this method, the target, usually a microscope slide, is covered with a suitable coating, which must be of fine-grain structure, so that even the smallest droplet impressions are distinct.

(a) Magnesium Oxide Layer: The layer was prepared by moving a burning magnesium ribbon to and fro under a microscope slide at a distance, such that the tip of the flame just cleared the glass. A 12 cm. length of 3 mm. ribbon gave a layer of adequate thickness.

When this target was exposed to the spray, the droplets striking the magnesium oxide layer, penetrated it and left a well-defined circular impression, which could be viewed under a microscope by strong transmitted light.

This method had the advantage of permanency and there were no evaporation or coalescence problems to consider. May[103] found from his droplet size measurements of "very nearly homogeneous" sprays from a spinning disk sprayer, that the ratio of true droplet size to impression size is constant at 0.86 for droplets > 20μ for any liquid.

(b) Carbon Layer: A fine layer of carbon was obtained on a microscope slide by holding it over a sooty kerosine flame. The droplet sampling procedure was the same as for the magnesium oxide method.

In this case also the ratio of impression size to the true droplet size has been investigated, and found to be 1.05.(63)

6.4 Average Droplet Size.

The sprays under investigation were very heterogeneous, the droplets varying over a ten-fold range in diameter at higher pressures, and over a fifty-fold range at lower pressures. It was therefore necessary to introduce an average value which would be suitably representative of the number and diameter range of droplets. The arithmetic average or arithmetic mean diameter was used in this work and called the Average Droplet Size. (A.D.S.). This average is simply $\Sigma N D_p / \Sigma N$. The introduction of this A.D.S. is equivalent to the replacement of the actual spray composed of droplets of different sizes, by a fictitious spray in which all the droplets are of the same size equal to the A.D.S.

Initial experiments carried out to find the suitability of the Automatic Particle Counter for droplet sizing by the carbon layer impression method, indicated that although a greater number of impressions might be counted by A.P.C., the value of A.D.S. given by it would be in error, since the upper size limit above 90.5 microns could not be clearly defined and assessed; and there were many droplets whose diameter was greater than 90.5 microns (the maximum size was about 220 μ). The lowest magnification, which could be employed was (x 23) and with that, the z values were 16, 32, 45.3, 64 and 90.5 microns. Hence visual counting was resorted to for droplet size measurement in subsequent experiments.

A Beck Optical Microscope with an eyepiece fitted with a calibrated linear scale was employed for counting and sizing of the droplets. A combination of an ocular (x 6) and either of two objectives (16 mm. and 4 mm.) made possible two magnifications of the order of (x 96) and (x 24).

Employing in turn each of the methods of droplet size measurement, the A.D.S. was obtained for sprays projected by a pressure of 8.5 Kg./sq.cm. by sizing and/or counting 500 droplets or impressions. The results, after applying the necessary correction factors, are shown in Table 6.2.

TABLE 6.2

Average Droplet Size of Sprays.

Comparison of sampling methods.

Sampling Method	A.D.S. microns
Immersion method	127.0
Gravimetric method	95.6
Magnesium Oxide Impression method	164.0
Carbon Layer Impression method	170.0

It is seen that the values of A.D.S. obtained by the immersion and gravimetric methods are much lower than those got from the impression methods. This suggests that the larger droplets hitting the liquid surface in the immersion method might have split, by virtue of their higher momentum, thus causing an increase in the number of smaller droplets and hence a lower A.D.S. In the gravimetric method, of course, failure to count all the droplets could have resulted in a lower A.D.S.

The results from the two methods of impression sampling are found to agree within the limits of experimental error. Of these, the carbon layer method was selected for use in subsequent experiments with high pressure sprays, since it had the important advantages over the magnesium layer method in that the carbon layer was less liable to break up when wet, and it provided a better light contrast between the impressions and the surrounding black medium.

6.5 The effect of Spray Pressure on Droplet Size.

The spray unit, described in 6.2 was used to give a uniform injection pressure at the nozzle, which could be caried over the range 35 - 210 Kg./sq.cm. (500 - 3,000 p.s.i.g.) Since the spray penetration was quite deep (about 4 metres), the spray was operated horizontally and exposed to the target by means of a shutter for a short period of 0.005 seconds.

Each target, consisting of a microscope slide covered with a fine-grained layer of carbon, was exposed to the spray for an equal amount of time in one of the same five positions at distances 0.92, 1.83, 2.75, 3.65 and 4.58 metres from the nozzle and in a position lying about half a metre below and parallel to the axis of the jet.

At each injection pressure, six targets were used and 80 impressions were sized on each target under the optical microscope. The A.D.S. was then obtained at each pressure, by finding the arithmetic mean diameter of these 480 impressions. The results are shown in Table 6.3 and the relationship between the injection pressure, the theoretical discharge velocity of the spray and the A.D.S. is shown in Fig. 6.3.

Degree of atomisation, as characterised by A.D.S. may be seen to increase with increase in the injection pressure. It appears that there is not a significant reduction in A.D.S. at pressures higher than about 150 Kg./sq.cm. (ca. 2000 p.s.i.).

·FIG.6·3.EFFECT OF SPRAY PRESSURE ON DISCHARGE VELOCITY AND A·D·S·

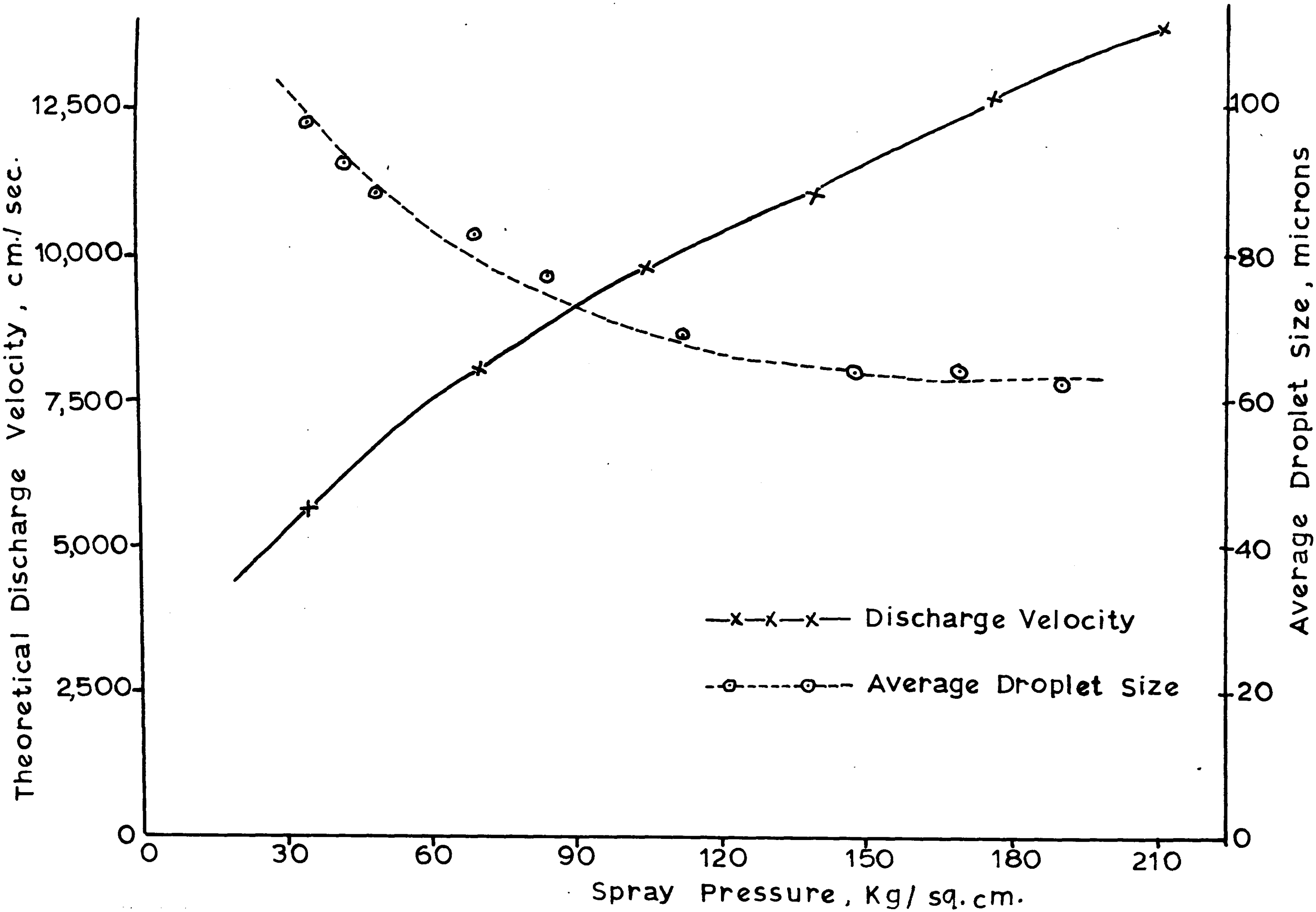

TABLE 6.3

Effect of spray pressure on Discharge Velocity and A.D.S.

Carbon Layer Impression Method - Optical Microscope Sizing

Spray Pressure		Theoretical Discharge Velocity cm./sec.	A.D.S. μ	Log P	Log ADS
p.s.i.g.	P kg/sq.cm				
500	35.15	5,640	98.5	1.5459	1.9934
600	42.18	6,180	93.0	1.6250	1.9685
750	49.56	6,900	88.5	1.7220	1.9469
1000	70.3	7,970	82.9	1.8470	1.9186
1200	84.36	8,740	77.5	1.9261	1.8893
1600	112.48	10,090	68.5	2.051	1.8357
2100	147.63	11,560	64.0	2.1691	1.8060
2400	168.72	12,380	64.4	2.2272	1.8089
2500	175.75	12,620	62.1	2.2448	1.7931
2750	190.16	13,260	63.3	2.2862	1.8014

A relationship connecting Log P and Log A.D.S. is shown in Fig. 6.4, and it is evident that the logarithm of the injection pressure of spray is inversely proportional to the logarithm of A.D.S. The best straight line linking the experimental points has a gradient of (- 0.28). Thus one relationship between the characteristics of spray and and the variables of the injection system can be given as

$$A.D.S. = K.\ P^{-0.28}$$

The relationship data has been discussed in detail in 6.9.

6.6 The effect of spray pressure on Droplet Size Distribution.

A number of tests were made to determine at various pressures the uniformity of the spray and the droplet size distribution. The technique was as already described. Droplet impressions were counted and sized over a wide range. The pressures investigated were 35.15, 70.3 and 147.63 Kg./sq.cm. (500, 1000 and 2100 p.s.i.g.). The results are given in Table 6.4 and the size distribution curves are drawn for the three pressures in Fig. 6.5.

It can be seen from the curves that an increase in injection pressure results in a greater spray uniformity, by the reduction of the number per cent of bigger droplets, particularly sizes > 100 μ. It can also be inferred by comparison with Fig. 6.3, that the improvement in atomisation with increased injection pressures is not only due to the decrease in the size of the smallest droplets, but is also

FIG. 6·4. EFFECT OF SPRAY PRESSURE ON AVERAGE DROPLET SIZE

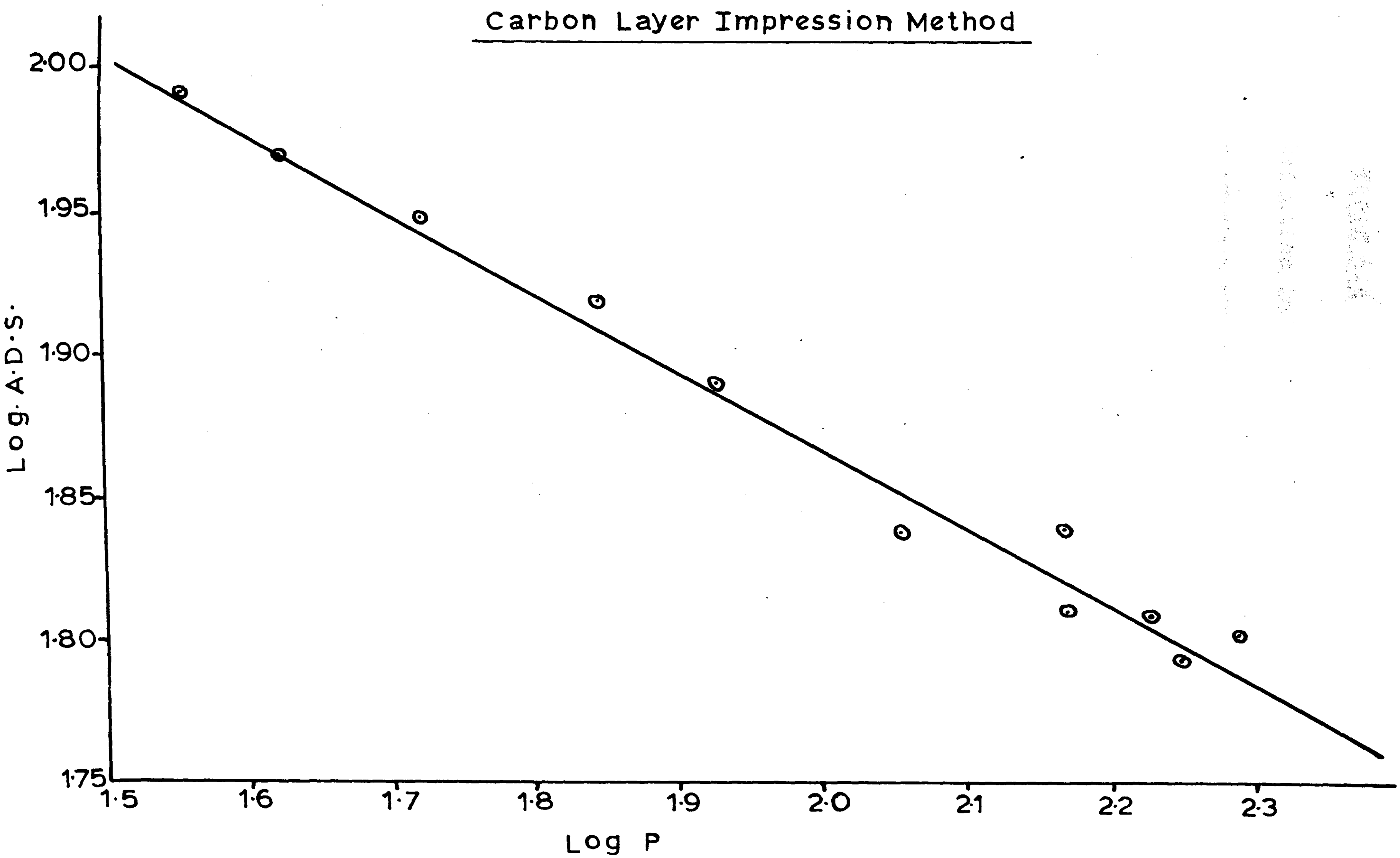

TABLE 6.4

Droplet Size Distribution in High Pressure Sprays.

Pressure p.s.i.g. :- kg./sq.cm:-	500 35.15	1000 70.3	2100 147.63
Mean size of droplet. μ	Percentage by number of each mean size		
14.3	2.7	5.5	6.1
28.6	6.1	10.7	15.0
42.9	7.5	13.1	20.3
57.2	10.5	14.1	18.5
71.5	11.6	12.1	12.7
85.8	12.1	10.3	8.3
100.1	11.5	8.1	6.2
114.4	9.5	5.8	4.3
128.7	7.0	4.5	3.1
143.0	5.3	3.3	2.0
157.3	4.0	3.0	1.2
171.6	3.3	2.6	1.0
185.9	3.1	2.4	0.6
200.2	2.9	2.2	0.3
214.5	2.8	2.1	0.4
$\Sigma N D_p$	9850.1	8284.6	6396.6
ΣN	100	100	100
A.D.S. = $\Sigma ND_p/\Sigma N$	98.5	82.9	64.0

FIG.6·5. DROPLET SIZE DISTRIBUTION IN HIGH-PRESSURE SPRAYS

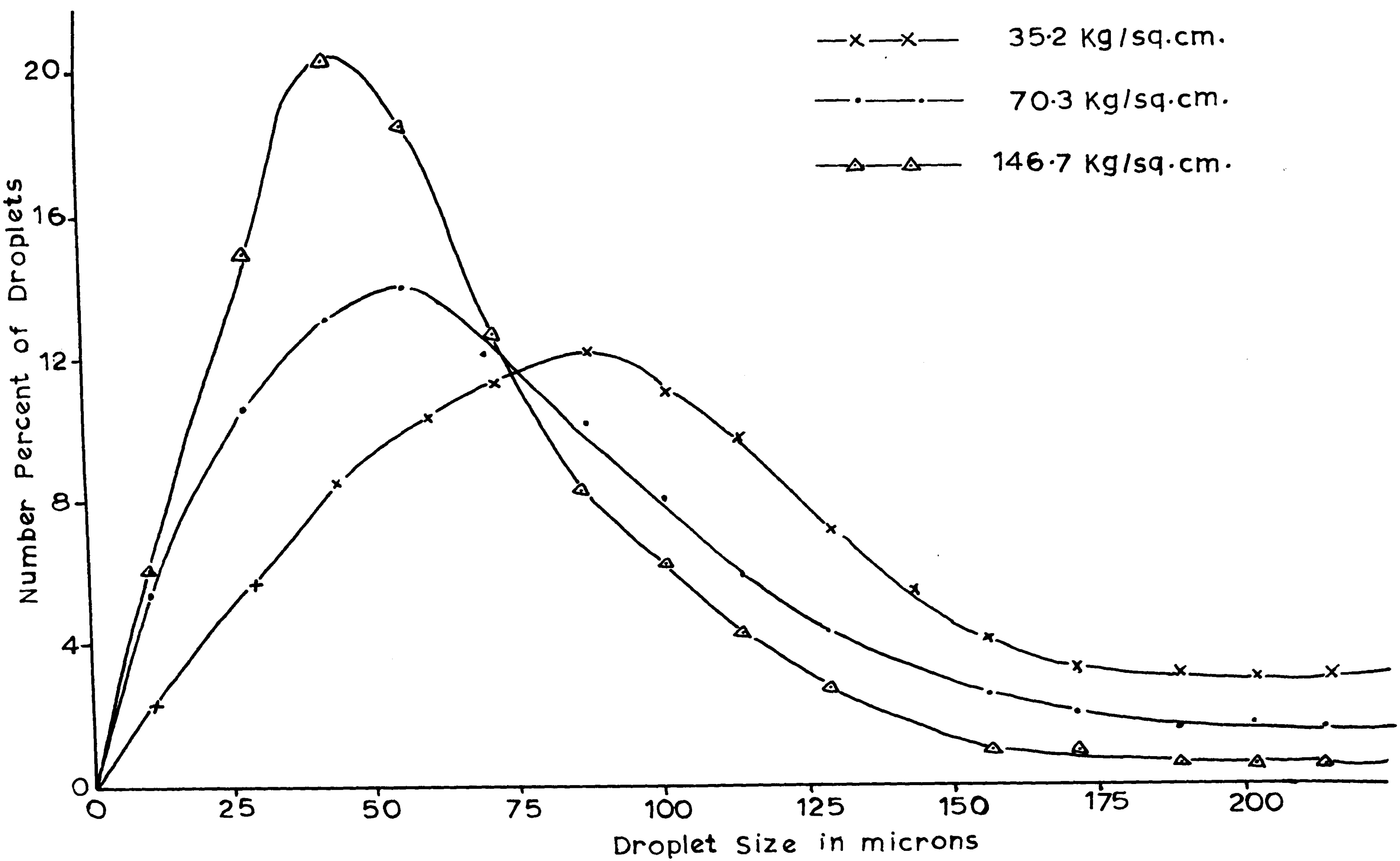

accounted for, by an increase in the number of small droplets (< 100 μ) and by a decrease in the number of large droplets (> 100 μ). The sprays are generally found to be very heterogeneous in character, especially at pressures lower than 70.3 Kg./sq.cm. (1000 p.s.i.). This heterogeneity may be attributable partly to the mode of atomisation in the spray cone.

6.7 The effect of sampling distance on A.D.S.

To determine whether there was a change in the A.D.S. with length of spray path, the spray was operated horizontally at a pressure of 70.3 Kg./sq.cm. (1000 p.s.i.g.) and targets were suitably placed at a number of distances from the nozzle in the path of the flying droplets.

An assessment of A.D.S. at the sampling positions indicated that there was no significant change in the value of A.D.S. along the length of spray up to about 2.7 metres from the nozzle and at a greater distance there was a slight progressive decrease in A.D.S. up to the total penetration of the droplets of 3.7 metres. The mean A.D.S. up to 2.7 metres was about 80 microns. At 3.7 metres the A.D.S. has dropped to about 60 microns. This may be attributed to evaporation of the droplets.

Since when used in the dust tunnel, as explained later, the water droplets traverse a relatively short distance before impacting on the wall it may be considered that the droplets suffer little change in diameter during their dust collecting flight.

6.8 Relationship between energy supplied and energy used up in atomisation.

Hunter[63] calculated the energy supplied for atomisation for spray pressures up to about 5 Kg./sq.cm. and compared it within the minimum energy required for atomisation. The study of the relationship was extended for spray pressures up to 200 Kg./sq.cm. (C.2800 p.s.i.g.) in the present work and Table 6.5 gives the summary of the calculations for energies in high-pressure sprays.

It may be easily seen that with increase of spray pressure, the ratio of minimum energy required for atomisation and the pressure energy supplied decreased. Thus, at higher pressures, most of the pressure energy was converted to the kinetic energy, thus enabling the droplets to acquire more penetrative power.

The relationship between logarithm of Ep and logarithm of Ea may be easily seen to be linear, since Ep is directly proportional to the spray pressure P and Ea is inversely proportional to the average droplet size A.D.S. The graph connecting Log P and Log A.D.S. gave a straight line with a gradient of (- 0.28).

TABLE 6.5

Energy for atomisation

Pressure		Ep	Ea	100 Ea
p.s.i.g.	P kg/sq.cm.	x 10^3 ergs/cm.	x 10^3 ergs/cm.	Ep
500	35.15	34,500	44.40	0.129
600	42.18	41,400	46.98	0.114
750	49.56	51,750	49.42	0.0954
1000	70.3	69,000	52.75	0.0764
1200	84.36	82,800	56.42	0.068
1600	112.48	110,400	63.8	0.0578
2100	147.63	144,900	68.2	0.047
2400	168.72	165,600	67.9	0.041
2500	175.75	172,500	70.4	0.0408
2750	190.16	189,750	69.0	0.0364

6.9 Determination of a functional non-dimensional relationship between the characteristics of the spray system and the Average Droplet Size.

The method of dimensional analysis has been used by several investigators to establish the relationship between the different variables of an injection system and the characteristics of sprays produced. Fraser, Eisenklam and Dombrowski(104) found the following relations between the properties of the liquid and the atomiser to hold :

$$D_p \quad \alpha \left(\frac{\overline{FN} \cdot \gamma}{P . \Theta} \right)^{1/3} \left(\frac{\rho}{\rho_a} \right)^{1/6}$$

If this is applied to a particular orifice and a particular liquid sprayed into air, it reduces to

$$D_p \quad \alpha \quad K1. \, P^{(-1/3)} \quad \text{or} \quad D_p = K.P^{(-0.33)}$$

A general formula of the nature $D_p = K.P^{-n}$ had also been established by many other workers in this field. Needham(105) found the index n to have a value of -0.275, while Joyce(106) obtained a value of -0.35. Both were derived from results of experiments with swirl atomisers and with continuous injection and using the method of substitute liquids for droplet size measurement. Molten wax of viscosity about 2.5 centistokes was used as a substitute liquid.

Muraszew[107] analysed data regarding swirl and plain atomisers discharging different liquids into the atmosphere and found the value of n to be 0.42. He included plain atomisers in the determination of this value.

Another important factor which may account for these slight discrepancies is the variety of methods of droplet measurement. Nevertheless, our relationship would seem to be in agreement with the relationships obtained by the other workers.

$$D_p = K.P^{(-0.28)}$$

The lower value of the index n may also be attributable to the fact that the spray obtained from the solid-cone spray was somewhat coarser than that given by the corresponding hollow-cone spray and hence the A.D.S. is larger.

A relationship could be sought between the average droplet size of the spray and the Reynolds Number of the issuing liquid jet, when spraying water at room temperature.

$$\text{Now Re} = \frac{v_L . D_o . \rho_L}{\eta_L}$$

$$= k1.v_L$$

$$= k2.\ P^{1/2}$$

$$\text{or } P = k3.Re^2 \qquad \ldots\ldots \quad (1)$$

We have already established from experimental results that

$$A.D.S. = k.\ P^{(-0.28)}$$

$$\text{or } P = k_4.(A.D.S.)^{\left(-\frac{1}{0.28}\right)} \qquad \ldots\ldots \quad (2)$$

From (1) and (2)

$$P = k_4(A.D.S.)^{-\frac{1}{0.28}} = k_3 Re^2$$

$$\text{Hence } A.D.S. = K.\ Re^{(-2 \times 0.28)}$$

$$= K.\ Re^{(-0.56)}$$

A graph connecting Logarithm of Re and Logarithm of A.D.S. will give a straight line with a gradient of 0.56.

Thus this non-dimensional relationship

$$A.D.S. = K.\ Re^{(-0.56)}$$

could be very useful in predicting the average size of droplets from sprays.

6.10 Summary.

Droplet size measurements were carried out successfully at high pressure ranges (35.15 - 210 Kg./sq.cm.) by the carbon layer impression method and the following relationship was found to hold good

$$D_p = K.\ P^{(-0.28)}$$

An increase in the injection pressure resulted in a decrease of average droplet size of spray (more pronounced at pressures below 140.6 Kg./sq.cm.) and in an increase of spray uniformity, which was brought about by reduction in the number of larger droplets in the spray.

The Automatic particle Counter was found not very suitable for such measurement, since droplet size ranges over 90.5 could not be definitely grouped.

A functional non-dimensional relationship was established, to enable prediction of average droplet size for a given orifice diameter and a given injection pressure.

$$A.D.S. = K. \; Re^{(-0.56)}$$

7. EFFECT OF HIGH PRESSURE AQUEOUS SPRAYS ON DUST SUPPRESSION.

7.1 Introduction.

Having studied the particle size distribution of the air-borne dust in the tunnel and the droplet size distribution of the high pressure spray, a quantitative determination was made of the effect of the high pressure spray on the knock-down of the air-borne dust particles.

Earlier workers[62] had sprayed air-borne dust with aqueous solutions of several wetting agents and found that at pressures up to 4.4 kg./sq.cm. an improvement in the dust-suppression efficiency did not appear to result. It was necessary to extend the tests to higher pressures, since the results would also indicate whether the lowering of the interfacial tension and increased wettability had any significant effect at such higher spray pressures on the capture of dust particles. Effect of change of throughput of liquid at constant pressure and effect of the relative velocity between the dust particles and the spray droplets, on dust suppression efficiency could be assessed, and it would be helpful to correlate the characteristics of the sprays and the dust suppression efficiency. From a practical point of view, the amount of water required to suppress a known amount of air-borne dust would be of some significance.

7.2 Initial experiments with high pressure water sprays.

The first series of experiments were carried out in the wind-tunnel, in order to compare, for the same spray nozzle, the effectiveness of hollow-cone spraying with that of solid-cone spraying on the dust suppression efficiency. The nozzle chosen was that already used for the droplet-size measurements. (Nozzle No.1 ; see Table 7.6).

The tests were made in the tunnel, with the air velocity set at about 100 cm./sec. and the dust machine adjusted to produce an air-borne dust cloud at a concentration of about 1500 p.p.c.c. Water was sprayed through the hollow-cone spray nozzle 1 upstream on the axis of the tunnel against the dust-laden air stream. The effect of spray pressure on dust suppression efficiency was studied quantitatively at 8 different atomisation pressures. At each pressure, when conditions in the tunnel and the spraying unit became steady, simultaneous dust sampling was done by means of thermal precipitators before and after the spraying unit. The T.P. dust samples were then counted under the Automatic Particle Counter and the results obtained are shown in Table 7.1.

Similar tests were then carried out with the same nozzle and at the same spray pressures, this time using a "drowned" spray (Plug I in Nozzle 1) and the results

Table 7.1

Effect of spray pressure on dust suppression efficiency

Liquid sprayed .. water ; Nozzle used .. Nozzle 1.

Air Velocity .. 100 cm./sec. ; Dust-concentration C. 1500 p.p.c.c.

Spray pressure		HOLLOW-CONE SPRAY					SOLID-CONE SPRAY				
			Dust-concentration p.p.c.c.					Dust concentration p.p.c.c.			
p.s.i.g	P Kg./sq.cm.	Through-put l./min.	Before the spray	Beyond the spray	Difference	Efficiency E%	Through-put l./min.	Before the spray	Beyond the spray	Difference	Efficiency E%
60	4.21	0.170	1400	1229	171	12.18	0.254	1322	1148	174	13.17
250	17.59	0.335	1324	1070	254	19.15	0.504	1247	973	274	22.00
500	35.15	0.474	1514	1128	386	25.48	0.680	1548	1116	432	27.96
1000	70.3	0.655	1455	970	485	33.36	0.964	1748	1083	665	38.02
1500	105.45	0.804	1595	921	674	42.20	1.168	1780	1001	779	43.77
2000	140.6	0.913	1617	833	784	48.50	1.381	1513	702	811	53.58
2500	175.75	1.039	1497	798	699	46.67	1.596	1658	808	850	51.25
3000	210.9	1.121	1402	761	641	45.71	1.709	1517	753	764	50.41

FIG.7·1. EFFECT OF HOLLOW CONE AND SOLID CONE SPRAYS ON DUST SUPPRESSION

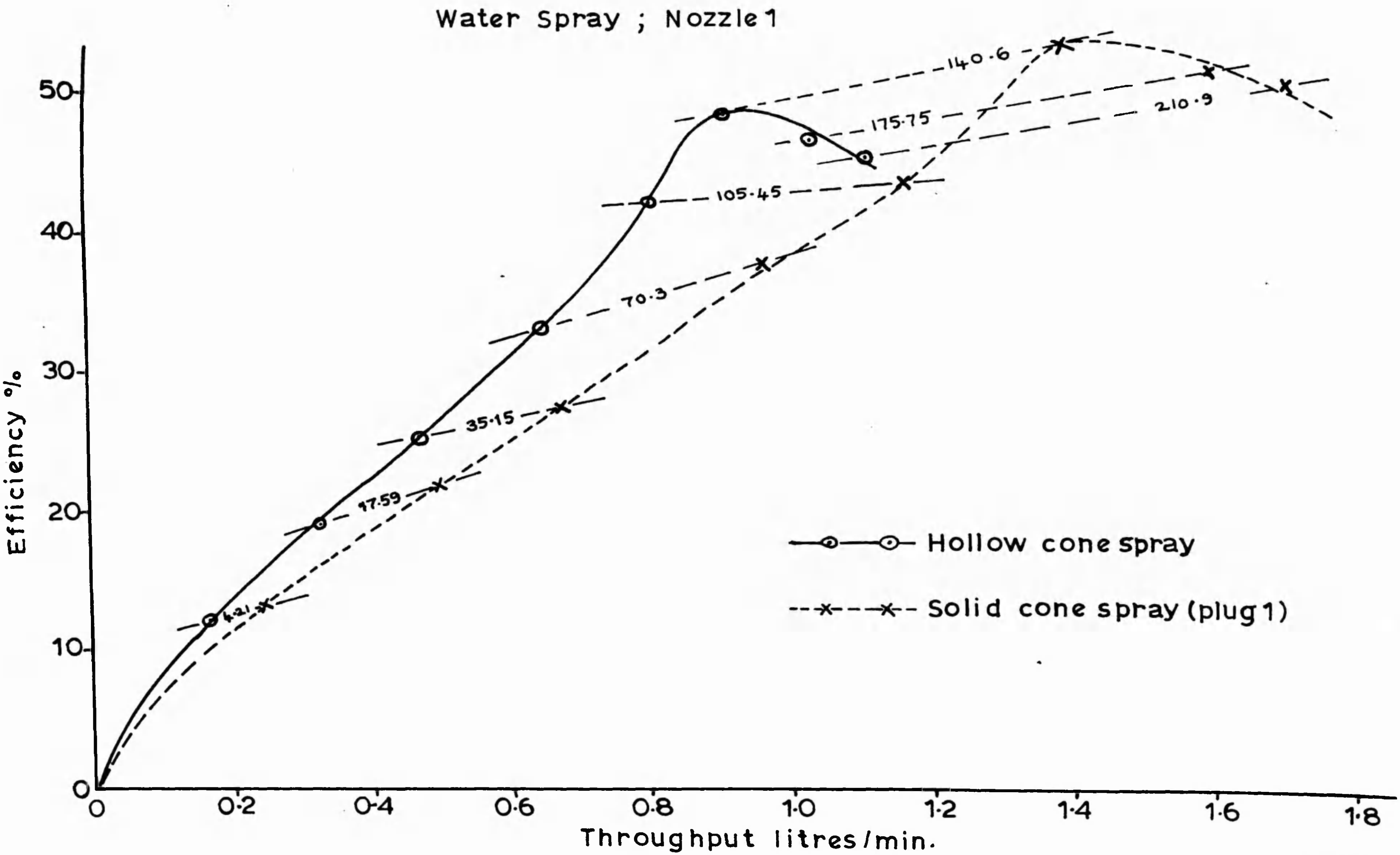

showing again the percentage of dust particles knocked down, are also tabulated in Table 7.1.

It may be seen from the table, that the efficiency of dust suppression increased with increase in spray pressure and, in general, the efficiency was found to be higher for the nozzle employing a drowned spray than for the same nozzle giving a hollow cone spray. Both types of spray showed similar gradation in the increase of dust suppression efficiency with the increase of spray pressure. Also it appeared that the maximum dust suppression was effected at a spray pressure of about 140.6 kg./sq.cm. (200 p.s.i.g.) with both nozzles, the efficiency being 48.5 per cent in the case of the hollow-cone spray and about five per cent higher for the solid-cone spray.

It is important to note that this higher dust suppression efficiency in the case of the solid-cone spray was achieved at the cost of a higher water usage. This is well illustrated in Fig. 7.1, in which the dust suppression efficiency is plotted against throughput for each nozzle. Comparison of the curves enables one to see the effect of throughput at constant pressure on the dust suppression.

It may be seen from Fig. 7.1 that the increase in dust suppression efficiency obtained with solid cone sprays is relatively insignificant, considering the increase in water usage. It is interesting to note that maximum efficiency seems to have been achieved with both hollow cone and solid cone sprays at 140.6 kg./sq.cm., at which spray pressure, the solid cone spray was found to be only five per cent more effective, even though its throughput was about fifty per cent more than that of the hollow cone sprays.

Comparison of dust suppression efficiencies obtained with those found by Deshpande[75] using the same nozzle indicate that although the maximum dust suppression efficiency was achieved at the same spray pressure (140.6 kg./sq.cm.), his values were generally somewhat higher. This may be due to the lower velocity of the dust-laden air-stream, at which he carried out his experiments, (60 cm./sec.), as is evidenced from the author's results on the effect of air velocity on dust suppression, discussed in 7.6 and 7.7.

7.3 Selection of Surface Active Agents.

It is generally agreed that the dust suppressing ability of a spray is dependent not only on the degree of atomisation achieved but also on the "wettability" of the dust to be suppressed.

Hunter[63] showed that above a certain value of applied pressure the degree of atomisation, achieved by using solutions of low surface tension, was similar to that obtained using water. Only at very low pressures (< 2 kg./sq.cm.) was any improvement gained by lowering the liquid surface tension. Glen[62] found that the inclusion of surface active agents in the spray solution did not result in an improvement in the dust suppression efficiency when the liquid was sprayed at pressures lower than 4.3 kg./sq.cm. It was therefore decided to investigate at higher pressures the effect of aqueous solutions of low surface tension on dust suppression. It was already known from Hunter's work that no improvement in atomisation should result, thus any improvement found must be due to increased wetting power.

The molecule of a wetting agent is relatively large and is composed essentially of two parts : one is characterised by its affinity for, and solubility in, water and is called the polar or 'hydrophilic' group; the other part has a strong affinity for oil or water-insoluble organic substances, and, consequently, is known as the non-polar or 'hydrophobic' group. In the wetting agent solution, it is claimed that these molecules orient themselves with the hydrophilic end of the molecules in the interior of the droplet and hydrophobic end at the surface. One wetting agent within each of the three generally recognised classes was selected for the subsequent experiments on dust-suppression. They were as follows[107] :-

(i) <u>Non-ionic Type</u>: Lissapol N, which is an aqueous solution of nonylphenol ethylene oxide condensate, containing a polyethylene glycol chain and is represented by

$$R - O - C_2H_4 (- OC_2H_4 -)_n . OH$$

(ii) <u>Anionic Type</u>: Calsolene Oil HS, which is an aqueous solution of the sodium salt of a highly sulphated oil ; and

(iii) <u>Cationic Type</u>: Fixanol C, which is anhydrous cetyl Pyridinium Bromide

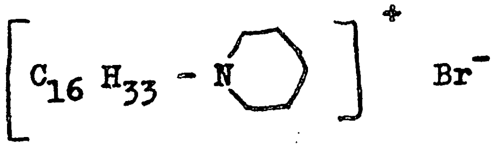

(i) and (ii), which were liquids, were readily soluble in cold water, while (iii), which was a brown soft solid, dissolved more quickly in hot water than in cold.

It was decided to produce sprays from aqueous solutions of these surface active agents, having static surface tension values of 60, 50 and 40 dynes/cm. and compare their dust suppression efficiency with that of pure water. The variation of static surface tension with concentration of a particular surface agent in water was determined by means of the du Nuoy tensiometer.[108]

This instrument measured the static surface tension by finding the force necessary to detach a platinum-iridium ring, 4 cm. in circumference, from the liquid surface. The ring was suspended from an arm fixed to the middle of a torsion wire. The front end of the wire was linked to a vernier pointer which moved over a scale calibrated directly in dynes/cm.

The results showing the lowering of surface tension obtained with increasing concentration of the agent in water are plotted in Fig. 7.2. From these curves the concentrations of the surface active agents to give surface tensions of 60, 50 and 40 dynes/cm. are tabulated in Table 7.2.

Table 7.2 /...

FIG.7·2. EFFECT OF CONCENTRATION OF SURFACE - ACTIVE-AGENTS ON STATIC SURFACE TENSION

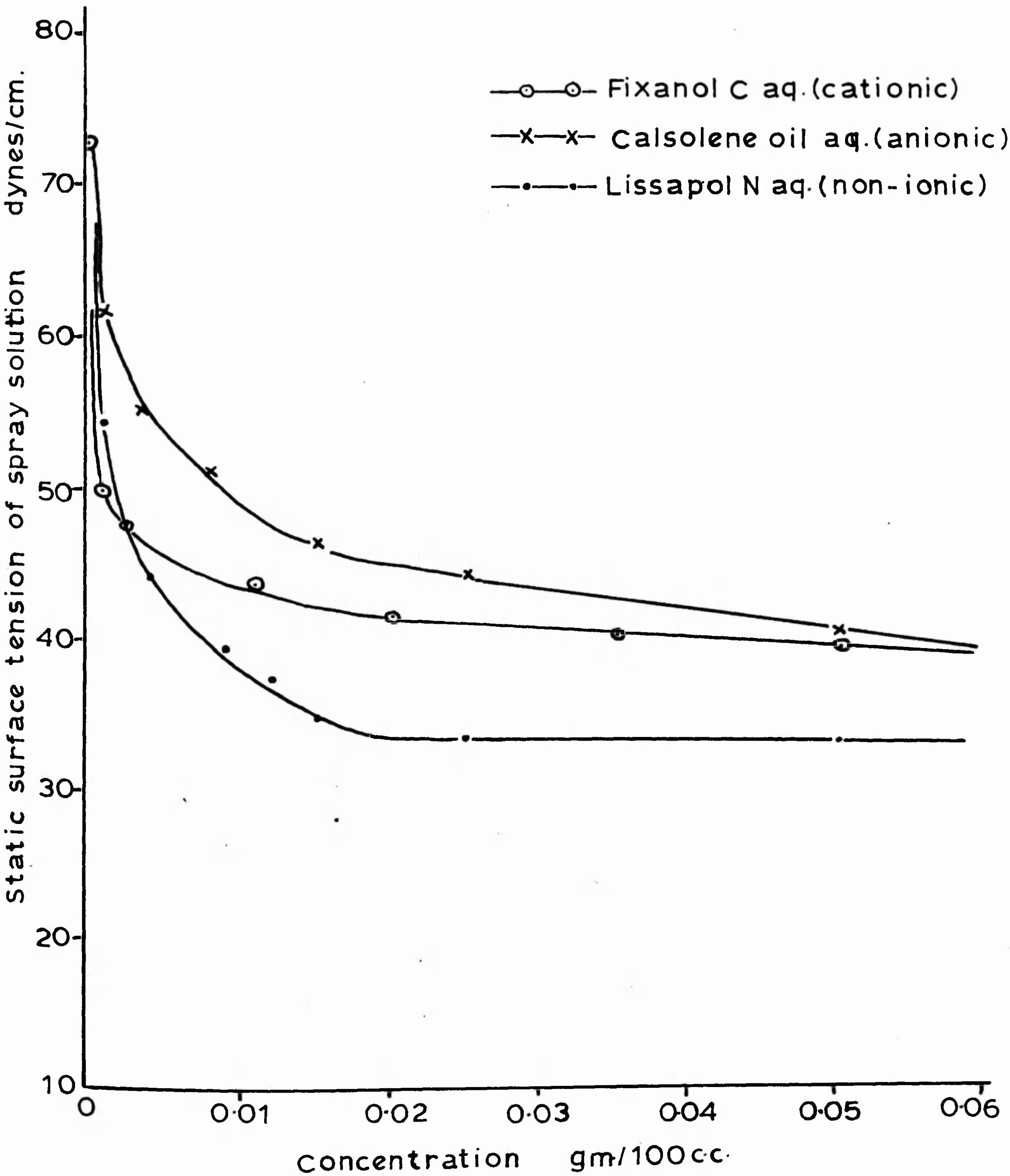

TABLE 7.2

Surface Tension of Surface active agent solutions

Type	Surface active agent solution	Concentration in gms/100 c.c.		
Surface Tension (dynes/cm.):		60	50	40
Non-ionic	Lissapol N	0.00066	0.0016	0.0085
Anionic	Calsolene Oil HS	0.00133	0.0094	0.08
Cationic	Fixanol C	0.0004	0.001	0.0415

It may be seen from the curves that concentrations of surface active agent less than 0.1% by weight, were sufficient to lower the surface tension from 72.8 dynes/cm. to values lower than 40 dynes/cm. It is also worthy of note that the rate of change of surface tension below 40 dynes/cm. with larger addition of the surface active agent was quite small, indicating the economic dis-advantages in using higher concentrations of these surface active agents.

7.4 Tests with surface active agent solutions at higher atomisation pressures.

The effect of spray pressures on the dust suppression efficiency was studied for the surface active agent spray solutions, at the same values of applied pressure as before. Three different concentrations of each type of surface active agent were used to give the required surface tensions of 60, 50 and 40 dynes/cm. respectively to the sprayed solution.

Air velocity in the wind tunnel was set at about 100 cm./sec. and the dust concentration was about 1500 p.p.c.c. The same nozzle (Plug 1 Nozzle 1 solid-cone spray), as used for experiments with water sprays, was used and when conditions were steady in the tunnel and in the spraying unit, dust sampling was carried out before and after the spray by thermal precipitators. The dust samples were then counted under the Automatic Particle Counter and the results obtained are shown in Tables 7.3, 7.4 and 7.5.

It may be seen from the tables that the increase in spray pressure up to 140.6 kg/sq.cm. increases the dust-suppression efficiency, for all the types of solutions sprayed. Comparison with the efficiencies using water (Table 7.1) indicates that efficiency has

Table 7.3

Effect of Spray pressure on dust suppression efficiency

Liquid sprayed .. Lissapol N solution ; Nozzle used : Solid-cone plug 1 - Nozzle 1.

Air Velocity .. 100 cm./sec. ; Dust concentration .. c. 1500 p.p.c.c.

Spray pressure		60 dynes/cm.				50 dynes/cm.				40 dynes/cm.			
p.s.i.g.	P kg/sq.cm	Dust conc$^{n.}$ p.p.c.c. Before the spray	After the spray	Difference	Efficiency E%	Dust conc$^{n.}$ p.p.c.c. Before the spray	After the spray	Difference	Efficiency E%	Dust conc$^{n.}$ p.p.c.c. Before the spray	After the spray	Difference	Efficiency E%
60	4.21	1278	1108	170	13.27	1664	1435	229	13.74	1790	1535	255	14.25
250	17.59	1271	989	282	22.19	1784	1376	408	22.87	1728	1322	406	23.52
500	35.15	1288	921	367	28.52	1373	965	408	29.78	1382	953	429	31.00
1000	70.3	1730	1069	661	38.23	1404	956	448	39.00	1688	1021	667	39.53
1500	105.45	1492	832	660	44.14	1436	781	655	45.73	1474	793	681	46.13
2000	140.6	1352	622	730	54.00	1429	640	789	55.25	1414	622	792	56.00
2500	175.75	1611	770	841	52.20	1578	733	845	53.57	1584	718	866	54.70
3000	210.9	1459	706	733	51.00	1708	802	906	53.05	1324	606	718	54.17

shown signs of increase with lowering of surface tension, the dust suppression efficiency in fact reaches the highest value, when a solution of surface tension of 40 dynes/cm. is sprayed.

Among the types of surface active agents, the cationic type Fixanol C showed higher values of dust suppression efficiency, than the other types. A maximum of 59.05 per cent was obtained for Fixanol C solution of surface tension 40 dynes/cm., as against 53.6 per cent for water at 140.6 kg./sq.cm.

Fixanol C would appear to have better wetting power than the others. This was evidenced also by an experiment made to test the relative wetting power of these surface active agents. A 50 c.c. (40 dynes/cm.) solution in water of each of the three surface active agents was prepared, and placed in a glass graduated cylinder. 50 c.c. of water was placed in a fourth cylinder. 2 gms. of experimental coal dust were placed on each liquid/air interface in the cylinder. It was found that the dust particles were wetted first by and sank first to the bottom of the cylinder of the Fixanol C solution. The relative wetting power, judged in this semi-quantitative way was found to be in the decreasing order of magnitude as follows : Fixanol C, Calsolene oil HS, Lissapol N and water.

In view of the above results it was decided to use Fixanol C solution as the spray liquid in further experiments to determine the effect of change of throughput at constant spray pressure and the effect of change of air velocity at constant spray pressure on dust suppression efficiency.

7.5 Effect of change of throughput at constant pressure on dust suppression efficiency :-

The water throughput of sprays can be varied at constant spray pressure by either of the two ways : (i) by changing the orifice diameter of the nozzle, in the case of hollow-cone sprays, and (ii) by keeping the same orifice diameter and changing the diameter of the hole in the plug, in the case of solid-cone sprays. Both the methods were utilised to find the effect of change of throughput at 140.6 kg./sq.cm. on the dust suppression efficiency.

For hollow-cone spraying, six nozzles were tested, including Nozzle 1 used in previous experiments. For solid-cone spraying, four plugs were tried in Nozzle 1, including plug 1 used for droplet size measurements. The characteristics of the hollow cone nozzles and solid-cone spray plugs are given in Tables 7.6 (i) and (ii) and the throughput curves are shown in Figs. 7.3 and 7.4.

Table 7.6 (i)

Nozzle characteristics for hollow-cone sprays

Nozzle Ref.	Orifice Diameter D_o cm.	Orifice length / Orifice diam.	Flow No. $\overline{FN}$	C_d	Cone angle (θ) degrees
1	0.051	0.36	0.2725	0.452	50
2	0.092	0.149	0.318	0.162	60
3	0.108	0.142	0.374	0.138	70
4	0.131	0.134	0.5745	0.144	75
5	0.154	0.107	0.729	0.133	80
6	0.165	0.077	0.851	0.134	110

Table 7.6 (ii)

Plug characteristics for solid-cone sprays

Nozzle No.1

Plug Ref.	Dia. of hole in plug. cm.	Flow No. $\overline{FN}$	C_d	Cone angle (θ) degrees.
1	0.05	0.408	0.68	40
2	0.062	0.461	0.766	37
3	0.078	0.6	0.995	33
4	0.085	0.636	1.05	18

FIG.7·3. THROUGHPUT OF HOLLOW CONE NOZZLES

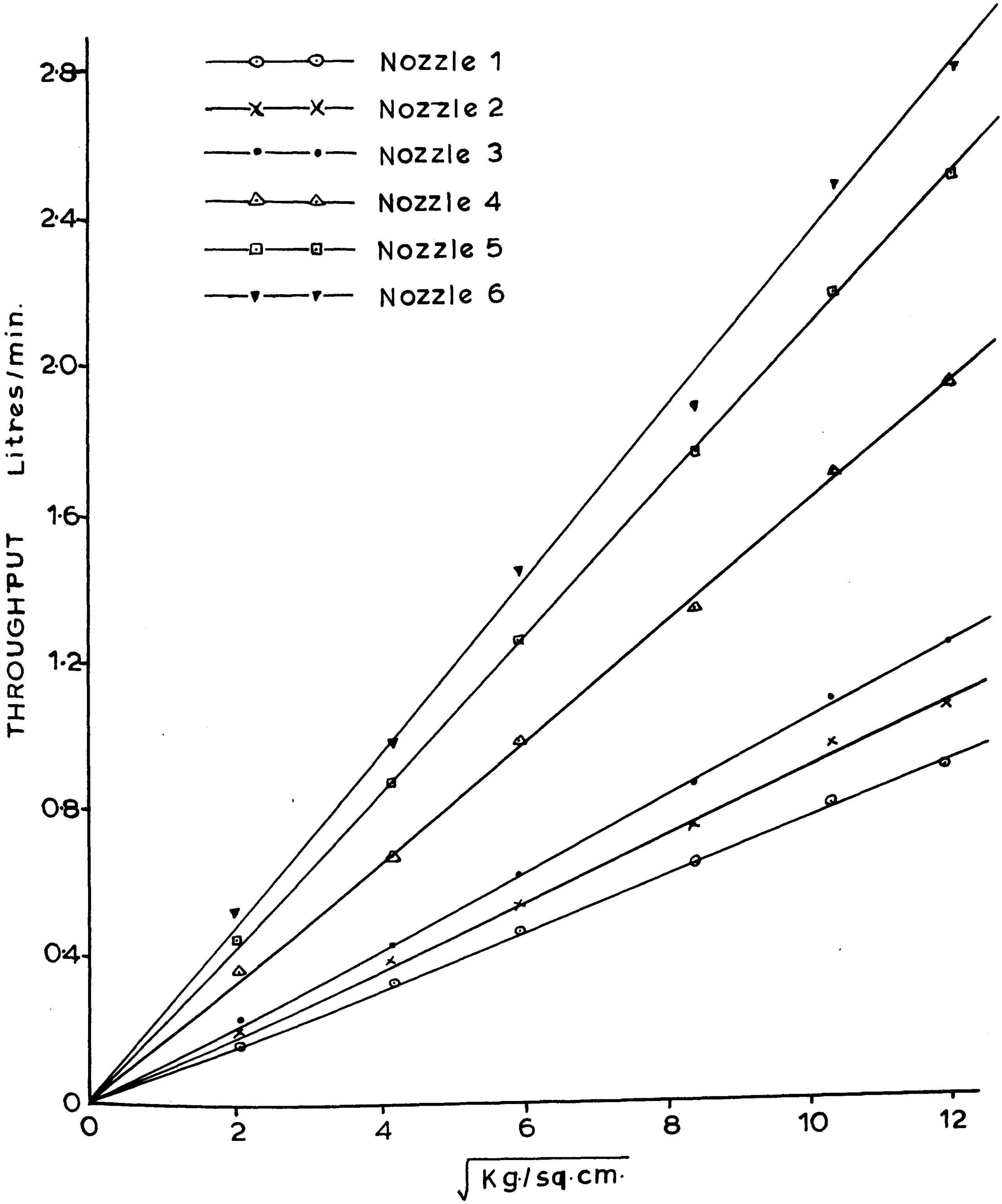

FIG.7·4.THROUGHPUT OF SOLID CONE NOZZLE 1

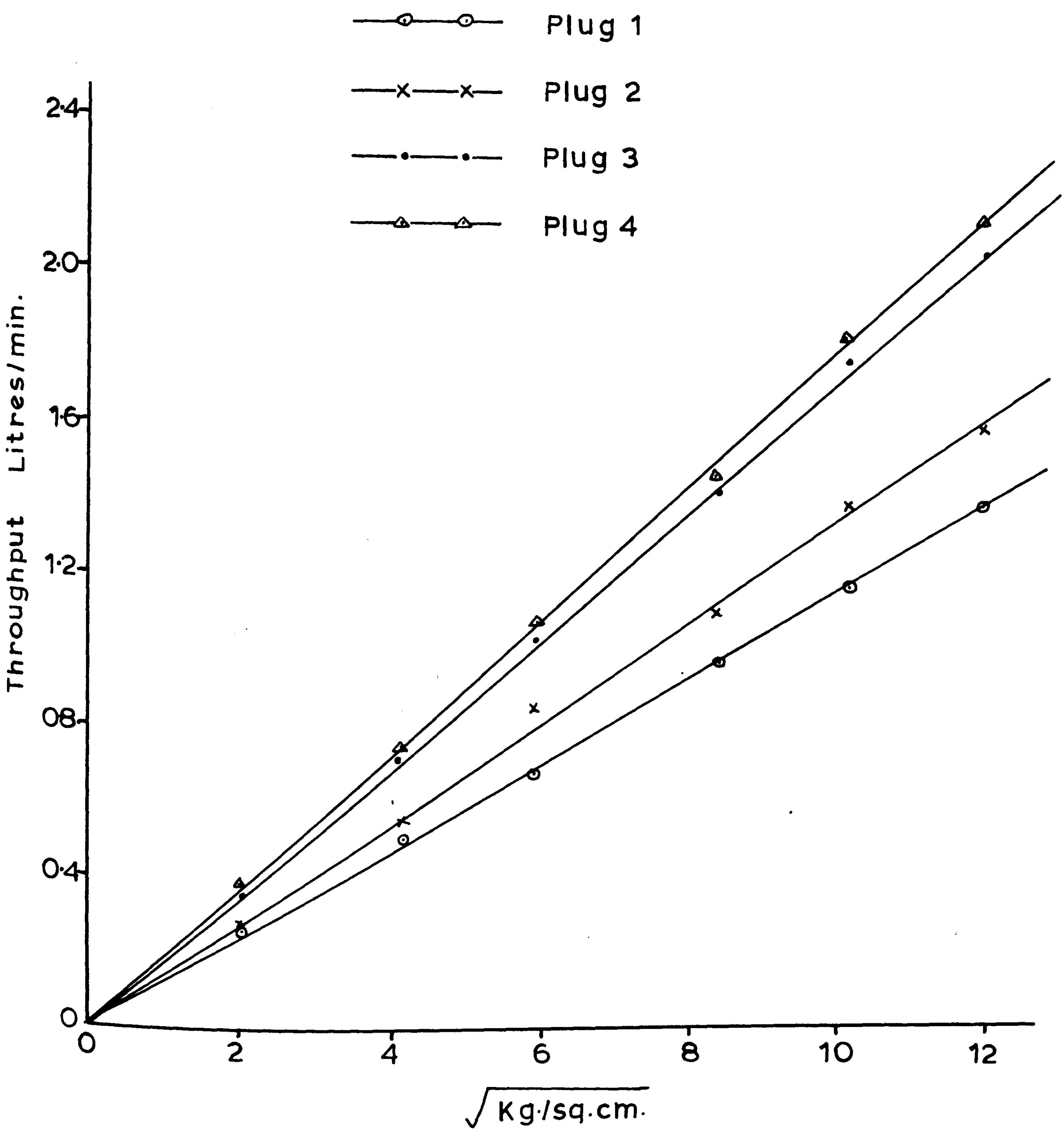

Fixanol C solution of surface tension 40 dynes/cm. was sprayed at a pressure of 140.6 kg./sq.cm., the spray nozzle facing upstream along the axis of the tunnel. The air-velocity in the tunnel was adjusted to 100 cm./sec. and the concentration of dust was set for about 1500 p.p.c.c. When conditions became steady, dust sampling was carried out before and after the spray and dust suppression efficiency calculated from the difference in the dust counts. Four solid cone plugs with Nozzle 1 and six hollow cone spray nozzles were tried in turn at the spray pressure of 140.6 kg./sq.cm. and the results obtained are shown in Tables 7.7 (i) and (ii).

As may be seen from the table, the dust suppression efficiency is found to increase with increase in throughput at constant pressure. The rate of increase in efficiency is seen to be higher for the solid cone sprays than for the hollow cone sprays at the same range of throughput. This may be attributable to the fact that in the former case a significant number of water droplets are initially injected parallel to the axis of the tunnel.

For example, for nearly the same throughput of about 2.85 litres/min. from hollow cone Nozzle 4 and solid cone Nozzle 1 Plug 4, the dust suppression efficiency was higher for the solid cone (67 per cent) than for the hollow cone (60.5 per cent).

Table 7.7 (i)

Effect of change of throughput on dust suppression at a constant spray pressure of 140.6 Kg./sq.cm.

Air Velocity .. 100 cm./sec. ; Liquid sprayed .. Fixanol C solution (40 dynes/cm.)

(i) HOLLOW CONE SPRAYS.

Nozzle Ref.		1	2	3	4	5	6
Throughput l./min.		0.913	1.070	1.242	1.954	2.515	2.812
Dust concentration p.p.c.c.	Before the Spray	1480	1658	1559	1440	1212	1764
	After the Spray	689	733	575	569	437	622
	Difference	791	925	984	871	775	1142
Efficiency E%		53.5	55.8	56.7	60.5	63.9	64.9

-

Table 7.7 (ii)

Effect of change of throughput on dust suppression at almost constant spray pressure.

Air Velocity .. 100 cm./sec ; Liquid sprayed .. Fixanol C solution (40 dynes/cm.)

(ii) Solid-cone sprays. (Nozzle No.1)

Plug Ref.	Spray Pressure		Through-put l./min.	Dust Concentration p.p.c.c.			Efficiency E %
	p.s.i.g	P Kg/sq.cm		Before the Spray	After the Spray	Difference	
1	2000	140.6	1.388	1470	602	868	59.0
2	2000	140.6	2.271	1620	568	1052	65.0
3	1850	130	2.770	1878	448	1310	69.8
4	1750	123	2.882	1682	553	1129	67.0

FIG. 7·5. EFFECT OF CHANGE OF THROUGHPUT ON DUST SUPPRESSION

at constant spray pressure of 140·6 kg/sq·cm.

Air Velocity ... 100 cm/sec ; Liquid sprayed ... Fixanol C aq. (40 dynes/cm.)

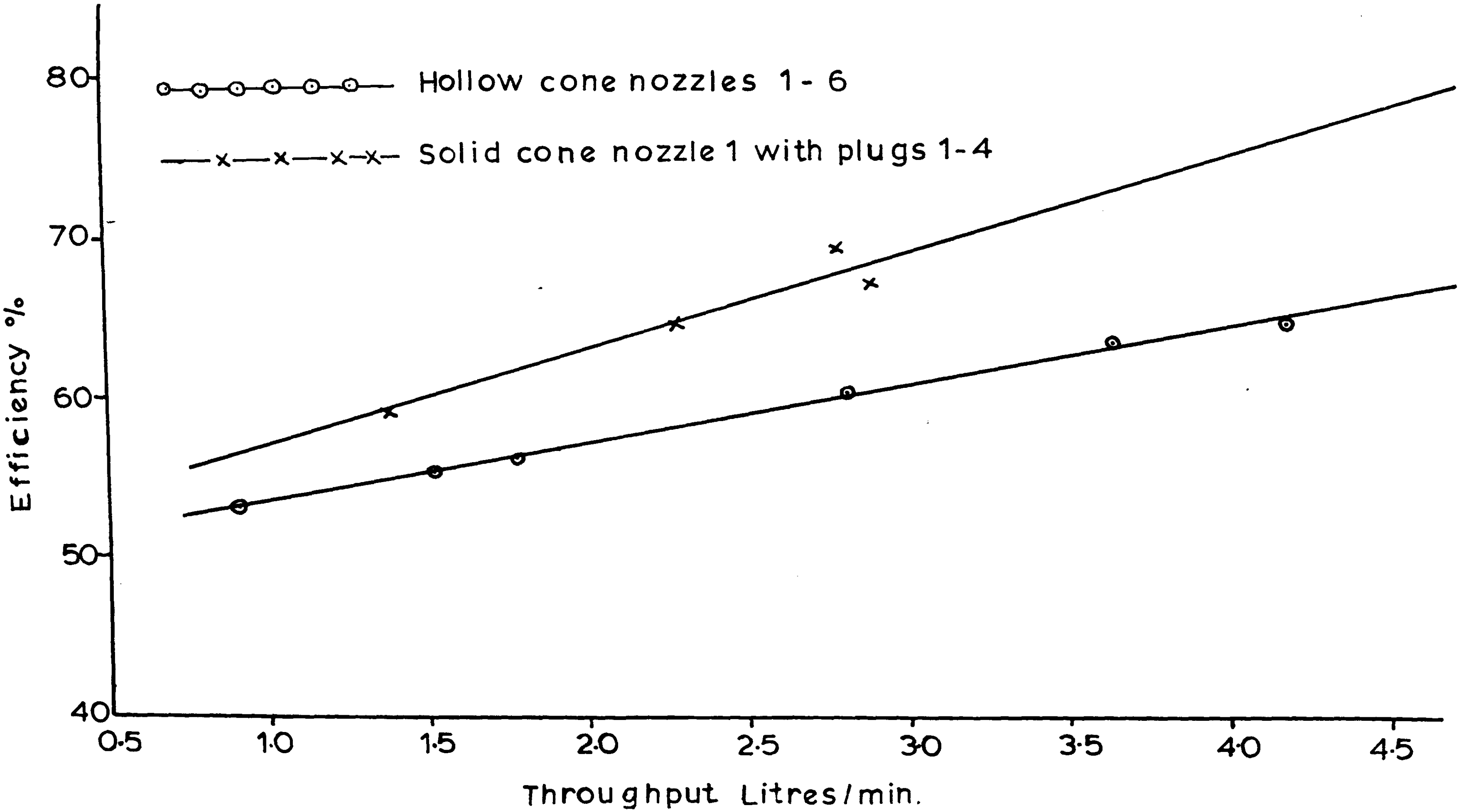

A graph connecting the throughput and the efficiency is shown in Fig. 7.5. There seems to exist a linear relationship between the throughput and the efficiency, for any particular nozzle and nature of spray. On comparison with Fig. 7.1, it is evident that the rate of increase in dust suppression efficiency is more pronounced with increasing spray pressures up to 140.6 kg/sq.cm. using the smaller nozzles, than with higher throughputs at 140.6 kg./sq.cm. obtained with bigger nozzles. It appears therefore that the spray pressure playes a more important part in dust suppression, than the amount of water sprayed. This is discussed in more detail in 7.7.

7.6 Effect of change of air velocity at constant spray pressure.

Theoretically, an increase in the velocity of the air in the tunnel would increase the relative velocity between the dust particle, which is assumed to follow the velocity and flow pattern of air, and the liquid droplet issuing against the dust laden air stream from the spray nozzle. To investigate, by quantitative measurement, the effect of change of air velocity at constant spray pressure, the following experiment was carried out.

The velocity of air in the tunnel was first set at 50 cm./sec. and the dust machine was adjusted to give

Table 7.8

Effect of air velocity on dust suppression

Hollow Cone Nozzle No.2 ; Spray pressure .. 140.6 kg./sq.cm.

Liquid sprayed .. Fixanol C solution (40 dynes/cm.)

Air Velocuty cm./sec.		50	100	175	250	375	500
Dust concentration p.p.c.c.	Before the spray	1348	1878	1266	1628	1708	1378
	After the spray	506	846	726	1005	1341	1252
	Difference	842	1032	540	623	367	126
Efficiency E%		62.5	55.0	42.3	38.3	21.5	9.14

FIG.7·6.EFFECT OF AIR VELOCITY ON DUST SUPPRESSION

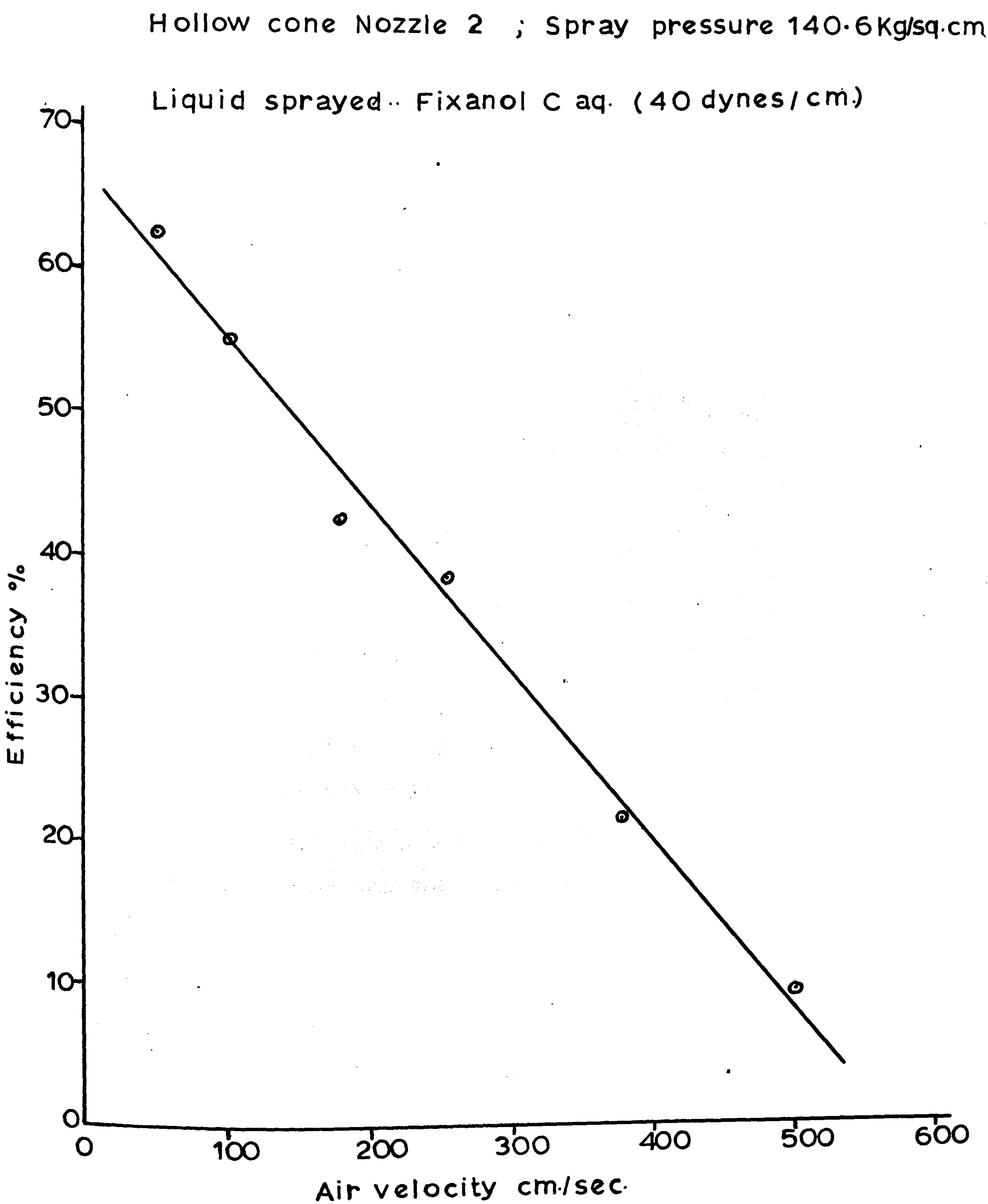

a dust concentration of about 1500 p.p.c.c. Fixanol C solution of surface tension 40 dynes/cm. was sprayed at a pressure of 140.6 kg./sq.cm. through Nozzle No. 2 (Hollow Cone), against the air stream. After steady conditions were reahced, dust sampling was carried out before and after the spray and from the dust counts obtained from the Automatic Particle Counter, the dust suppression efficiency was calculated. The test was repeated under the same conditions, but by changing the air velocity in turn to 100, 175, 250, 375 and 500 cm./sec. The results obtained are shown in Table 7.8.

From the results, it is surprising to note that the efficiency decreased rapidly, with increase in air velocity. The dust suppression efficiency dropped from 62.5 per cent at 50 cm./sec. to about 10 per cent at 500 cm./sec.

In practice with spraying in the tunnel, it was found on inspection that the spray cloud was considerably deformed and the spray cone reduced in size at higher air velocities. Thus the initial penetration of the greater number of the droplets was reduced and a proportion of the dusty air could bypass the spray. This effect is illustrated in Fig. 7.10.

The graph connecting the dust-suppression efficiency and the air velocity in the tunnel seems to indicate a linear relationship (Fig. 7.6) and it appears that there is a drop of efficiency of about 1.8 per cent for every 10 cm./sec. increase of air velocity.

7.7 Discussion of results.

It was found in general, that these small high pressure sprays were able to remove a considerable proportion of < 10 μ air-borne coal dust from the air in the wind tunnel (up to a maximum of about 70 per cent, depending upon the spray liquid, nature of spray, spray nozzle and spray pressure employed and the velocity of air-borne dust in the tunnel). The results are best considered under their appropriate sub-section headings.

Effect of spray pressure : (Tables 7.1, 7.3, 7.4 and 7.5; Fig. 7.1)

As might be expected, increase in spray pressure generally causes an increase in dust suppression efficiency. Irrespective of the solution sprayed, all the experiments showed a gradual increase in the dust suppression efficiency, with increase of spray pressure up to 140.6 kg/sq.cm. The maximum efficiency seems to have been reached at a spray pressure of about 140 kg/sq.cm. and there appears to be a slight reduction in the efficiency beyond this spray pressure.

When all the results for the Tables 2 and 5(c) are plotted together, an approximate proportionality appears to exist between the dust suppression efficiency of the particular nozzle and the logarithm of the liquid spray pressure (Fig. 7.7). It is evident from the tables and graph that there is not much to be gained, in increasing the spray pressure above 140.6 kg./sq.cm. It was already shown in Chapter 6.8, that the amount of energy required to produce the spray at higher pressures is very high and hence, it is not commensurate with the return in dust suppression. It is also worthy of note, that increase in the spray pressure is accompanied by an increase in the throughput of the spray and hence reduces the dust-water ratio. As is shown later, there appears to be an optimum spray pressure of about 140 kg./sq.cm., beyond which the additional throughput of sprayed liquid does not contribute towards any significant increase in dust suppression efficiency. On the contrary, it only helps to reduce the dust-water ratio.

The spray variables that are dependent on the pressure at which the spray liquid is applied to a given orifice are :-

(i) the angle which the spray cone subtends at the orifice (the cone angle) ;

FIG.7·7. EFFECT OF SPRAY PRESSURE ON DUST SUPPRESSION EFFICIENCY

Nozzle 1

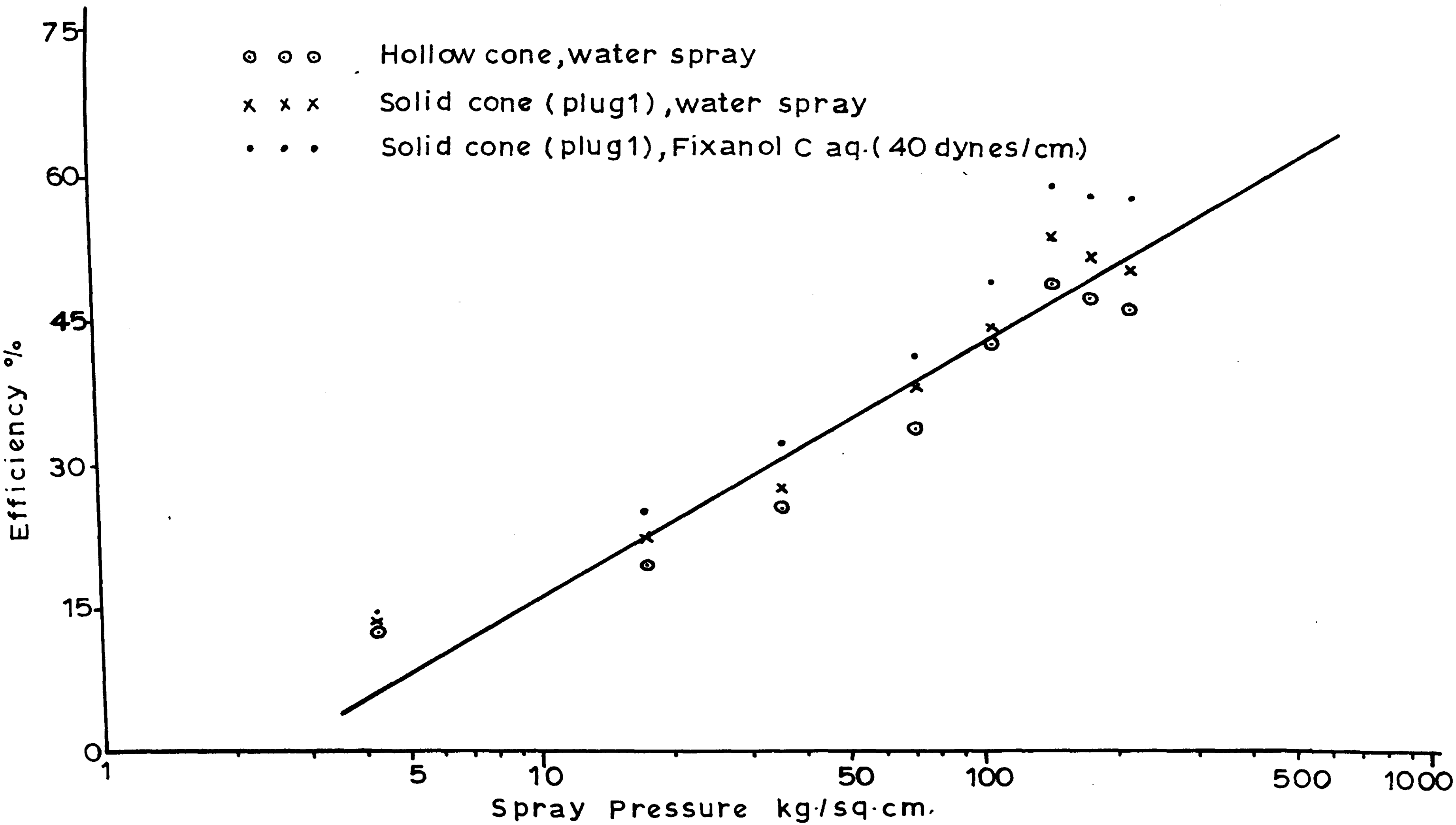

(ii) the liquid flow-rate, which increases as the square root of the spray pressure;

(iii) the initial velocity and penetration of the spray droplet. The latter will, in practical cases, depend on the velocity of the oncoming dust-laden air stream, and

(iv) the average droplet size produced by the spray.

It has been shown[62] that for the nozzles employed in these tests, the cone is fully developed at a pressure of about 100 p.s.i.g. and the cone angle does not change greatly at higher pressures. In practice, moreover, a certain amount of deformation of the spray cone takes place, especially at higher air velocities and this makes the difference between the cone angles of the nozzles employed, insignificant for all practical purposes.

If the increased dust suppression efficiency at increased spray pressures were merely due to the increased flow rate and consequently to the rate of increase of liquid droplets ejecting out of the spray nozzle, one might expect the dust suppression efficiency to vary approximately as the square root of the applied spray pressure. In Fig. 7.8, the logarithms of all pressure variation results for nozzle 1 (hollow cone and solid cone water sprays, and

FIG. 7·8. EFFECT OF SPRAY PRESSURE ON EFFICIENCY

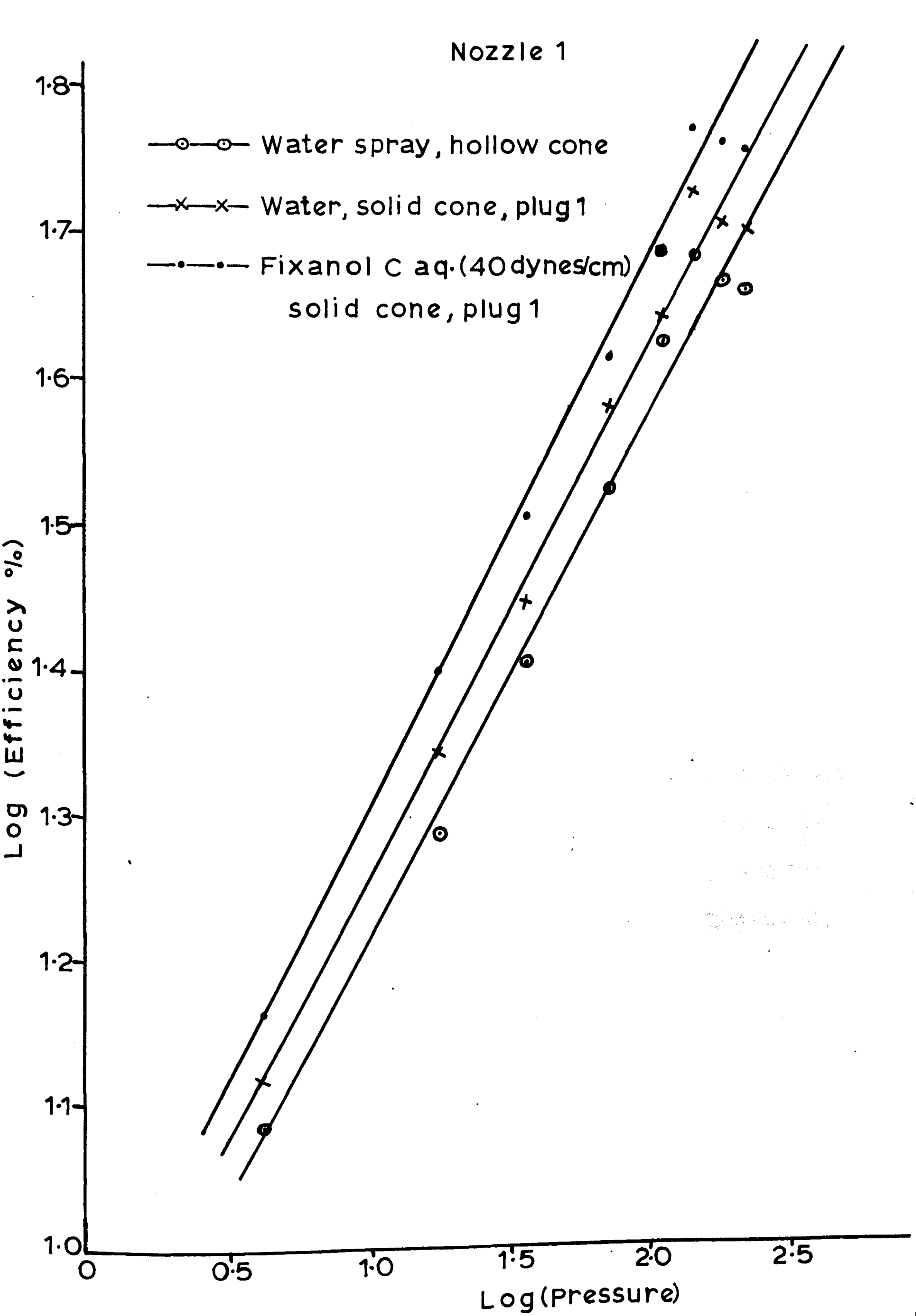

Fixanol C sprays) are plotted against the logarithm of the dust suppression efficiency and in all the cases straight lines with gradients of 0.385 can be drawn through the points, thus giving a general relationship between the spray pressure and dust suppression efficiency.

$$E \quad \alpha \quad (P)^{0.385} \qquad \ldots\ldots \; (1)$$

which is somewhat lower than the efficiency obtainable from the relationship $E \, \alpha \, P^{0.5}$.

The increased initial velocity and penetration at higher spray pressures should have a positive influence on the dust suppressing efficiency. But however, since the spray nozzle is placed facing the dust-laden air stream, the liquid droplet emerging from the nozzle will decelerate rapidly to zero velocity and, if it has not reached the tunnel wall, will then be accelerated down-stream with the air. Thus only for quite a small proportion of its life, will it have a velocity controlled by the spray pressure.

Again, from our experiments described in Chapter 6, it was shown that the logarithm of the average droplet size in high pressure sprays is inversely proportional to the logarithm of the spray pressure. viz.

$$A.D.S. = k. \, (P)^{-0.28}$$

If one may take, as a measure of the number of liquid droplets produced per minute, the ratio

Volume flow rate/Average Droplet Size

and since volume flow rate α $P^{(0.5)}$

and average droplet size α $P^{(-0.28)}$

then Number of droplets per minute $= k.\ P^{(0.5+0.28)}$

$= k.\ P^{(0.78)}$

Thus if the dust suppression efficiency were dependent on the number of droplets produced per minute, it should increase as the $(0.78)^{th}$ power of the spray pressure. This is quite high in comparison with the experimental results which show that the efficiency increases only as the $(0.385)^{th}$ power of the Spray pressure (Fig. 7.8).

This tends to confirm the already well recognised fact that "number of droplets" alone is not the controlling factor in dust suppression. Not all droplets have an equal chance of capturing a dust particle.

The smaller the droplet size, the more difficult does it become for it to make a successful capture of a dust particle owing to the nature of the flow pattern of the air around the droplet. It has been shown in Chapter 6, that a decrease in the average droplet size at higher spray pressures was brought about by an increase in the number of smaller sized droplets rather than by a decrease in the smallest size. This would mean that at higher spray pressures, the number of smaller size droplets being greater, chances of collision and consequent capture of the dust particles by these droplets is less, and this could explain the lower dust suppression efficiency obtained. This subject will be dealt with more fully later in this thesis. It is of interest to note that it has been suggested[109] that there may be a decrease in the efficiency of atomisation of spray nozzles at very high pressures due to pressure deformation of the orifice.

Effect of solid-cone spraying :(7.2; Table 7.1; Fig.7.1)

Comparison is made between hollow-cone spraying and solid-cone spraying in Table 7.1 and Fig. 7.1. Using the same nozzle (No. 1) and spraying water, it is seen that the dust suppression efficiency for the solid-cone spray shows nearly the same gradation, as that for the hollow cone spray, and a maximum efficiency of 53.58 per cent was recorded for solid-cone spray at the spray pressure of 140.6 kg./sq.cm., while it was 48.5 for the hollow cone spray.

The graphs showing the relationship between the logarithm of spray-pressure and the logarithm of efficiency are shown in Fig. 7.8 and it may be seen that the nature of spraying devices does not significantly affect the relationship, even though the efficiency values for the solid cone sprays are higher than those of hollow cone sprays.

It was to be expected that the solid-cone spray would give a better dust suppression efficiency, because for the same spray pressure, the solid cone spray nozzle had a throughput about 1.5 times that of the hollow cone nozzle. The increase, however, in dust suppression efficiency with the solid-cone spray, does not greatly justify the large increase of throughput of the spray. Whereas the increase in throughput is about 50%, the increase in dust suppression efficiency is only of the order of 10 per cent of the efficiency obtained by hollow-cone sprays. As may also be seen from the dust-water ratios calculated later in this chapter, the number of particles of dust knocked down per c.c. of liquid sprayed is actually lower for the solid-cone spray, than for the hollow-cone spray. (Figs. 7.12 and 7.13).

Effect of surface active agents :(7.4; Tables 7.3,7.4,7.5)

The results shown in Tables 7.3, 7.4 and 7.5 seem to indicate that in general the wetting agents give a small increase in dust suppression efficiency. The increase in efficiency with spray pressure, seems to show a similar gradation to that of pure water sprays and the maximum efficiency was again reached at about 140.6 kg./sq.cm.

Of the three surface active agents, the cationic type - Fixanol C - gave better results than the other two. At the spray pressure of 140.6 kg./sq.cm., however, the dust suppression obtained by using Fixanol C solution of surface tension 40 dynes/cm., was only about 6 per cent higher than that obtained by using water alone. With calsolene oil HS, the increase in dust suppression was only about 4 per cent and with Lissapol N about 3 per cent. It would seem that the use of surface active agents is not very advantageous from an economic point of view.

These results suggest that measurement of the air-solution surface tension alone does not indicate the utility of a wetting agent. Adhesion tension is necessary to cause the solution to adhere to the dust particles. Coal has a high adsorptive power for air and hence to wet extremely fine particles of coal dust, the adhesion tension for the sprayed liquid must be strong enough to work through the film of air on the surface of the coal dust. The wetting power of the spray solution is enhanced, if the power of the wetting agent in question for contact wetting,

FIG.7·9. EFFECT OF SURFACE TENSION OF SPRAYED LIQUID ON DUST SUPPRESSION

Nozzle 1 solid cone (plug 1); Spray pressure...140·6 kg/sqcm

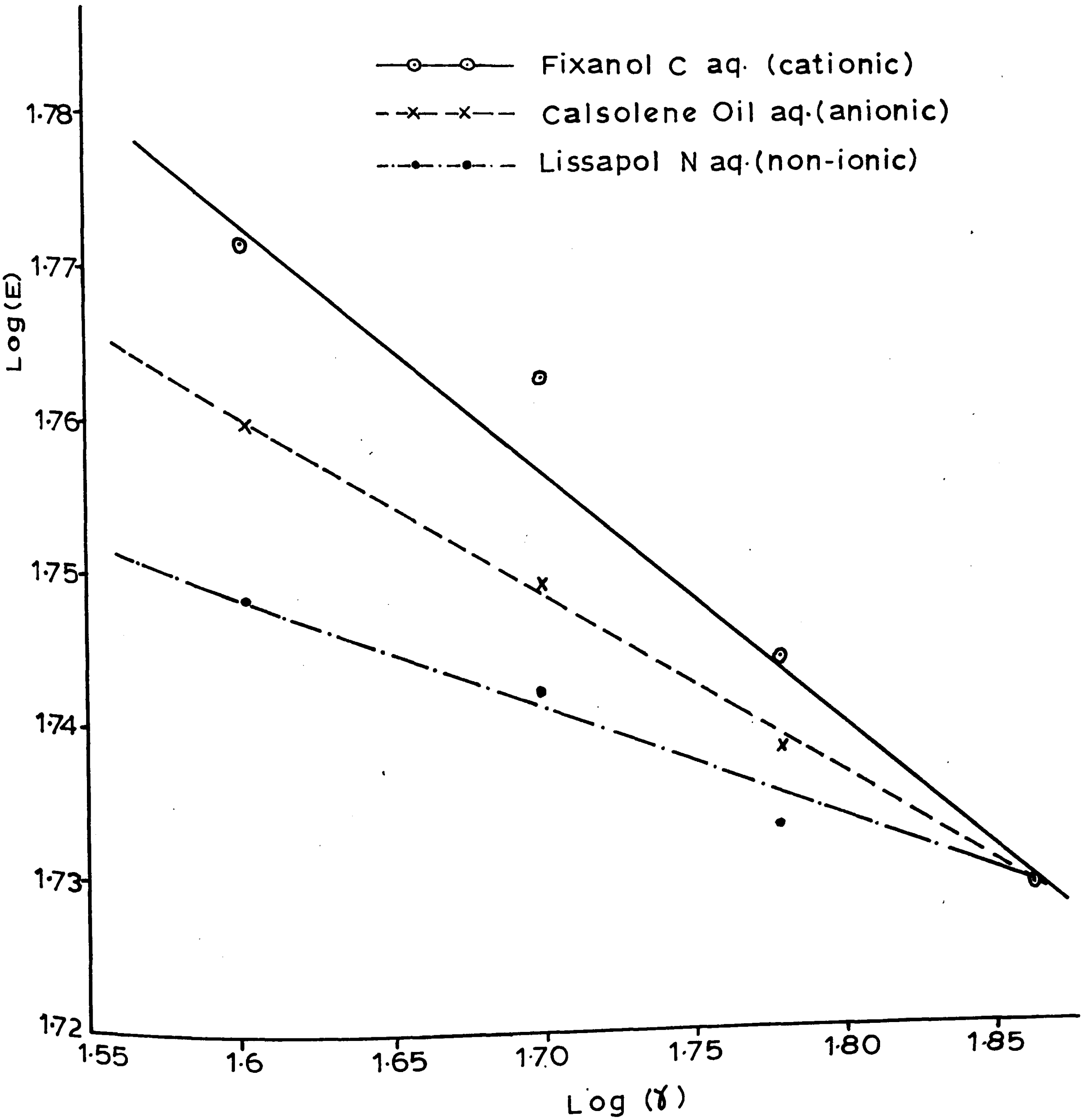

immersional wetting and spreading wetting is high[110].

The results in Tables 7.3, 7.4 & 7.5 seem to indicate that the wetting power for coal of the cationic type of wetting agent - Fixanol C - is higher than that of the other two. A graph connecting the logarithm of surface tension and logarithm of dust suppression efficiency with these wetting agent solutions at a spray pressure of 140.6 kg./sq.cm. is shown in Fig. 7.9 and there seems to be a general relationship between the surface tension of sprayed liquid and dust suppression efficiency, as given by

$$E \quad \alpha \quad \gamma_l^{(-n)} \qquad \ldots. \quad (2)$$

where $n = 0.165$ for cationic surface active agent,

$n = 0.118$ for anionic surface active agent,

and $n = 0.074$ for non-ionic surface active agent.

Hence combining (1) and (2), $E \quad \alpha \quad (P)^{0.385}.(\gamma_l)^{(-n)}$

The increase in dust suppression can be attributable only to the greater wetting power of the solutions sprayed, since it has already been shown[63] that at higher spray pressures, reduced surface tension does not produce any significant effect on atomisation.

<u>Effect of change of throughput at constant pressure</u>:(7.5; Table 7.7; Fig. 7.5)

As might be expected, there is an increase in dust suppression with increase of liquid throughput (Table 7.7; Fig. 7.5). It is interesting to note that the rate of increase in dust suppression efficiency is higher for the solid cone (with the increase of diameter of hole in the plug), than for the hollow cone nozzles.

It may be seen from the figure that the rate of increase of dust suppression efficiency with throughput was nearly constant at constant spray pressure. The figures were about 6 per cent increase for every additional litre/minute throughput for the solid cone nozzles and about 3.7 per cent increase per litre/min. for the hollow cone nozzles.

The greater efficiency in the case of solid cone nozzles may be due to the deeper penetration of droplets by virtue of the higher axial velocity of a high proportion of the droplets in the issuing jet. Consequently, there would be less deformation of the spray pattern by the counter current air flow.

<u>Effect of air velocity in the tunnel</u>: 7.6; Table 7.8, Fig. 7.6.

With the liquid sprayed upstream, one would expect that increase in air velocity should contribute to an increase in the dust suppression efficiency, as the relative velocity between the liquid droplet and dust particle is thereby increased. The results in Table 7.8 show that in the wind tunnel this did not in fact happen. From Fig. 7.6, it may be seen that there was a steady drop in the dust suppression efficiency with increase of air velocity in the tunnel. The efficiency which stood at 62.5 per cent with the air velocity of 50 cm./sec. dropped down to 9.14 per cent, when the air velocity was increased to 500 cm./sec., i.e. a decrease of about 1.8 per cent for every 10 cm./sec. increase of air velocity.

Inspection of the effect of the flowing air on the spray cone provided a clue to this unexpected variation It could be seen that the deformation of the spray cone shortened the forward travel of the droplet, so that the overall size of the cone was reduced. This effect is sketched in Fig. 7.10. Owing to this deformation, dusty air was able to bypass the droplets.

FIG.7·10.EFFECT OF AIR VELOCITY ON SPRAY CONE

(a) Low air velocity

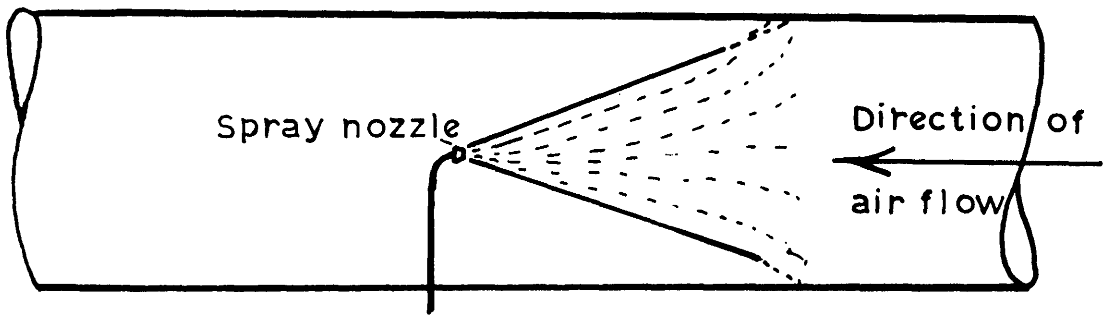

(b) Medium air velocity

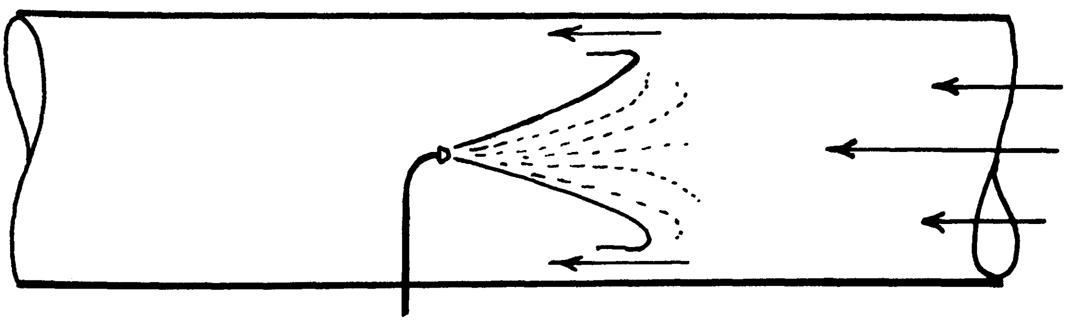

(c) High air velocity

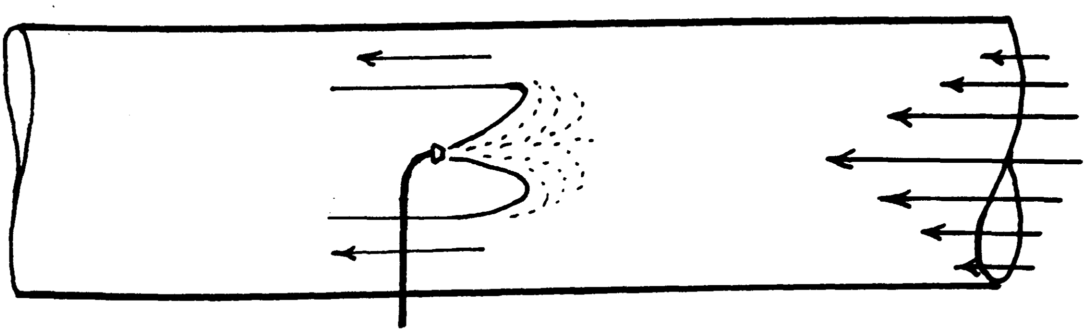

Effect of spraying on size distribution of residual dust:

As can be seen from Fig. 7.11, the residual dust was, like the initial dust, counted under the Automatic Particle Counter in five size ranges - 0.5 - 1.0μ, 1.0 - 2.0μ, 2.0 - 2.83μ, 2.83 - 4.0μ and 4.0 - 5.66μ. In general, about 75 per cent of the particles greater than 5.66 microns in diameter were removed and about 65 per cent of the particles of size 0.5 - 5.66 microns. The comparative histograms shown, indicate that the sprays, irrespective of the nature of the spray device, spray pressures, throughputs, and air velocities, do not appear to be particularly selective in suppressing any one size range of dust over the ranges counted.

Dust-Water Ratio.

A knowledge of the volume of water required to remove a certain amount of dust from air is of value, when spray capacities have to be decided upon the when taking into consideration the nuisance created by wet conditions in a particular mining operation. The volume of water required may be assessed by calculating a dust-water ratio. The ratio chosen in this work was the number of particles of coal dust knocked down per c.c. of atomised water.

FIG.7.11. SIZE DISTRIBUTION HISTOGRAMS

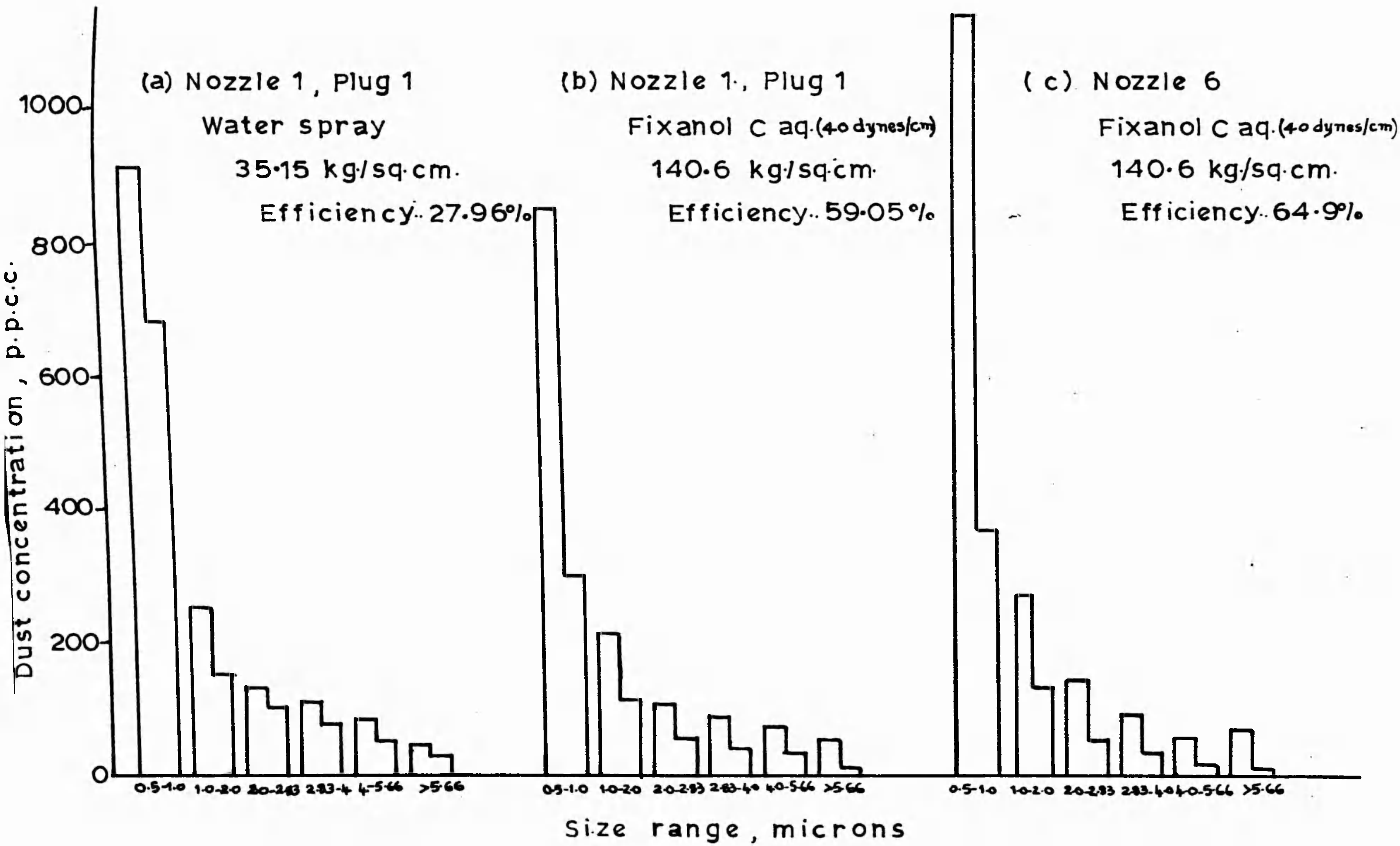

This seeming inconsistence of units may be tolerated, since use of any larger, more practical volume units such as the litre or gallon results in a very large number for the final ratio value. If a density is selected for the coal substance together with an average particle diameter, one may calculate the weight of coal dust removed from air suspension per litre of liquid sprayed.

The dust-water ratio calculations are tabulated in Table 7.9 and the effect of throughput on dust-water ratio is illustrated in Figs. 7.12 and 7.13. It is worthy of note that the dust-water ratio is higher for a hollow-cone spray than for a solid cone spray and the rate of decrease of the ratio with increase of throughput is more or less the same, irrespective of the nature of the spray device and the liquid sprayed.

This would appear to underline the fact that increased throughput does not result in a corresponding increase in dust suppression and that there is little to be gained (from the point of view of dust-water ratio) by increasing the orifice diameter of the nozzle to obtain high throughput at high pressure.

Table 7.9

Dust-water Ratios*

Nozzle No.1 ; Air velocity .. 100 cm./sec.

Dust concentration .. 1500 p.p.c.c.

Spray Pressure		Throughput litres/min.		Hollow cone-water spray		Solid cone Plug 1 - water		Solid cone Plug 1 Fixanol C-40 dynes/cm.	
p.s.i.g	P kg/sq.cm	Hollow cone	Solid cone	Particles removed per minute $\times 10^6$	Dust-water ratio $\times 10^6$	Particles removed per minute $\times 10^6$	Dust-water ratio $\times 10^6$	Particles removed per minute $\times 10^6$	Dust-water ratio $\times 10^6$
60	4.21	0.17	0.2536	18,030	106.2	19,520	77.0	21,650	85.5
250	17.59	0.335	0.504	28,250	84.5	32,520	64.5	37,380	70.4
500	35.15	0.474	0.68	37,780	79.7	41,350	60.7	47,500	69.8
1000	70.3	0.655	0.964	49,300	75.2	56,300	58.4	60,600	62.9
1500	105.45	0.804	1.168	62,450	77.7	64,700	55.4	72,350	61.9
2000	140.6	0.913	1.381	71,800	78.6	79,200	57.3	87,350	63.1
2500	175.75	1.039	1.57	68,980	66.4	75,600	48.2	85,200	54.2
3000	210.9	1.121	1.72	67,600	60.2	74,500	43.4	84,700	49.2

* Dust-water ratio = Number of dust particles removed/1 c.c. of liquid sprayed.

FIG. 7·12. RELATIONSHIP BETWEEN THROUGHPUT AND DUST-WATER RATIO

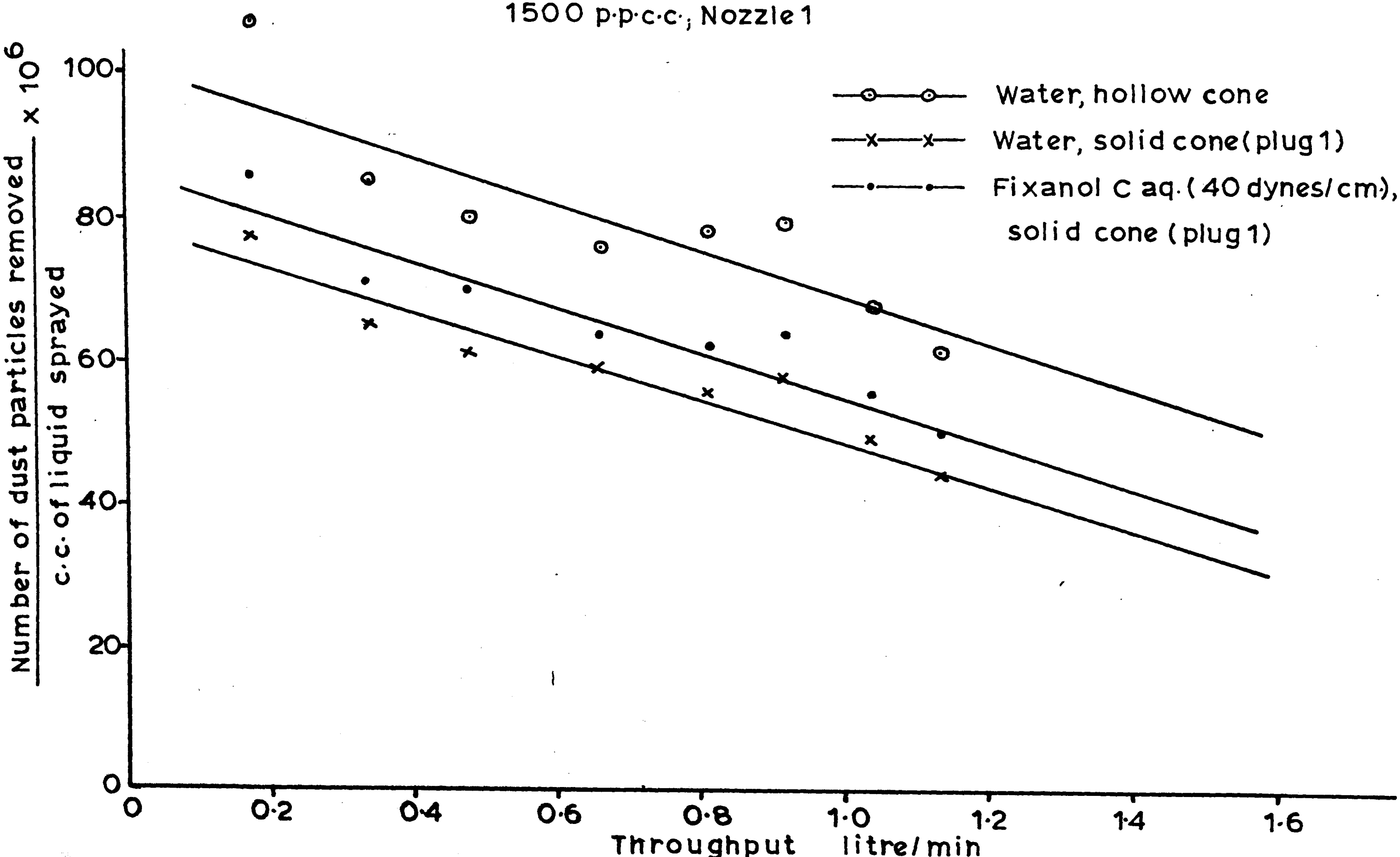

FIG.7.13. EFFECT OF SPRAY PRESSURE ON DUST-WATER RATIO

1500 p.p.c.c.; Nozzle 1; Water spray

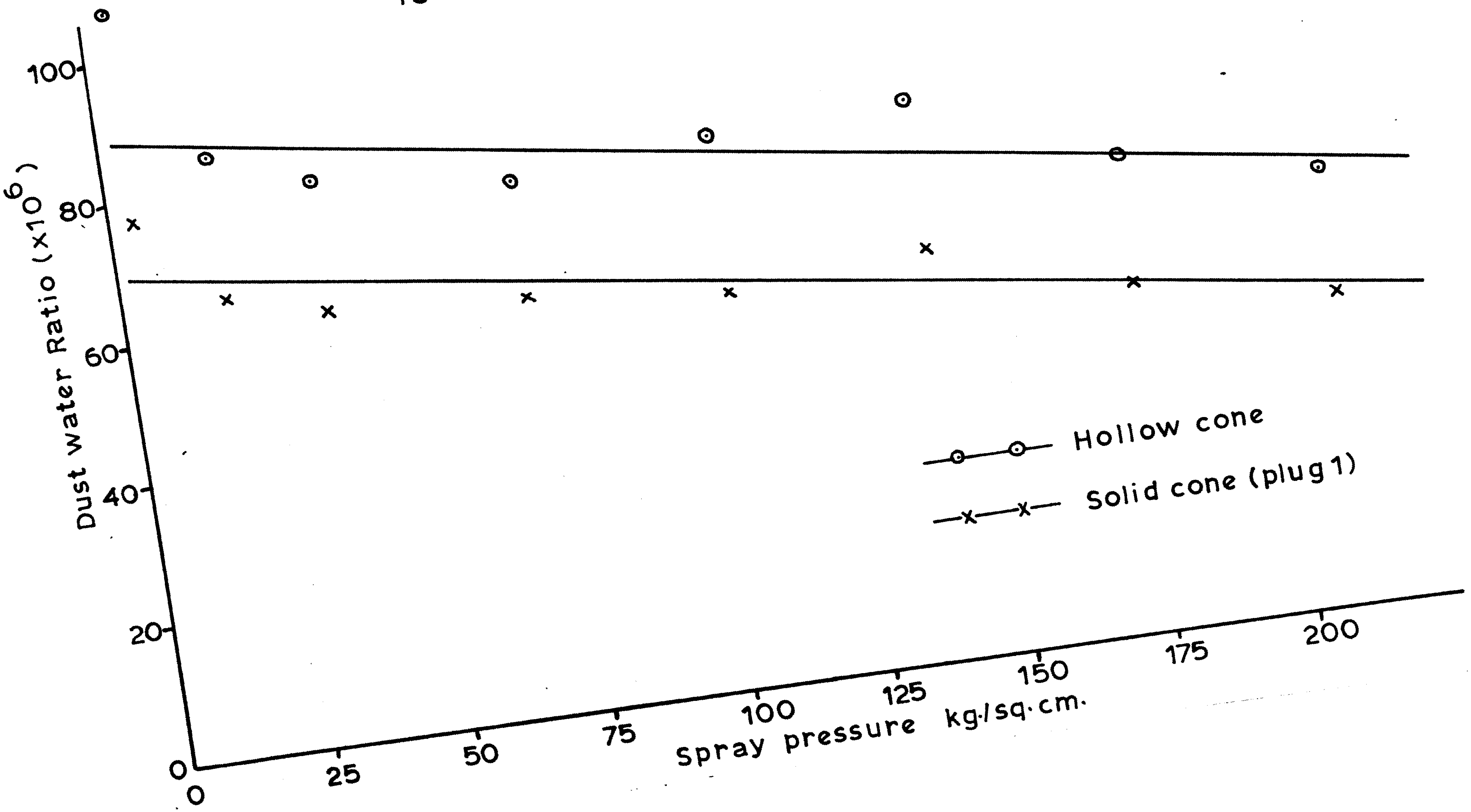

8. EFFECT OF TANDEM SPRAYING ON DUST SUPPRESSION.

8.1 Introduction.

In the process of spraying through a single nozzle along the axis of the tunnel counter to the dust-laden air stream it had been found that even at an air velocity of about 100 cm./sec. there was some deformation of the spray cone. It was thought that the bad effects of this deformation could be reduced somewhat by placing a second spray cone behind the first, i.e. a two stage spraying system. From this idea grew the conception of "tandem" spraying, i.e. the arrangements of a number of equally spaced nozzles all set on the axis of the tunnel, one behind the other and all spraying counter current to the dusty air flow. When the distance between nozzles was fixed the largest number of nozzles that could be used at one time would be controlled by the water output of the pump at a particular pressure and the length of the dust tunnel. It was hoped that such an arrangement might furnish a significant increase in the dust suppression efficiency. A comparison of the dust-water ratios for tandem sparying would also indicate whether any increase in dust suppression efficiency gained by tandem spraying was gained at the price of excessive water usage.

8.2 Experiments with tandem sprays.

Owing to the limited capacity of the pump the nozzle with the smallest orifice diameter, Nozzle 1, was chosen for the tests. Even with that nozzle, tandem spraying with six nozzles was found to be limited to a pressure maximum of about 140.6 kg./sq.cm. (2000 p.s.i.g.)

The throughput of sprays, from one to six nozzles in tandem was measured during the experiments and are shown in Table 8.1 and Fig. 8.1. It was found that with two identical nozzles in tandem, the spray throughput at any constant pressure was not twice that for a single nozzle. This was confirmed for tandem spraying with 3, 4, 5 or 6 nozzles. It may be seen from Table 8.1 that the tandem spraying (with identical nozzles) was accompanied by a nearly constant increase per nozzle in the relative overall flow number (i.e. calculated by setting the flow number of one nozzle = 1.0) for each additional nozzle in tandem (about 0.35).

Experiments with single nozzle have been described earlier (7.2). Preliminary tests with two nozzles in series indicated that the second spray could effectively operate without interfering with the first spray, if the second nozzle was placed behind the first nozzle, at a

Table 8.1

Throughput of Tandem Sprays

Nozzle 1 Hollow Cone

Number of nozzles in tandem		Single	Two	Three	Four	Five	Six
Spray pressure		Throughput litres/min.					
p.s.i.g.	P kg/sq.cm						
500	35.15	0.474	0.625	0.780	0.951	1.130	1.320
1000	70.3	0.655	0.901	1.089	1.350	1.560	1.800
1500	105.45	0.804	1.100	1.352	1.669	1.941	-
2000	140.6	0.913	1.280	1.550	1.912	-	-
2500	175.75	1.039	1.451	1.770	2.181	-	-
Overall Flow No.		0.2725	0.361	0.457	0.560	0.642	0.740
Flow No. per nozzle		0.2725	0.181	0.152	0.140	0.128	0.123
Relative overall FN		1.0	1.325	1.680	2.054	2.355	2.720
Increase in Relative overall FN		-	0.325	0.355	0.374	0.301	0.365

FIG. 8·1. THROUGHPUT OF TANDEM SPRAYS

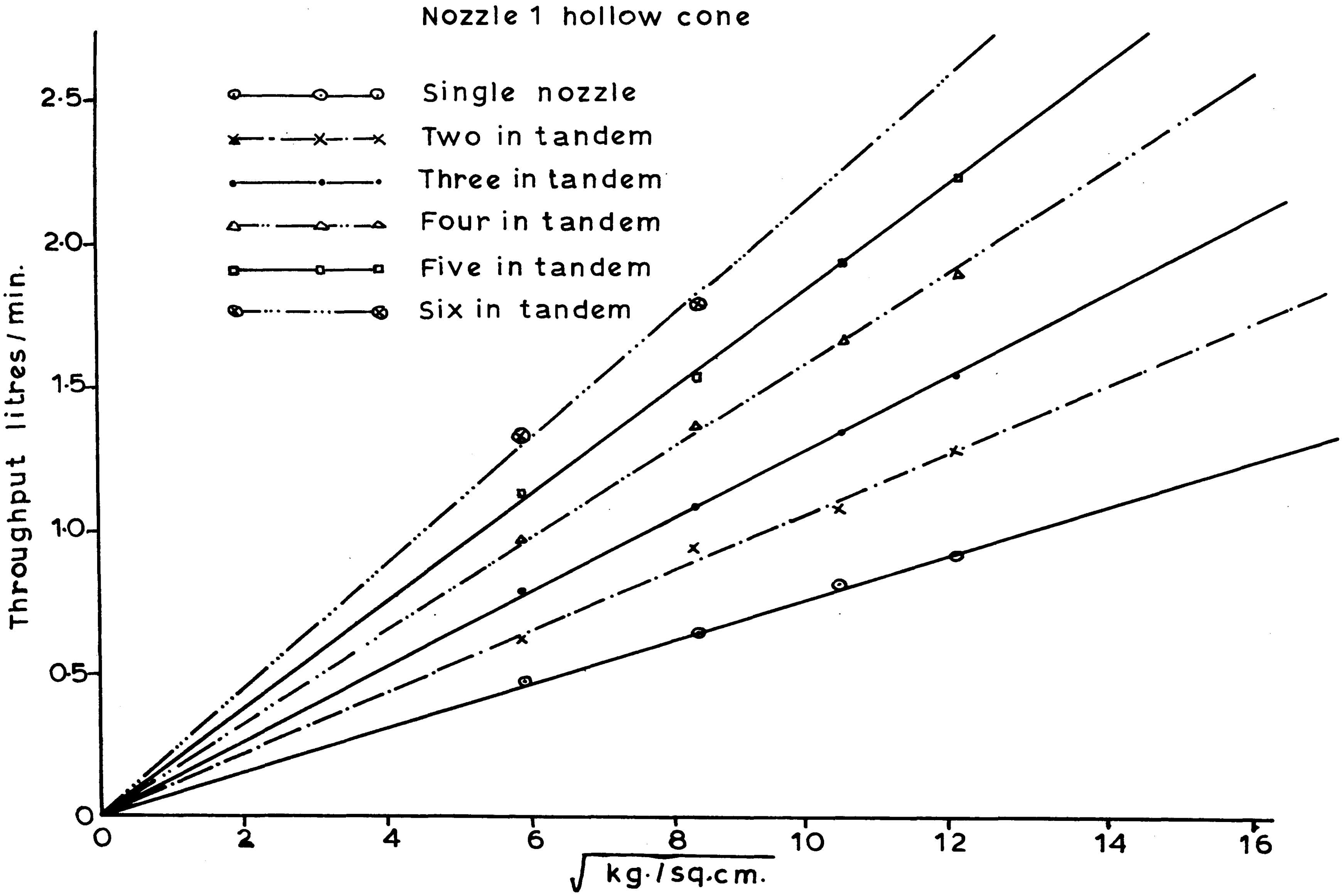

distance not less than 15 cms. Since the nozzles could not be too near the second dust sampling point, it was decided to set the distance between any two adjacent nozzles at 15 cms. The arrangement of nozzles for tandem spraying is shown in Fig. 8.2. The stems carrying the nozzles could be easily corrected for orientation and were easily detachable from the main water feed pipe.

In the first instance two nozzles were placed in tandem facing up-stream. The air velocity was set to 100 cm./sec. and the dust concentration in the wind tunnel was about 3000 p.p.c.c. Water was sprayed through the tandem sprays at a constant pressure of 35.15 kg./sq.cm. When conditions in the tunnel and spraying unit became steady, simultaneous dust sampling was carried out before and after the spray, by means of thermal precipitators. The dust samples were then counted under the Automatic Particle Counter. The tests were repeated at a number of higher pressures.

Such tests were repeated for arrangements of three, four, five and six nozzles in turn and at similar values of applied pressure. A summary of the effect of spray pressure and the effect of number of nozzles in tandem on dust suppression efficiency is given in Table 8.2. Tables 8.3 (a), (b), (c) and (d) give detailed accounts

FIG. 8·2. DIAGRAM ILLUSTRATING TANDEM SPRAYING IN WIND TUNNEL

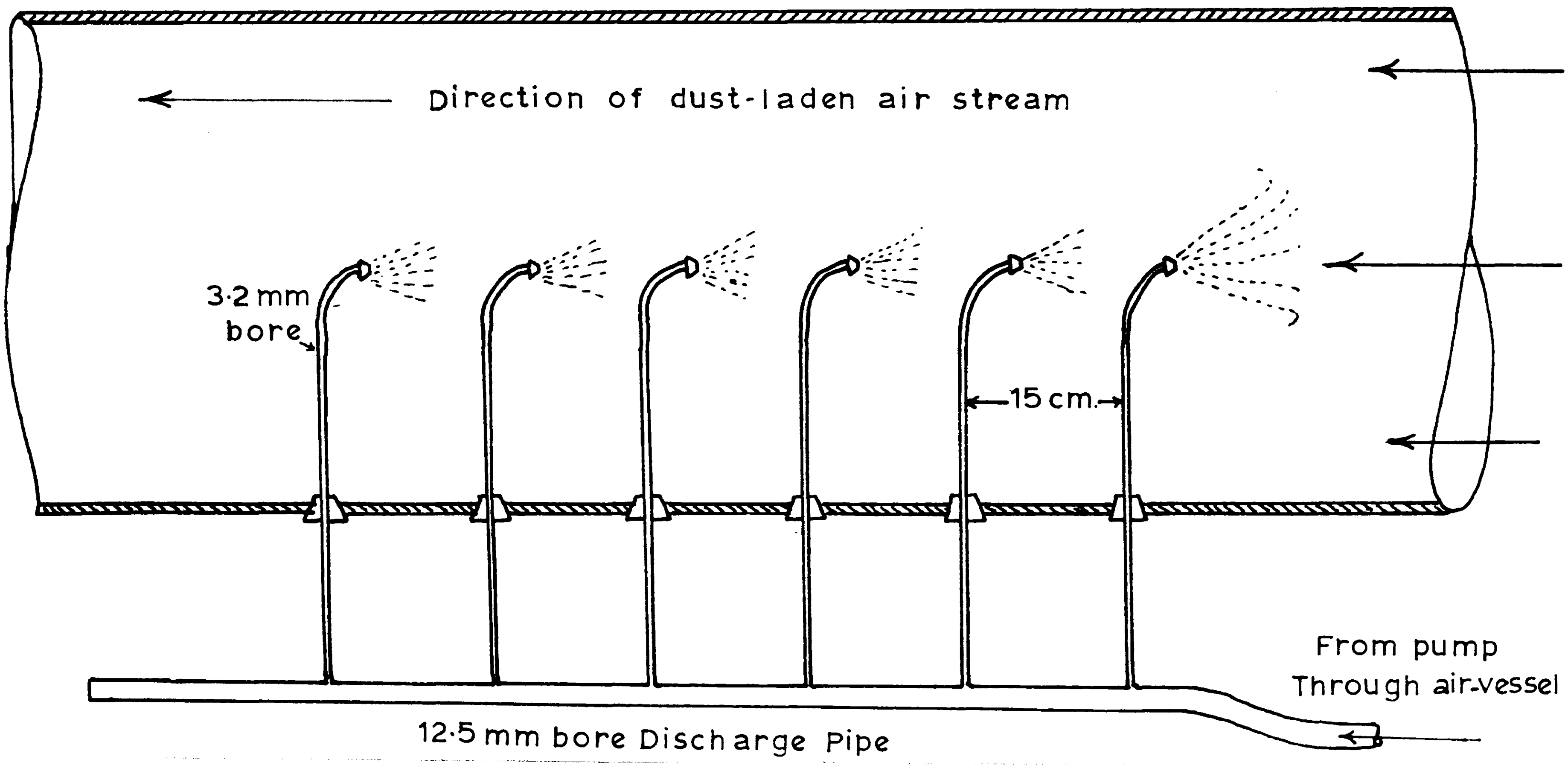

Table 8.2

Effect of Tandem Spraying on dust suppression

Summary

Type of nozzle used : Nozzle 1 Hollow Cone ; Liquid Sprayed .. Water

Air Velocity .. 100 cm./sec. ; Dust concentration .. C. 3000 p.p.c.c.

Spray pressure		Dust-Suppression Efficiency E% with no. of nozzles in tandem.					
p.s.i.g.	$P_{kg/sq.cm}$	Single	two	three	four	five	six
500	35.15	25.48	30.20	33.80	40.60	43.60	48.80
1000	70.3	33.36	37.80	41.30	46.60	50.20	56.10
1500	105.45	42.20	47.95	55.20	60.10	66.00	-
2000	140.6	48.50	53.70	59.80	68.00	-	-
2500	175.75	46.67	53.45	57.50	67.20	-	-

Table 8.3 (a)

Effect of Tandem spraying on dust suppression

Two Nozzle Spraying

Nozzle used .. Nozzle 1 Hollow cone ; Liquid sprayed .. water

Air Velocity .. 100 cm./sec. ; Dust concentration .. c. 3000 p.p.c.c.

Spray pressure	p.s.i.g.	500	1000	1500	2000	2500
	kg/sq.cm.	35.15	70.3	105.45	140.6	175.75
Dust Concentration p.p.c.c.	Before the spray	3131	3392	3005	3634	3242
	After the spray	2186	2110	1545	1683	1510
	Difference	945	1282	1460	1951	1732
Efficiency E%		30.2	37.8	47.95	53.70	53.45

Table 8.3 (b)

Effect of Tandem spraying on dust suppression

Three Nozzle Spraying

Nozzle used .. Nozzle 1 Hollow Cone ; Liquid sprayed .. water
Air Velocity .. 100 cm./sec. ; Dust concentration .. C. 3000 p.p.c.c.

Spray Pressure	p.s.i.g.	500	1000	1500	2000	2500
	kg./sq.cm	35.15	70.3	105.45	140.6	175.75
Dust Concentration p.p.c.c.	Before the spray	3182	3590	3634	3392	3242
	After the spray	2105	2110	1626	1367	1377
	Difference	1077	1480	2008	2025	1865
Efficiency E%		33.8	41.3	55.20	59.80	57.50

Table 8.3 (c)

Effect of Tandem spraying on dust suppression

Four Nozzle Spraying

Nozzle used .. Nozzle 1 Hollow cone. Liquid sprayed .. water
Air Velocity .. 100 cm./sec. Dust concentration .. c. 3000 p.p.c.c.

Spray pressure	p.s.i.g.	500	1000	1500	2000	2500
	kg/sq.cm.	35.15	70.3	105.45	140.6	175.75
Dust Concentration p.p.c.c.	Before the Spray	3131	3786	3590	3463	3684
	After the Spray	1855	2023	1431	1107	1204
	Difference	1276	1763	2159	2356	2480
Efficiency E%		40.6	46.6	60.1	68.0	67.2

Table 8.3(d)

Effect of Tandem spraying on dust suppression

Five and Six nozzle spraying

Nozzle used .. Nozzle 1 Hollow cone ; Liquid sprayed .. water

Air Velocity.. 100 cm./sec. Dust concentration .. C.3000 p.p.c.c.

No. of Nozzles in tandem		Five			Six	
Spray pressure	p.s.i.g.	500	1000	1500	500	1000
	kg./sq.cm.	35.15	70.3	105.45	35.15	70.3
Dust concentration p.p.c.c.	Before the spray	3120	3392	3005	3634	3242
	After the spray	1754	1688	1023	1862	1423
	Difference	1366	1704	1982	1772	1819
Efficiency E%		43.6	50.2	66.0	48.8	56.1

of the data obtained for two-nozzle, three-nozzle, four-nozzle, five-nozzle and six-nozzle arrangements.

As may be seen from Table 8.2, there is a significant increase in dust suppression efficiency, with increase in the number of nozzles in tandem. It is interesting to note that the increase in dust suppression efficiency with increase of spray pressure shows a similar gradation for any number of nozzles in tandem. The maximum dust-suppression efficiency (for the tandem sprays up to 4 nozzles in tandem) appeared to have been effected at about 140.6 kg./sq.cm. Owing to the limited capacity of the pump at higher pressures it was not possible to test this point more fully.

In general, the rate of increase in dust-suppression with number of nozzles in tandem is much higher for any spray pressure than that produced by increasing throughput at constant pressure in one nozzle through increase of orifice diameter. For example, at 140.6 kg./sq.cm. spray pressure, a single spray nozzle gives an efficiency of 48.5 per cent (7.5) as against 68 per cent, given by 4 spray nozzles in tandem. The increase in throughput, as may be seen from Table 8.1, is only 1 litre/min. Thus the rate of increase in dust suppression is about

$\frac{68 - 48.5}{3}$ = 6.5 per cent for each additional nozzle or

19.5 per cent per an increase of 1 litre/min. throughput. This is quite high, compared with about 4 per cent increase obtained (chapter 7.6) by changing the throughput at constant pressure by varying the nozzle diameter. This would indicate that an increase in throughput by having a number of small diameter nozzles in tandem is much more effective and advantageous, than employing a single nozzle of greater diameter.

8.3 Discussion of Results.

The results are best considered under the following headings :-

Effect of spray pressure and number of nozzles in tandem on dust suppression: (Tables 8.2, 8.3 (a),(b),(c),(d); Figs. 8.3 and 8.4)

A graph connecting the logarithm of spray pressure and the logarithm of dust suppression efficiency is shown in Fig. 8.3 for the tandem sprays and it may be seen that a linear relationship of about the same gradient is obtained for any number of nozzles in tandem. Between the spray pressures of 35.15 and 140.6 kg./sq.cm. the following relationship seems to hold good for tandem sprays,

$$E \propto (P)^{0.455}$$

For a single nozzle, it was shown in Chapter 7 (Fig. 7.8) that an approximate relationship of the type

$$E \propto (P)^{0.385}$$

FIG. 8·3. EFFECT OF SPRAY PRESSURE ON DUST SUPPRESSION WITH TANDEM SPRAYS

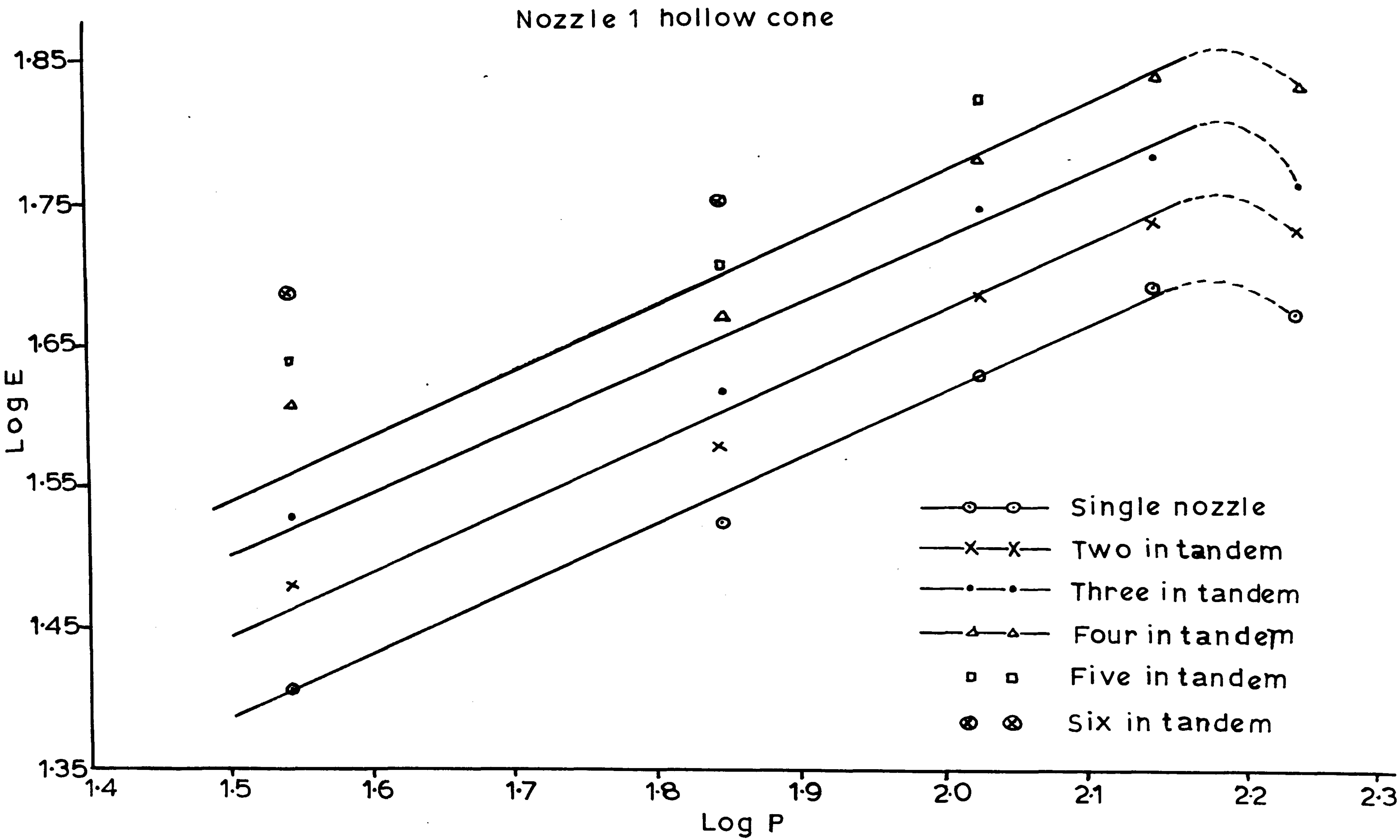

was found to exist for the whole range of pressures.

The value of index (0.455) for tandem sprays is much nearer to (0.5), which would tend to confirm the hypothesis that the increased dust suppression at increased pressures was mainly due to the increased water flow rate and hence one should expect the dust suppressing efficiency to vary as the square root of the applied pressure.

The relationship between the Overall Flow Number of the tandem sprays and the number of nozzles used in tandem was shown in Table 8.1 to be approximately linear. The Flow Number increased by about 0.094 for every additional nozzle (No.1) in tandem. The effect of the number of nozzles in series on dust suppression efficiency is illustrated in Fig. 8.4. It is interesting to note that the rate of increase in dust suppression efficiency with additional number of nozzles in tandem was higher for pressures above 70.3 kg./sq.cm. than for pressure lower than 70.3 kg./sq.cm. As was the case with the single nozzle, the maximum dust suppression efficiency was seemingly effected at about 140.6 kg./sq.cm. (2000 p.s.i.g.) whatever the number of nozzles in tandem.

<u>Hypothetical maximum dust suppression efficiency with tandem sprays</u>: It was clear from the foregoing discussion that there was a significant increase in dust suppression efficiency with small nozzles in tandem, without

FIG. 8·4. EFFECTS OF SPRAY PRESSURE AND NUMBER OF NOZZLES IN TANDEM ON DUST SUPPRESSION

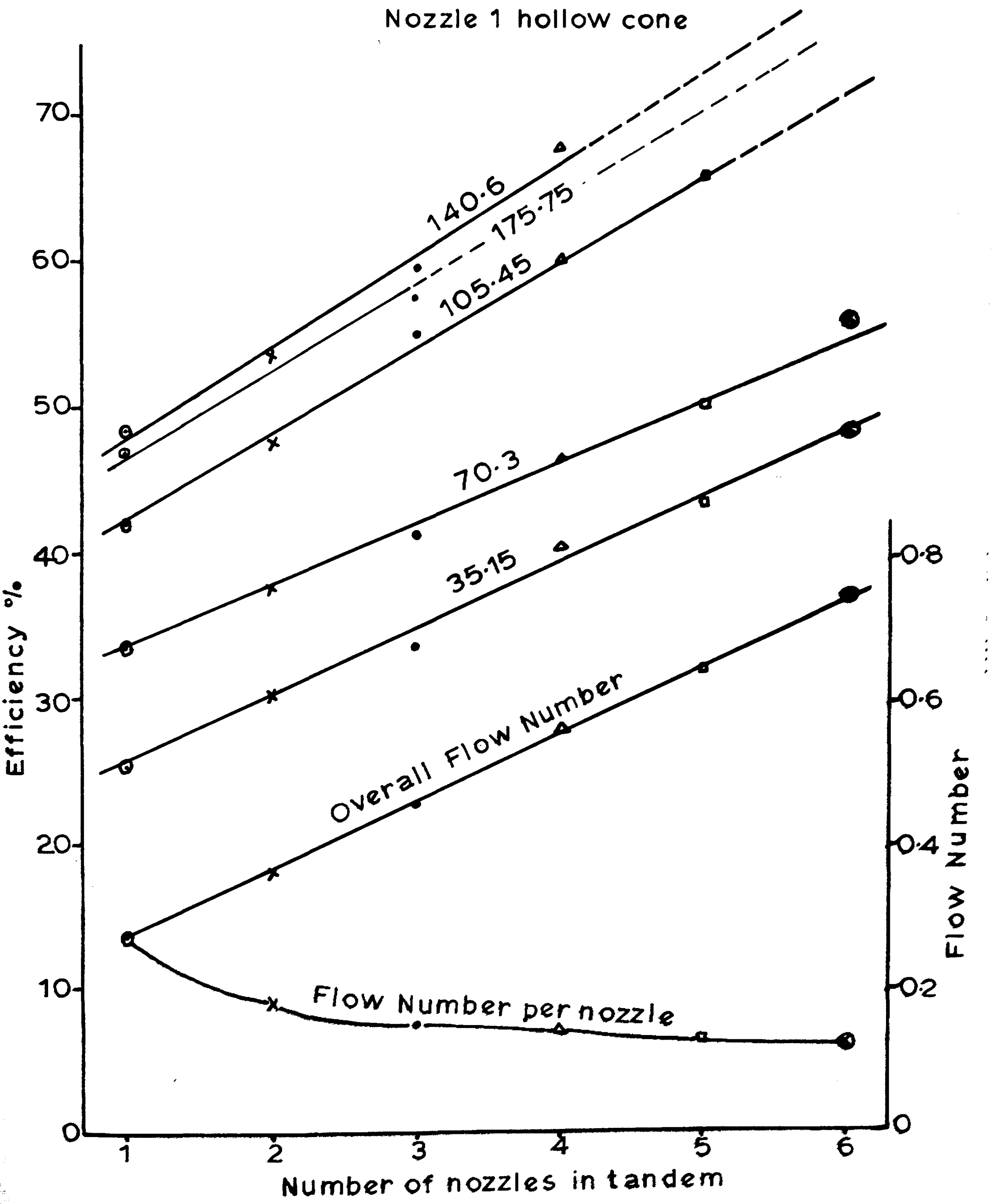

excessive water usage. Fig. 8.4 also indicated that the maximum dust suppression was effected at 140.6 kg./sq.cm. and the rate of increase of dust suppression for every additional identical nozzle (nozzle 1 Hollow cone) in series was about 6.5 per cent.

Now, a graph connecting the throughput of these tandem sprays at 140.6 kg./sq.cm. and the dust-suppression efficiency showed an approximately linear relationship for the range of up to four nozzles in tandem (Fig.8.5). Unfortunately the capacity of the water pump prevented more than four nozzles being tested at this pressure. If and when a large pump becomes available this study should be extended to a larger number of nozzles to see how far this linearity extends. Were it to extend right up to a 100 per cent efficiency of dust suppression for sprays at 140.6 kg./sq.cm., as is shown by the dotted portion of the line in Fig. 8.5, a total throughput of 3.58 litres/minute of water sprayed through ten identical nozzles (nozzle 1) in tandem at 140.6 kg./sq.cm. would be required to achieve 100 per cent dust suppression. Since it is quite possible that the linearity does not extend to 100 per cent dust suppression, a larger number of nozzles may well be required in practice. Further experiment is required to test this point.

FIG. 8·5. POSTULATION FOR 100 PERCENT DUST SUPPRESSION BY TANDEM SPRAYING AT 140·6 Kg/sq·cm.

Water spray; Hollow cone Nozzle 1; Air velocity 100 cm/sec.

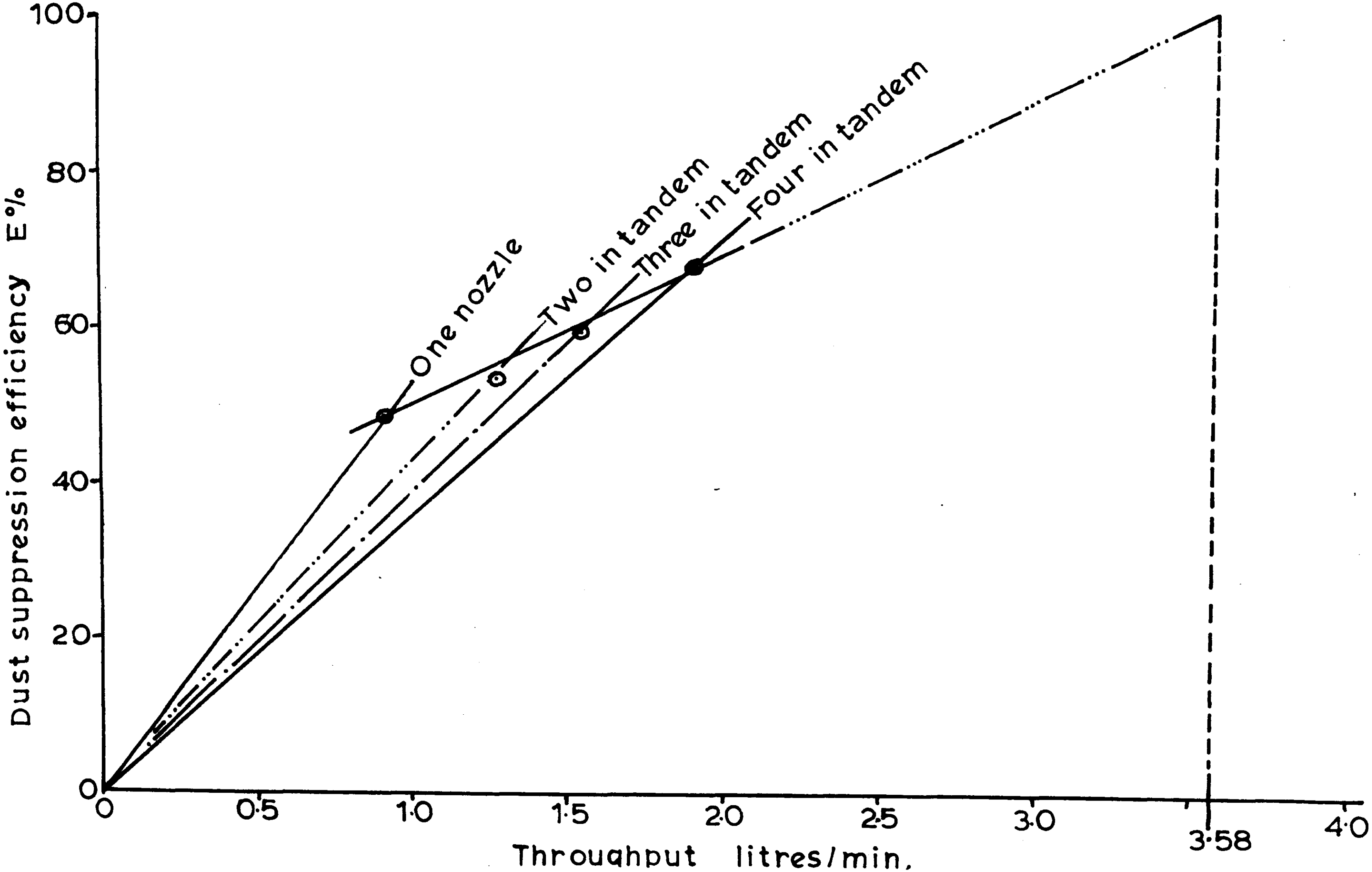

<u>Dust-water ratios</u>: The dust-water ratio, which is expressed as the number of dust particles removed per one c.c. of water sprayed, was calculated for all the tandem sprays and for all the spray pressure ranges and the ratio was plotted against the water throughput, as shown in Fig. 8.6.

As was the case with the single nozzle spraying, a straight line with a negative gradient can be drawn through these points. The dust-water ratios are always found higher for lower pressures and throughputs and the ratio steadily decreases with increase in spray pressure and water throughput. This indicates that whatever be the nature of spray, there is always at higher spray pressures, a sacrifice of the dust-water ratio to achieve greater dust suppression efficiency.

It is also possible that a higher dust-water ratio at lower pressure may be attributable to the larger number of relatively larger droplets being produced by the sprays under these conditions, which would increase the probability of collision with dust particles. Consideration, however, of the line drawn in Fig. 8.6 will show that it is virtually a line of constant water pressure covering the range of nozzles used. This would suggest that the phenomenon of reduced dust-water ratio at elevated water pressure is primarily a throughput effect. Extra water droplets are being produced which are not as efficiently utilised since

Table 8.4(a)

Dust-water Ratios* for Tandem Spraying

Nozzle used .. Nozzle 1 Hollow cone ; Liquid sprayed .. water

Air Velocity .. 100 cm./sec. ; Dust concentration .. 3000 p.p.c.c.

No. of nozzles in Tandem .. Single					Two			Three		
Spray Pressure		Through-put l./min.	Total no. of particles removed/min. x 10^6	Dust-water ratio x 10^6	Through-put l./min.	Total No. of particles removed/min. x 10^6	Dust-water ratio x 10^6	Through-put l./min.	Total No. of particles removed/min. x 10^6	Dust-water ratio x 10^6
p.s.i.g	P kg/sq.cm									
500	35.15	0.474	75,560	159.4	0.625	89,400	142.9	0.780	100,000	127.9
1000	70.3	0.655	98,600	150.4	0.901	111,800	124.2	1.089	122,000	121.0
1500	105.45	0.804	124,900	155.4	1.100	141,800	128.8	1.352	163,100	120.9
2000	140.6	0.913	142,600	157.2	1.280	158,900	123.9	1.550	176,800	114.1
2500	175.75	1.039	137,960	132.8	1.451	158,000	109.1	1.770	170,000	96.1

* Dust-water Ratio = Number of dust particles/1 c.c. of liquid sprayed.

Table 8.4(b)

Dust-water Ratios for Tandem Spraying

Nozzle used .. Nozzle 1 Hollow cone ; Liquid sprayed .. water

Air Velocity .. 100 cm./sec. ; Dust concentration .. 3000 p.p.c.c.

No. of Nozzles in Tandem ..		Four			Five			Six		
Spray Pressure		Through-put	Total No. of particles removed/min.	Dust-water Ratio	Through-put	Total No. of particles removed/min.	Dust-water Ratio	Through-put	Total No. of particles removed/min.	Dust-water Ratio
p.s.i.g.	P kg/sq.cm	l./min	$\times 10^6$	$\times 10^6$	l./min	$\times 10^6$	$\times 10^6$	l./min	$\times 10^6$	$\times 10^6$
500	35.15	0.951	120,000	126.2	1.130	128,900	114.0	1.320	144,100	109.2
1000	70.3	1.350	137,600	102.0	1.560	148,300	95.1	1.800	166,000	92.2
1500	105.45	1.669	177,900	106.4	1.941	195,000	100.5	-	-	-
2000	140.6	1.912	201,000	105.2	-	-	-	-	-	-
2500	175.75	2.181	198,500	90.7	-	-	-	-	-	-

FIG. 8·6. DUST-WATER RATIOS FOR TANDEM SPRAYS

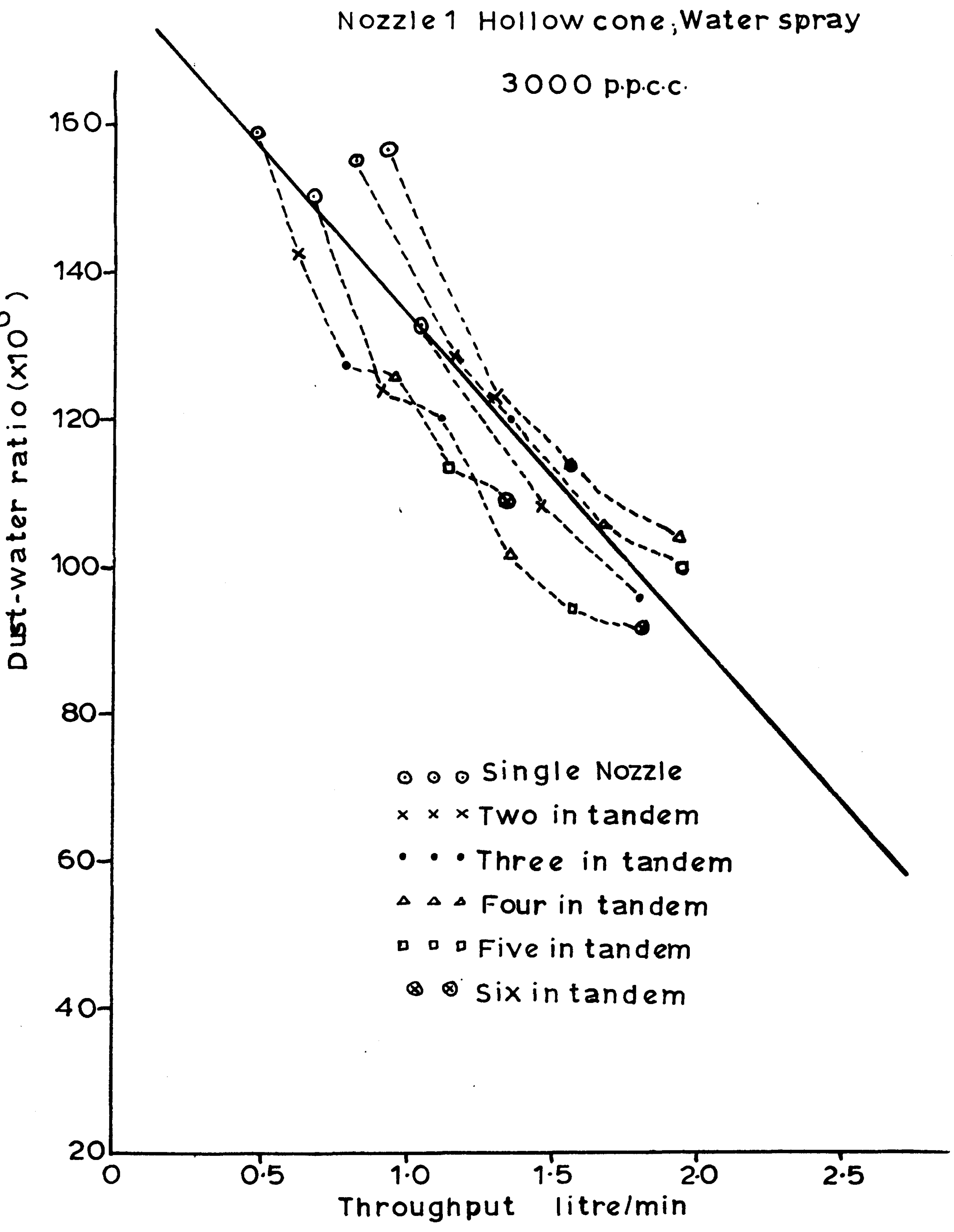

they pass through a path already partly cleared of dust particles.

Comparison with the dust water ratios resulting from increasing throughput through increase in nozzle diameter indicates that water is being more efficiently utilised in the tandem spraying technique.

9. GENERAL DISCUSSION AND CONCLUSIONS

The precise mechanism of suppression of airborne dust by spray droplets is somewhat complicated. It is generally postulated that the liquid droplets strike the dust particles and actually wet them, thus enabling the particle to penetrate into the droplets. This wetting action would cause the "captured" dust particles to settle rapidly, by virtue of the increased size and weight. Terrel(111) suggested that the dust suppression may also be attributable to the mechanical sweeping action of the descending droplets which might bring down particles of size, too small to be efficiently wetted.

In the case of particulate matter difficult to wet, such as the coal dust used in our experiments, the capability of the droplet to capture the particle is reduced, because of the high interfacial tension between the droplet and the dust particle, the entry of the particle into the drop being resisted by surface tension forces.

Considering the impact and penetration of a liquid droplet by a spherical non-wettable dust particle, the minimum velocity of the droplet required for penetration can be theoretically calculated, neglecting any induced mass effects associated with the impact and assuming that the deformed surface of the drop conforms exactly to the shape of the embedded surface of the particle.

As penetration proceeds, work is done against the surface tension force, at the expense of the kinetic energy of the particle. The particle can thus enter the drop, only if its incident kinetic energy is sufficient to allow it to penetrate to such a depth that the drop is able to close behind it, viz.

Kinetic energy (K.E.) $\nless$ work required to be done by the particle against surface tension

$$\nless \frac{2}{3} \pi d_p^2 . \gamma_1 . \qquad .... \quad (1)$$

Pemberton(112) deduced that the particle will be assumed to be captured and retained by the droplet, when the velocity of impact is such that its component normal to the surface of the drop is greater than the value, given by

$$\left(\frac{8 \gamma_1}{\rho_s . d_p} \right)^{1/2}$$

The velocity required for penetration will, no doubt, increase with the angle of incidence of the particle with the droplet and also with the approach to equality of the masses of particle and drop.

The average droplet size of high pressure sprays (30 - 200 kg./sq.cm.) ranged from 60 to 100 microns in our experiments. The average diameter of the particles in the experimental cone dust was found to be 1.57 microns, as sampled by the thermal precipitators and 2.43 microns, as sampled by the salicylic acid filter. A value of 2 microns for the particle diameter was taken to calculate the minimum velocity required for the penetration of droplet by dust particle, considering in turn water (of surface tension .. 72.75 dynes/cm.) and other surface active agent solutions of surface tension 60, 50 and 40 dynes/cm. The values are tabulated in Table 9.1.

Table 9.1

Theoretical minimum velocity of droplet for penetration

Surface tension of liquid sprayed dynes/cm.	72.75	60	50	40
Minimum velocity of droplet. cm./sec.	1509	1370	1250	1119

It is thus seen that a reduced surface tension of the liquid sprayed (provided the droplets from the liquid also have the same surface tension values at equilibrium) requires lower penetration velocities for impact and capture of similar dust particles.

Comparison of this table with Table 6.3 will show that much larger values of theoretical initial discharge velocities of water droplets were available, even at a low pressure of 35.15 kg./sq.cm., with the solid cone Nozzle 1. For example, at 35.15 kg./sq.cm. the theoretical initial axial velocity of the water droplets is 5,640 cm./sec., and this is almost four times the theoretical minimum velocity of droplets required for penetration and capture of dust particles. Thus it is evident from theoretical consideration, that the initial velocity of the droplets at the high-pressure ranges at which our experiments were carried out, far exceeded the minimum velocity required for penetration of water droplet by the dust particle. Owing to the decelerating effect of the air on the water droplet this high intial value is of course only maintained over a relatively short portion of the droplet flight and the low values of dust suppression obtained in practice indicate partly that the discharge velocity must drop very rapidly. There may also be a considerable amount of bouncing off the dust particles after impaction due to the grazing angle of incidence of the droplet with the dust particle.

Adhesion tension is another important factor in the complete wetting and capture of coal dust particles. This force of attraction between the molecules of the dust and those of sprayed liquid, is required to be high to cause the droplets to adhere to the dust particles and to cause flocculation, thereby increasing the mass of the combined particles and causing them to fall. In adhesion tension, there are three forces to be considered - the air surface tension of the solid, the air surface tension of the liquid and the interfacial tension between solid and liquid. When the droplet is placed in contact with the solid particle, it spreads until it reaches equilibrium. Any point at the edge of the droplet is then subjected to these three forces and the adhesion tension of the liquid on the solid is given by the difference between the surface tension of the solid and of the interfacial tension of the solid and liquid, i.e.

$$Sa = \gamma_s - \gamma_i = \gamma_l . \mathrm{Cos}\ \alpha$$

and thus reduction of the surface tension of the sprayed liquid should provide an increase in adhesion tension between the droplet and the particle and hence increase "wettability".

In practice, as was seen in 7.4, there was generally only a slight (often insignificant) increase in dust suppression efficiency produced by spraying surface active agent solutions. With Fixanol C of surface tension 40 dynes/cm., the efficiency increased by a maximum of about 6 per cent, as compared with water sprays (59.05% and 53.58%). It is perhaps worth noting, however, that the solution of Fixanol C which gave a surface tension of 40 dynes/cm., was very dilute, having a concentration of only about 0.04 gm. of surface active agent per 100 ml. of water.

The ultimate action in wetting is to achieve rapid spreading over the surface of the dust particle. Three types of wetting have to be considered in the estimation of wetting power - "contact" wetting, "immersional" wetting and "spreading" wetting. The tendencies of coal particles to be wet by and adhere to liquid droplets have been discussed by Owings.(110)

The small increase of dust suppression efficiency when spraying surface active agent solutions of low surface tension may only be attributable to spreading or creeping wetting. The change in free surface energy in spreading is equal to the sum of the solid-liquid interfacial tension and the surface tension of the liquid minus the surface tension of the solid. viz.

$$\gamma_i + \gamma_1 - \gamma_s = \gamma_1 - Sa$$

and the loss in free energy is

$$Sa - \gamma_1 = \gamma_1 (\text{Cos } \alpha - 1)$$

The added wetting agent reduces the surface tension of the liquid and hence the angle of contact of the droplet. The smaller contact angle, the greater is the spreading rate. The results in Tables 7.3, 7.4 and 7.5 indicate the rate of spreading, as characterised by the dust suppression efficiency, and as influenced by the nature or type of surface active agent. It would appear that a cationic wetting agent may spread more quickly over the surface of the dust particle than the anionic type and the non-ionic type. This last would appear to be only slightly better in wetting power than pure water.

The efficiency of dust suppression obtained in actual practice, by spraying surface active agent solutions, is not as high as might be expected because of one or more of the following reasons, for which quantitative measurements could not be easily made:

(i) Loss of "contact wetting" and "immersional or capillary wetting" powers of the sprayed liquid, due to its lowered surface tension. The tendency to wet by contact is measured by γ_1(Cos α + 1) and hence, addition of surface active agents to water would tend to decrease the contact-wetting power of the liquid, since the contact angle is lowered.

Immersional wetting becomes important, in suppressing porous particulate matter such as coal, by sprays. Coal has a high adsorptive power for air; as the ratio of the surface area to the mass of the particle increases, the greater is the adsorption. Therefore, to wet extremely fine particles of coal dust, the adhesion tension for water must be sufficiently great to work through the film of air on the surface of coal dust. The tendency of immersional wetting to occur is measured by $\gamma_1 . \cos \alpha$. Lowering of the surface tension of the liquid would thus appear to reduce immersional wetting.

(ii) Higher value of 'dynamic' surface tension of liquid sprayed. It was shown by Hunter[63] that reduced surface tension of the spray solution was not effective in increasing the 'atomisation' of sprays at higher pressures. This apparent failure to produce finer sprays of lower Average Droplet Size by surface active agents might possibly indicate that a value of synamic surface tension, intermediate between the values at the instant of formation of the new surface and at equilibrium adsorption of surface active agent, may be operative for the sprays. The new surfaces are formed too quickly for adsorption of the surface active agent to be complete and hence the static surface tension of the sprayed droplet is not actually to be taken as the surface tension of the solution.

(iii) Besides these characteristics of spray solutions, other factors in the actual collision process between the liquid droplets and the dust particles, such as the deformation of spray cone, may also contribute towards the low increase in dust suppression efficiency obtained by spraying surface active agent solutions.

Another useful theoretical attack on the problem of dust suppression by water sprays may be made through a study of the fundamental dynamics of the collision process between the dust and the sprayed droplets.

For convenience in such a theoretical treatment of the hydrodynamic capture of particulate matter, an idealisation of a system of small aqueous droplets encountering a cloud of smaller dust particles is made by considering the relative motion of only a single liquid droplet and a single dust particle in air. Both the bodies are assumed to be spherical and the water droplet is considered to be appreciably larger than the dust particle, so that the flow pattern under consideration is that of the air and the dust particle around the water droplet. [For the range of our experiments carried out at high spray pressures, the average droplet size can be taken as 80 microns, and the average particle diameter of dust in the wind-tunnel can be taken as 2 microns].

The dust particle, in this ideal system, is assumed to be so small that it does not affect the flow pattern of the stream. It is also assumed that the apparent weight of the particle is negligible compared with the viscous force. Since the Reynolds number of such a particle is very low (less than unity), the drag of the fluid on it is given by Stokes' law. The water droplet has a motion relative to the dust-laden air, by virtue of being sprayed from a pressure nozzle; but it is convenient to reduce the relative motion of the dust particle and the droplet to the motion of the particle in the air stream flowing around a stationary droplet.

In the spraying process, the ejected droplet will sweep out through the air a tube of cross-section equal to its diameter and in so doing may capture, sweep against, or sweep just past the dust particle. Theoretically, it is assumed that each impact results in a capture, but in practice, bouncing can occur with a probability depending on the relative velocity and the angle of incidence of each on the other.

The probability of capture of the particle by the droplet depends upon the balance of viscous and inertial forces acting on the particle as the droplet approaches it. If viscous forces are neglected and only inertial forces are considered, collision leading to capture will occur if the dust particle lies within the tube swept out by the water droplet. If the dust particle is given an effective diameter (the value of which may be taken as 2 microns in our case), the diameter of the tube has to be increased to allow for the diameter of the particle, viz. an impact will occur, if the minimum distance of the trajectory of the particle from the droplet surface is equal to or less than the effective radius of the dust particle. On the other hand, if viscous forces only are operative, the dust particle will tend to get carried away from the swept path of the droplet, along with the deviated streams of fluid. In practice, the impact and capture of dust particles is influenced by both viscous and inertial forces and collision efficiencies lie between zero and 100 per cent.

A sketch illustrating the grazing trajectory of a small dust particle for capture by a liquid droplet in an idealised system is shown in Fig. 9.1. It is assumed that the particle and the droplet will just collide, when the particle trajectory's nearest approach to the droplet surface is half the effective particle diameter, i.e. dp/2.

If the fluid forces on the dust particle can be taken to follow Stokes' law and thus the magnitude of the viscous drag on the particle to be linearly proportional to the relative velocity of the particle in the fluid, the

FIG.9·1. GRAZING TRAJECTORY OF DUST PARTICLE AND LIQUID DROPLET

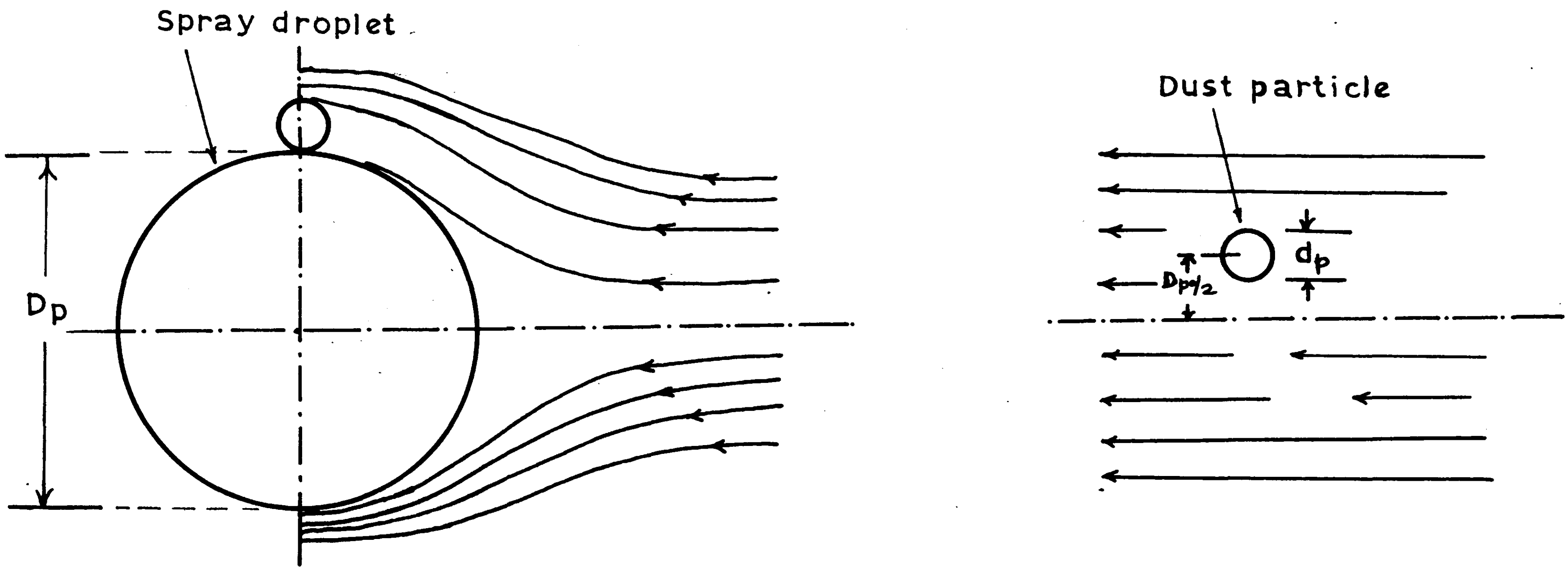

equations of motion can be written in terms of the fluid flow pattern around the droplet and the equations of motion are shown, by dimensional analysis, to depend on one characteristic dimensionless group, known as the "particle parameter" K,

$$\text{where} \quad K = \frac{1}{9}\left(\frac{dp}{Dp}\right)^2 \cdot \frac{\rho_s}{\rho_l} \cdot Re_{(droplet)}$$

$$\text{or} \quad = (\rho_s \cdot d_p^2 \cdot V_r)/(9\ \eta_a \cdot Dp).$$

Since the velocity of the fluid due to the flow pattern round the droplet is non-linear, the equations of motion of the particle are non-linear and hence their solution involves step-by-step plotting of each possible trajectory of the dust particle, as it approaches and tends to be swept round the larger sphere.

The trajectory, which corresponds to a grazing collision, is found by trial and error. This is the grazing trajectory, whose distance of nearest approach to the droplet surface is $d_p/2$ and whose distance from the line through the centre of the droplet when still at larger distances from the droplet is $D_{po}/2$. The circular area corresponding to the distance $D_{po}/2$ from the centre line of the droplet is known as the "capture cross-section" y_o^2, or, alternatively, as the "collection efficiency" E_c [67] which is defined as

$$E_c = \pi ({D_{po}/2} + {d_p/2})^2 / \pi ({D_p/2})^2$$

$$= (D_{po} + d_p)^2 / D_p^2$$

It is the ratio of the number of particles striking the droplet, to the number which would strike it, if the stream lines were not deflected around the droplet.

A number of workers(66)(67)(68)(69)(70)(71)(72) have computed values of E_c in terms of K, notable among them being Langmuir and Blodgett(66) and Fonda and Herne(67), who have evaluated particle trajectories and collision efficiencies in viscous and in potential flow pattern around droplets. Employing the diameter of the droplet as the unit of length, Fonda and Herne derived by a computer technique a dimensionless capture cross-section (y_o^2) and plotted curves relating various nearest distances of approach (r_m) of the trajectory to the centre of the droplet for both viscous and potential flow. Colision will take place where

$$r_m = (d_p + D_p) / D_p$$

The fluid flow pattern, which is assumed to be characterised by the flow of dust laden fluid round the droplet, has a significant influence on the collection efficiency. The latter is generally smaller for viscous than for potential flow at equal values of K, because in the former case, the fluid streamlines pass further from the sphere due to the stagnation of the fluid at the surface. In practice, the potential flow pattern is approximately valid in front of the droplet, when the Reynolds Number of the sphere is very large and the viscous flow pattern is appropriate when this Re is very small. The analysis of potential and viscous flow patterns around a sphere is given by Lamb.[113] The flow pattern is characterised by the Reynolds Number for the droplet, which is itself a measure of the relative importance of inertial and viscous forces within the fluid.

It is of interest to determine the range of capture cross-section covered in the high pressure aqueous spray work described here. The high pressure sprays (35.15 - 190.16 kg./sq.cm.) projected against the dust-laden air stream from the solid cone Nozzle 1 Plug 1 (Chapter 7.2) are considered for this treatment and using the data provided by Fonda and Herne, the range of capture cross-section is calculated for the whole range of spray pressures employed; making use of the experimental values of average droplet size at each spray pressure and taking a mean effective particle diameter of 2 microns. The results of these calculations are shown in Table 9.2.

Table 9.2

Range of Particle Parameter K and theoretical collection efficiencies for droplets from high pressure spray nozzles
(Plug 1 Nozzle 1)

Range of spray pressure ...	35.15 - 190.16 kg./sq.cm.
Range of calculated theoretical initial discharge velocity of sprays ...	5,640 - 13,260 cm./sec.
Counter-flow air velocity ...	100 cm./sec.

Range of Renolds Number of droplets in air:

for D_p = 60 microns ...	243.5 - 566.0
for D_p = 80 microns ...	323.0 - 752.5
for D_p = 100 microns ...	404.0 - 940.5

Range of Particle Parameter K (d_p mean - 2 microns)

for D_p = 60 microns ...	29.65 - 68.95
for D_p = 80 mkcrons ...	22.25 - 51.85
for D_p = 100 microns ...	17.85 - 41.45

Theoretical Capture Cross-section y_o^2

for rm = 1.033 ...	1.0318 - 1.0520
for rm = 1.025 ...	1.0030 - 1.0297
for rm = 1.020 ...	0.9848 - 1.0145

Theoretical Collection Efficiency Ec%

	Potential flow	Viscous flow
for D_p = 60 microns	96.5 - 98.5	83.0 - 90.0
for D_p = 80 microns	96.0 - 98.0	79.0 - 88.0
for D_p = 100 microns	94.0 - 97.5	75.0 - 86.0

It may be noted from the table that the experimental wind tunnel had a very efficient capture cross-section and therefore dust-suppression efficiencies, as high as the theoretical collection efficiencies (75.0 - 90.0 per cent for viscous flow and 94.0 - 98.5 per cent for potential flow fluid patterns) should have been achieved by the sprays, in the pressure-range employed. The values calculated, however, correspond to the initial projection velocity of the spray droplets. On discharge against the air stream, the droplets decelerate rapidly due to the resistance of the air and come to a halt, before getting carried away downstream with air. Under these conditions, the capture cross-section decreases rapidly and a calculation of the capture cross-section for a 80 micron droplet brought to momentary rest in a counter flow of air moving at 100 cm./sec., gives its value as low as 0.225. The mean capture cross section will then lie somewhere between the maximum values given in Table 9.2 and this minimum value.

Walton and Woolcock[68] made experimental measurements of the collection efficiency of water droplets for airborne dust particles of methylene blue over the range D_p 0.5 mm. to 2 mm., d_p 2.5μ to 5.0μ and droplet velocity 200 cm./sec. to 670 cm./sec. and compared it with theoretical predictions given by Fonda and Herne. Their reasoning has been adopted and modified to suit our experimental conditions to enable the calculation of dust suppression efficiencies resulting from the continuous spraying of a moving dust cloud in the cylindrical wind tunnel.

If a small interval of time Δt is considered during which water is sprayed in droplets of effective diameter D_p (equivalent to the Average Droplet Size at each spray pressure), at a total volume throughput rate of Q_w and the penetration of the droplets is S, the number of droplets produced will be equal to

$$(Q_w \, \Delta t) \; / \; (\tfrac{\pi}{6} D_p^3)$$

If $\bar{y}_o^2$ is the average capture cross-section over the range of spray S,

Effective volume of air denuded of dust will be

$$= \quad (Q_w . \Delta t / \tfrac{\pi}{6} D_p^3) \;\; \bar{y}_o^2 \; (\pi \, D_p^2/4) \; S$$

$$= \quad 3 \, Q_w . \, \bar{y}_o^2 . \Delta t . S / 2 \, D_p$$

Let the volume of air flowing through the tunnel in the same time Δt be $Q_a . \Delta t$

Thus fraction of the total dust removed

$$= \; (3 \, Q_w . \bar{y}_o^2 . \Delta t . S) \; / \; (2 \, D_p . Q_a . \Delta t)$$

If Δn is the change in dust concentration effected by spraying, the above relationship becomes

$$\frac{\Delta n}{n} \; = \; (3 \, Q_w . \bar{y}_o^2 . \Delta t . S) \; / \; (2 \, D_p . Q_a . \Delta t)$$

Thus for a logarithmic diminution in dust concentration,

$$n_1 \; = \; n_o . \exp \left[(- 3 \, Q_w . \bar{y}_o^2 . S) \; / \; (2 \, D_p . Q_a) \right]$$

where n_o and n_1 are the dust concentrations before and after the spray respectively

Hence $\log_e (n_1/n_o) = (-3\, Q_w . \bar{y}_o^2 . S) / (2\, D_p . Q_a)$

or $\log_{10}(n_1/n_o) = (-1.5\, Q_w . \bar{y}_o^2 . S) / (2.3\, D_p Q_a)$

and nozzle efficiency $E = \dfrac{n_o - n_1}{n_o} 100$

$= [1 - (n_1/n_o)]100.$

From the experimental values of dust suppression efficiencies, it is then possible to calculate the value of the actual effective capture cross-section $\bar{y}_o^2$ in the wind tunnel and this can be compared with the value, obtained from the particle parameter K using Fonda and Herne's data (see Table 9.2).

The solid cone spray from Nozzle 1 Plug 1 at a spray pressure of 140.6 kg./sq.cm. has been chosen to illustrate the calculations and the data appear in Table 9.3.

The value for y_o^2 was also calculated for the water droplet of 65 micron diameter under the same conditions using Fonda and Herne's data. A value of 54.2 was obtained for the particle parameter K, resulting in a value of 1.041 for the capture cross-section (y_o^2). It is important to note that this value has been calculated from the initial discharge velocity of spray droplets, whereas the value of

Table 9.3

Example for the calculation of Average Capture Cross-Section in Wind-tunnel

Nozzle 1   Plug 1   Solid cone   Water spray

Water pr. P = 140.6 kg./sq.cm.

Water throughput = 0.964 litres/min.(Fig.6.2)

Average Droplet Size = 65.0 microns (Table 6.3)

Air Velocity = 100 cm./sec.

Initial dust concentration (n_o) = 1513 p.p.c.c.(Table 7.1)

Final dust concentration (n_1) = 702 p.p.c.c.

Dust suppression Efficiency (E) = $\frac{n_o - n_1}{n_o}$ = 53.58

Spray cone angle = 40°

Q_w = water flow rate = $\frac{964}{60}$ = 16.07 c.c./sec.

Q_a = air flow rate = $\frac{\pi}{4} \times (18)^2 \times 6.4516 \times 100$

= 164.9×10^3 c.c./sec.

S = penetration = $9 \times 2.54 / \sin 20°$ = $\frac{22.86}{0.3420}$

= 66.9 cms.

$\therefore \log_{10} (702/1513)$

$= (-1.5 \times 16.07 \times \bar{y}_o^{\,2} \times 66.9) / (2.3 \times 65 \times 10^{-4} \times 16.49)$

i.e. $\log_{10} 0.4642 = (-\,0.654\, \bar{y}_o^{\,2})$

$\therefore (-\,\bar{y}_o^{\,2}) = (-\,0.3333) / (0.654)$

or $\bar{y}_o^{\,2} = 0.51$

y_o^2 calculated from the experimental value of dust suppression efficiency is an overall average effective value of capture cross-section in the wind tunnel. It can be shown that the value of y_o^2 drop to 0.3, when a 65 micron droplet (A.D.S. at a spray pressure of 140.6 kg./sq.cm.) comes to rest with respect to the tunnel. Hence, if an average value for y_o^2 is taken over the range S, the resulting figure for the effective capture cross-section is $\frac{1.041}{2} = 0.5205$, which is very close to the value calculated from the experimental results on dust suppression (0.51).

Thus it is seen that the experimental results of dust suppression compare well with the theoretical collection efficiency calculation.

The experiments with tandem sprays, described in Chapter 8, provide an attractive rate of increase in the dust suppression efficiency, as compared with single sprays. The best system for optimum efficiency was found by experiment to be four-nozzle tandem spraying at 140.6 kg./sq.cm. The efficiency was found to increase by almost 20 per cent, (48 to 68%) by the addition of three more nozzles in tandem and with a throughput of only about twice that of the single spray.

CONCLUSIONS:

The average droplet sise of high pressure sprays (in the range 35.15 - 210.6 kg./sq.cm.) varied inversely as the $(0.28)^{th}$ power of the spray pressure and hence a non-dimensional relationship connecting the average droplet size and the Reynolds Number of the issuing jet was established as follows :

$$A.D.S. \quad \alpha \quad Re^{(-0.56)}$$

This would enable predictions to be made of average droplet size, for a particular orifice and a particular spray pressure.

Generally, the dust suppression efficiencies obtained in practice were not as high as might be expected. This would indicate that the capture cross-section for the droplets in the tunnel was considerably reduced, by the rapid deceleration of the droplets and by the deformation of the spray cone due to the resistance of oncoming dust-laden air streams. Taking an average capture cross-section at nearly one half the value makes the theoretical predictions comparable.

The solid cone sprays gave about five per cent higher efficiencies than hollow cone sprays from the same nozzle. Maximum dust suppression seems to have been effected at about 140.6 kg./sq.cm. for all nozzles and types of liquids sprayed, thereby suggesting an optimum value of spray pressure for the best dust suppression efficiency with a minimum reduction in the dust-water ratios. The dust-water ratios in general decrease with increased water throughput and hence, a balance was necessary to be struck between the values of spray pressure and dust-water ratios, for an optimum dust suppression efficiency.

The surface active agents in spray solution generally effected a small increase in dust suppression efficiency. The cationic type - Fixanol C - of surface tension 40 dynes/cm. gave the maximum efficiency of 59.05 per cent with Nozzle 1 Plug 1 solid cone - about 6 per cent higher than that for water sprays with the same nozzle. The anionic and non-ionic types were in decreasing order of merit, though all three gave generally slightly higher figures for dust suppression than pure water. Nevertheless, the utility of these agents, to effect just about 6 per cent increase in dust suppression efficiency, is questionable on economic considerations.

The dust suppression efficiency was found in practice to decrease rapidly with increase in air velocity. One shoudl theoretically expect an increase in dust suppression, since increase in air velocity increases in turn the relative velocity between the water droplet and the dust particle and also the turbulence. However, due to the deformation and reduction of spray cone at higher air velocities, this decrease in efficiency is mainly attributable to the failure of the droplets to impact on the dust particle and hence to the by-passing of a proportion of the dust particles past the spray without colliding with the droplets.

Logarithmic relationships were found to exist between the spray pressure and dust suppressing efficiency and also between the surface tension and dust suppressing efficiency at the high pressure range (35.15 - 210.6 kg/sq.cm.) The dust suppression efficiency under these experimental conditions, could be represented as a function of the spray pressure and surface tension of sprayed liquid as follows :-

$$E = k. (P)^{0.455}. (\gamma_1)^{-0.12}$$

It was also found from experiments with different nozzles, that the spray pressure played a more important part in effecting dust suppression than the amount of water sprayed.

The results also indicated that high pressure sprays did not appear to be selective in suppressing any particular size-range of the dust particles from the air. The size distribution of the dust particles remaining in the air was found almost the same as that determined before spraying.

In general, the dust suppressing efficiency was found to increase linearly with increase in the water throughput of the spray and this is evident from results quoted in 7.5.

Tandem sprays showed a greater dust suppression efficiency with little increase in throughput of spray. The maximum dust suppression efficiency was seen to be effected at a spray pressure of 140.6 kg./sq.cm. and at this pressure was found the best rate of increase of dust suppression efficiency with number of nozzles added in tandem and hence with increase in throughput. As compared with a single spray at 140.6 kg./sq.cm., a 4 nozzle tandem spray required only twice the throughput at a gain of about 20 per cent in dust suppression efficiency.

This amounted to a rate of increase of about 6.0 per cent in dust suppression efficiency with one of every additional nozzle in tandem spray.

The trend of dust suppression effected at 140.6 kg/sq.cm. with tandem sprays suggested that almost 100 per cent dust suppression in the tunnel may be possible with a tandem spray system at 140.6 kg./sq.cm., and utilising about 10 nozzles (Nozzle 1 Hollow cone) in tandem at a minimum throughput rate of 3.58 litres/min. This hypothetical value is of great interest, in that such values of dust suppression efficiencies cannot be effected by a single spray nozzle, due to the reduced capture cross-section of droplets as the air resistance decelerates them. It also underlines the fact that better dust suppression could be effected by a series of small diameter nozzles in tandem, rather than by a single larger diameter nozzle.

Suggestions for future work.

(a) The effect of aqueous sprays of constant droplet size on moving dust clouds of constant particle size should be studied. This would enable one to find the optimum value of droplet size, if any, for the most efficient capture of dust particles of a particular size. The constant droplet size could be achieved by a rotary cup atomiser.

(b) Experimental investigations should be made of the velocity of water droplets within a spray over the range from initial ejection to the limit of experimental penetration. This would enable suitable practical values of average capture cross-section to be obtained.

(c) The new dust-feeder, described in Apprendix 2, could be developed more fully, with instrumentation for measurement of pressures, so that a more accurately reproducible range of dust concentrations could be studied in the tunnel.

(d) Radial sprays, projecting a thin screen of spray-liquid-barrier across the section of the tunnel, could be studied.

(e) Other arrangements of multiple sprays should be studied in the tunnel.

APPENDIX I

PARTICLE SIZE ANALYSIS OF EXPERIMENTAL DUST BY SEDIMENTATION METHOD.

Air-borne dust flowing in the wind tunnel had been sampled, simultaneously, through gravimetric salicylic acid filters and by thermal precipitators and their dust-counts compared in Chapter 5. It was felt that an independent check should be made of particle size of dust fed to the dust-machine hopper and this was done using the I.C.I. sedimentation apparatus, which is a modified form of Andreason Sedimentation pipette. (See Fig. A.1.1).

The Sedimentation pipette consisted of two glass tubes equipped at the top with stop cocks and encased in a water jacket to prevent temperature variation. There was an outlet at the foot of one of the tubes and a side arm above this led off to the foot of the other glass tube.

A 2% Sodium citrate solution was used to completely fill the clear water reservoir and fill two-thirds the sedimentation tube. About 0.3 gm. of the sample of experimental dust was then accurately weighed out, moistened with a little glycerol and dispersed in about 10 ml. of the citrate solution. A pipette was used to place this suspension in the settling tube and an air current introduced to obtain even distribution and prevent sticking to the wall of the tube.

FIG.A·1·1· I.C.I. SEDIMENTATION APPARATUS

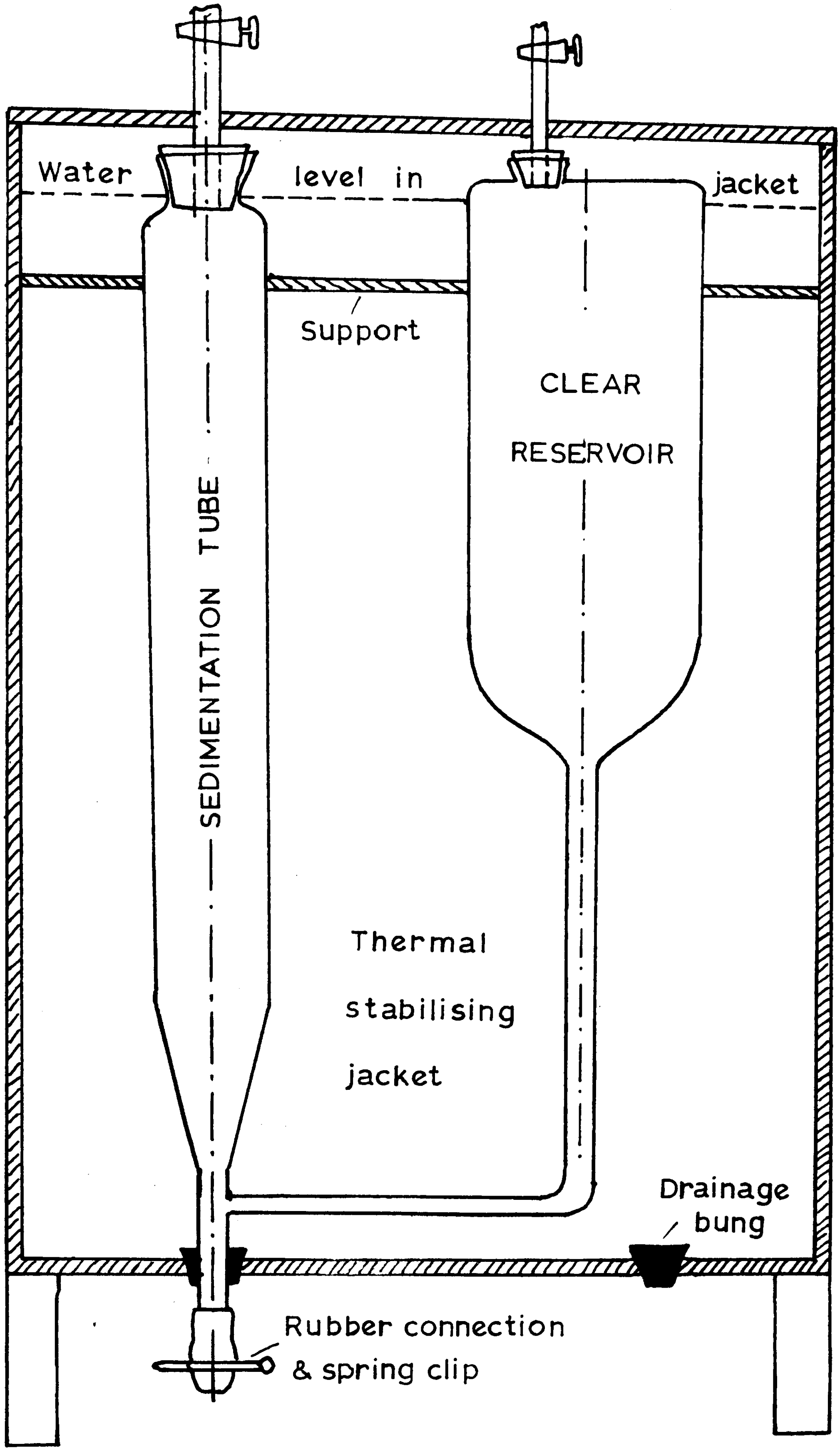

By manipulating the taps on the top of the tubes, clear liquid was passed from the reservoir to the sedimentation tube via the side arm and, after a final air injection to restore uniformity, the test was started.

During the run the tap on top of the sedimentation tube remained closed, while that on the clear liquid reservoir remained open. Thus when a sample was taken by releasing the spring clip at the outlet, the liquid flowed from the reservoir via the outlet, carrying with it the particles which had settled out with the minimum of disturbance to the liquid in the sedimentation tube.

Incremental samples were taken at calculated intervals and the results computed assuming hydrodynamic similarity of dust particles and obedience to Stokes' Law.

$$V_t = h'/t = g.d_p^2(\rho_s - \rho_1) / 18\,\eta$$

This equation was used to calculate the time of settlement of a particular range of particles, and in appropriate units, it reduced to

$$t = \frac{h'\ \eta\ 10^7}{5.45(\rho_s - \rho_1)d_p}$$

For this determination, the mean particle diameters were arranged in a $\sqrt{2}$: 1 starting from 89 microns (76 - 106μ), so that the sampling times would become convenient multiples of 't'. t was found to have a value of 302 seconds, at the end of which the sample withdrawn would have a characteristic mean diameter of 89 microns

Table A.1.1

Size* - distribution of experimental coal dust by Sedimentation method.

Size range microns	Mean size microns	Wt. of increment gms.	True wt. of sample gms.	No. of particles x 10^6	No. %
106 - 76	89.0	0.2444	0.1577	0.33	0.010
75.99 -253	63.0	0.0867	0.1183	0.71	0.021
52.99-37.5	44.5	0.0551	0.0543	0.953	0.028
37.49-26.5	31.5	0.0559	0.0804	4.03	0.120
26.49-18.8	22.2	0.0314	0.0428	5.59	0.166
18.79-13.2	15.7	0.0200	0.0197	7.14	0.211
13.19- 9.4	11.1	0.0203	0.0281	31.5	0.934
9.39- 6.6	7.9	0.0125	0.01118	28.0	0.83
6.59-4.69	5.6	0.0034	-	-	-
4.68- 3.3	3.79	0.008	0.0118	286.0	8.48
3.29- 2.4	2.86	0.0042	-	-	-
< 2.39	-	0.017	0.0154	3010.0	88.40

* "Size" in hydrodynamic similarity refers to the diameter of a sphere having the same density and Stokes' law terminal velocity as the particle.

and then samples were collected at intervals of 2t, 4t, 8t, etc. These were collected in numbered tubes and the weight of coal particles present was found by centrifuging and drying to constant weight. The relationship between the true weights of dust samples in particular size ranges and the measures had been derived by Stairmand[114]

The results are shown in Table A.1.1 and the summary is given in Table A.1.2.

Table A.1.2

Summary of Size Analysis of experimental dust by Sedimentation

Size range microns	< 3.29 μ	3.29 - 6.59 μ	> 6.59 μ	Total
Number percentage Size frequency	88.40	8.48	3.12	100.00

These results should be compared with the dust size-counts of samples actually taken from the dust-laden air streams in the wind tunnel by means of thermal precipitator and salicylic acid filter. (Table 5.2). The number percentage in all size ranges seem to agree quite closely, giving allowance for errors in sampling.

APPENDIX II

A NEW DUST FEEDING DEVICE

It was found in practice that the dust feeding machine used in our experiments for injecting dust into the tunnel (see 2.2.1) was not very effective in achieving exactly repeatable dust concentrations, since its action depended on the dust groove being completely filled with dust, by the scapers. The position of the scraper and the clearance between the dust-disc and the hopper were also found to have an influence on the filling of the dust-groove and consequently on the dust concentration in the tunnel. Hence a new dust feeding machine was developed, which would give more predictable dust concentrations and which depend less on manual adjustments of the apparatus.

The new machine, built of glass, is shown in Fig. A.2.1 and was found to give a more repeatable dust concentration, which could be varied over a wide range. It is in fact a modified form of the apparatus described by Shale.[115]

The feeder was of the counterflow pulsating type, which injected dust into the gas stream. The dust-bed was kept 20 cms. high, while the air-inlet and dust-outlet nozzles were 4.0 mm. and 2.5 mm. in diameter respectively. The pulsating air supply was obtained from the exhaust of a vacuum pump, which maintained a pressure of 15 cm.w.g. A constant frequency of 800 impulses of air per minute was

FIG. A2·1. A NEW DUST FEEDER

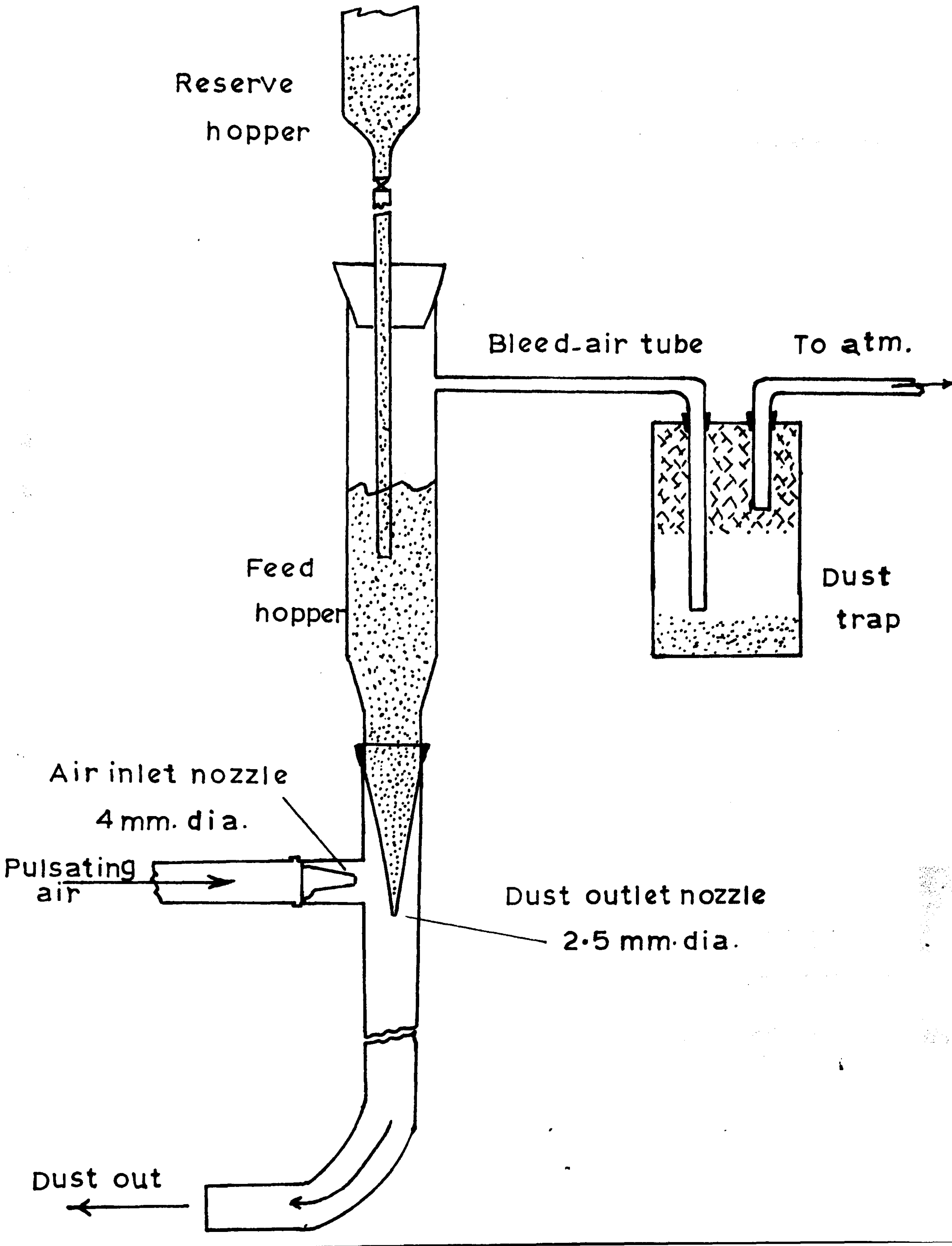

employed during the experiments. It is possible that a variation in impulse-frequency would affect the dust feed rate.

The pulsating air was admitted to the feeder at a controlled rate through the orifice just above the level of dust-outlet nozzle. In practice, it was found necessary to include a filter or oil-trap in the passage of the pulsating air, to remove any oil droplets that might be carried with the air from the pump.

At each impulse peak, a small quantity of the carrier air flowed up through the dust-outlet nozzle and the dust bed and escaped through a bleed-air tube above the dust bed. At the low-pressure point in each impulse, the air flow through the nozzle reversed and a small increment of dust was entrained by the pulsating carrier-air stream into the tunnel-axis. Thus there was an intermittent discharge of dust from the outlet nozzle. Since the increments of dust were small, the dispersion was virtually continuous. As this injected dust was carried forward along the length of tunnel by the turbulent air stream from the centrifugal fan, the dust was well dispersed.

The new dust feeder was set in position, to inject dust along the axis of the tunnel and test runs were carried out, to find the dust concentration along the length of the tunnel, at air velocities of 100, 250 and 500 cm./sec. Allowing some time to reach steady conditions in the tunnel,

FIG. A2·2. NEW DUST FEEDER: EFFECT OF AIR VELOCITY ON DUST CONCENTRATION IN TUNNEL

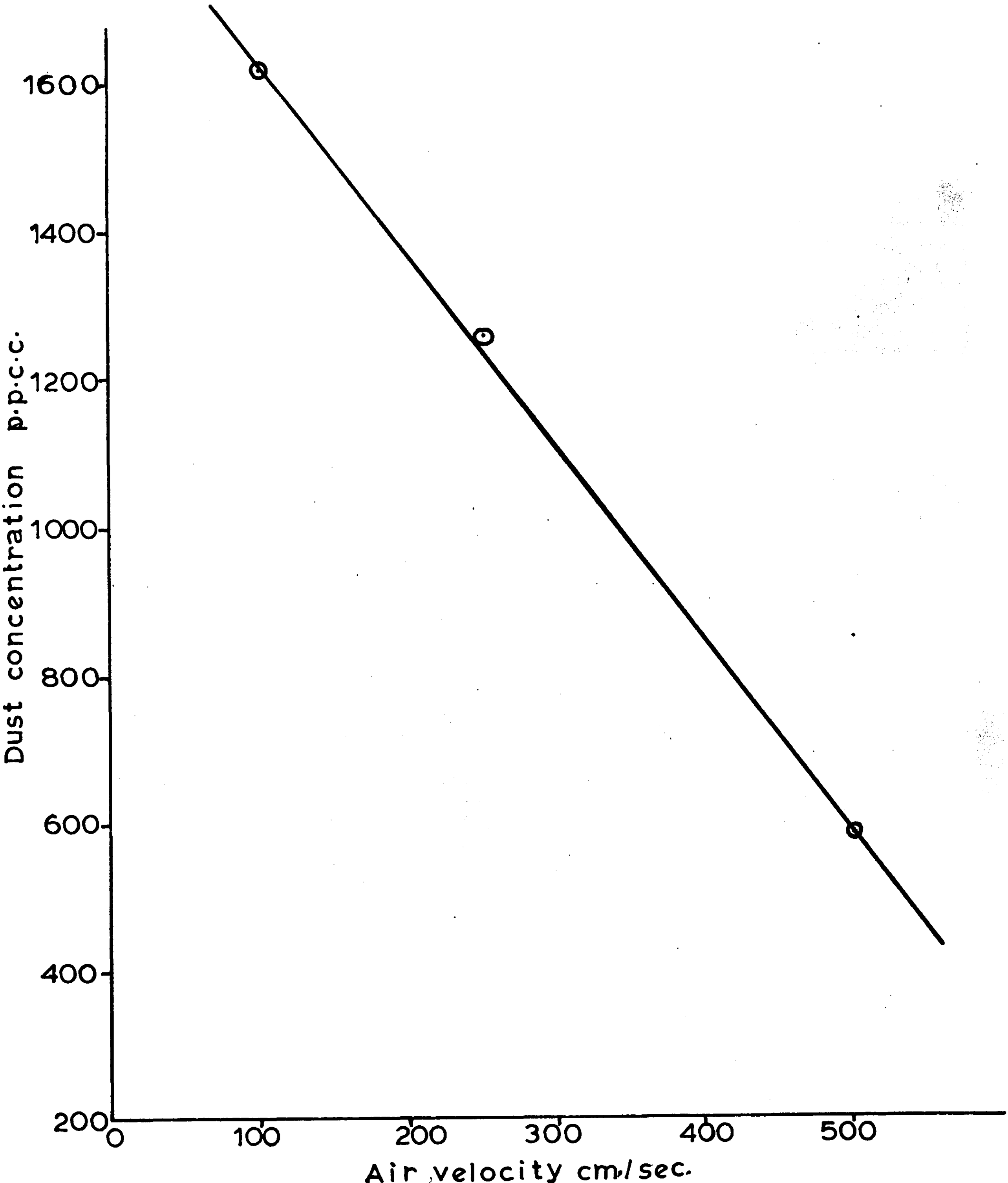

simultaneous dust sampling was carried out at each of these three air velocities by means of thermal precipitators. The dust concentrations obtained are shown in Table A.2.1.

Table A.2.1

Dust concentration in the tunnel from the new dust feeder

Air Velocity		Dust concentration p.p.c.c.		
ft/min.	cm/sec.	At T.P.1	At T.P.2	Difference
200	100	1602	1638	36
500	250	1250	1272	22
100	500	582	583	1

This would indicate a linear relationship between the air velocity and the dust concentration in the tunnel, for this particular dust feeder. This is illustrated in Fig. A.2.2. Hence it is possible to predict the dust concentration in the tunnel for any particular dust feeder employed.

Dust-feed rates would however be increased, by reducing bleed-air rates or increasing operating pressures. Larger orifices in the air-inlet and dust outlet nozzles and shallower dust-beds would also increase the dust-feed rates. Calibrations for different set of nozzles and operating conditions would prove highly useful, in selecting the dust-feeding apparatus, for any required dust-concentration range.

REFERENCES

1. Green, H.L., and Lane, W.E: 'Particulate clouds: Dust, Smokes and Mists', E. and F.N. Spon Ltd., London, 1957, 4.

2. B.S.S. No. 410, British Standards Institution, 1943.

3. Jones, W.R.: Silicotic lungs: the minerals they contain, J. Hyg., 33: 307, 1933.

4. Middleton, E.L.: The etiology and pathogenesis of Pneumoconiosis, Proc. conf. of experts on Pneumoconiosis, I.L.O., 1, 300, 1950.

5. Gibbs, W.E.: Clouds and Smokes, J. and A. Churchill, London, 1924.

6. Hartmann, I., Nagy, J., and Brown, H.R.: "Inflammability and explosibility of metal powders", U.S. Bur.Mines, Rept. Invest. 3722, 1943.

7. Hartmann, I., Copper A., and Jacobson, M.: Recent studies on the explosibility of cornstarch; U.S. Bur. Mines, Rept.Inves. 4725, 1950.

8. Thorp, P.: Dust suppression in coal-mines, Iron and Coal Trades Review, 176, 553, 1958.

9. International Labour Organisation: Pneumoconiosis, a list of references, studies and reports; Series F. (Ind. Hygiene) No.15, 1932.

10. Greenburg, L.: The classification of dusts which cause pulmonary disability, Proc.conf. of experts on pneumoconiosis, I.L.O., 2, 64, 1950.

11. Zenker, F.A., Deustch.Arch.klin.Med., 116, 2, 1866.

12. Proust, A., Bull.Acad.Med., Paris, Ser.2,3,624.

13. Hamlin, L.E.: Journal of the American Medical Association, Chicago, 1949, 139; 14; 909-912.

14. King, E.J.: 'Recent Research in Pneumoconiosis', Rep. of Symp. on Pneumoconiosis, The Chest and Heart Assoc.; 1959.

15. Gough, J.: J.Path. and Bact., 86, 4, 1947.

16. Heppleston, A.G.: J.Path. and Bact., 51, 67, 1954.

17. Boyd, W: Pathology for the physician, Henry Kimpton, London, 1958, 225-232.

18. Stewart, M.J. and Faulds, J.S.: J.Path. and Bact., 1934, 39, 233.

19. Agricola, G. (1494-1555), De Re Metallica, Translated from Latin Ed. 1556 by H.C. and L.C. Hoover, Mining and Scientific Press, San Francisco, 1912.

20. Smith, J.M.: "A review of the work of the Silicosis Medical Bureau, Johannesburg", Proc.Conf. on Silicosis, Inst. of Min.Eng. and Inst.Min.Met., 1947, p.88.

21. Caplan, A.: Dust prevention in Kolar Gold Fields, ibid, 33.

22. Macbain, G.: The working Foundryman and his chest, Report on Symp. on pneu., Chest and Heart Assoc., 1960.

23. Fletcher, C.M. and Gough, J.: "Coal-miner's Pneumoconiosis", Brit.Med.Bull. 7:42(1950).

24. Warner, C.G.: Air-borne dust problem in coal-mines, The Iron and Coal Trades Review, 174, 911, 1957.

25. Digest of Pneumoconiosis Statistics, Ministry of power, 1961, p.10.

26. Gooding, C.G. Pneumoconiosis Field Work in the Scottish Coalfield, Rep. on Symp. on Pneum., Glasgow 1960, p.106.

27. S.M.R.E. Annual Report No. 51, 1958.

28. McCrae, J.: The Ash of Silicotic lungs, South African Institute of Medical Research, Johannesburg, 1913.

29. Mavrogordato, A.: Value of the Konimeter, being an investigation into the methods and results of dust-sampling as practised in the mines of Witwatersrand, South African Inst. of Med.Res., 1923.

30. Gardner, L.U. and Cummings, D.E.: The reaction to fine and medium sized quartz and aluminium oxide particles. Am.J.Path., 9, 751, 1933.

31. Tebbens, B.D., Schulz, R.Z., and Drinker, P.: The potency of Silica particles of different size, J. Indust. Hyg. and Toxicol., 27: 199, 1945.

32. "Chronic Pulmonary Disease in South Wales Coal-Miners: I - Medical Studies, and II - environmental studies", Spec.Rep.Ser.Med.Res.Coun., London; Nos. 243(1942); 244(1943).

33. Finderson, W.: Pflügers Arch., 236, 367, 1935.

34. Davies, C.N.: Inhalation risk and particle size in dust and mist; Brit. J. Industr. Med., 6, 245, 1949.

35. Van Wijk, A.M., and Patterson, H.S.; J.Industr.Hyg., 22, 31, 1940.

36. Landahl, H.D. and Black, S. ; J.Industr.Hyg., 29, 269, 1947.

37. Wilson, I.B., and La Mer, V.K. ; J.Industr.Hyg., 30, 265, 1948.

38. Brown, J.H., Cook, K.M., Ney, F.G., and Hatch, T.: Influence of particle size upon the retention of particulate matter in the human lung, Am. J. Pub. Health, 40: 450, 1950.

39. Davies, C.N.: Dust Sampling and lung disease; Brit.J.Industr.Med., 9, 120, 1952.

40. Cited by Graham, J.I. and Jones, T.D.: The Suppression of dust in coal-mines of Great Britain, Proc. of Conf. on Pneumoconiosis, Inst. of Min. Engrs., and Inst. Min. and Metall., London, 1947, 121.

41. National Coal Board, Report and Accounts for 1949, H.M.S.O., 29.

42. Taylor, S.E., Discussion on Evans W.D.'s paper "Properties of air-borne dusts in relation to pneumoconiosis", Trans.Inst.Min.Metall., London, 25, 65, 1955-56.

43. Boyle, W., How Britain Controls Dust, Coal Age, Feb. 1957, p.87.

44. Knaggs, C.R., Approach to dustless mining, Iron and Coal Trades Review, 313, 174, 1957.

45. Richmond, J. Report on the reduction of air-borne dust concentration at loading points by application of water sprays, NCB Sci.Dept.

46. N.C.B. inf. Bull. 55/144, 1955.

47. Wood, W.A., Steam for underground dust suppression. The Iron and Coal Trades Review, 315, 177, 1958.

48. Linacre, E.T., The salt-crust method of roadway treatment, S.M.R.E., Rep. No. 94, 1954.

49. Meyer, W.E. and Ranz, W.E., 'Sprays', Encyc.chem. Tech., 12, 703, 1954.

50. Rayleigh, (Lord): 'On the instability of jets', London Mathematical Society Proc., 10, 4, 1878-'79.

51. Castleman, A.: 'The resistance to the steady motion of small spheres in fluid', N.A.C.A. Tech. Note, No.231.

52. Haenlein, A.: 'On the disruption of a liquid jet', Forsch. Geb. Ingenieurwesens , A, 2, 4, 139, 1931.

53. Weber, C.: 'On the disruption of a liquid jet', Zeitschrift für angewandte Mathematik und Mechanik, 11, 2, 136, 1931.

54. Wehlig, H. : 'On the physics of fuels sprays in diesel engines', Automobiltechnische Zeit, 37, 16, 411, 1934.

55. Schweitzer, P.H. : Mechanism of disintegration of liquid jets, Jour. of Appl.phys., 8, 513, 1937.

56. Thiemann, A.E. : 'The viscosity of air is more important than its density for fuel sprays', Automobiltechnische Zeit, 37, 16, 400, 1934.

57. Strazhewski, L.: 'The spray range of liquid fuels in an opposing air-flow', Techn. Phys. U.S.S.R., 4,6,438, 1937.

58. Oschatz, W.: 'An investigation on atomisation and sprays', Forsch. Geb. Ingenieurwiesens B., 11, 5, 296, 1940.

59. Nukiyama, S. and Tanasawa, Y. : 'An experiment on the atomisation of liquid by means of air stream'; Soc.Mech.Engrs. Japan, Trans., 4, 86, 138, 1938 and 5, 63, 68, 1939.

60. Ohnesorge, W.V. : "The formation of drops from nozzles and the disruption of a stream of liquid", Verein Deutscher Ingenieure Zeitschrift, 81,16,220,1937.

61. Castleman, R.A. Jnr.: 'The Mechanism of atomisation of liquids', Bureau of Standards. Jour.Res. U.S. Dept. of Commerce, 6, 281, 1931.

62. Glen, W.: Ph.D. Thesis, University of Glasgow, 1954.

63. Hunter, G. : Ph.D. Thesis, University of Glasgow, 1959.

64. Fraser, R.P., Eisenklam, P. and Dombrowski, N.: Liquid atomisation in chemical engineering, Brit.Chem.Eng., Oct. 1957.

65. Best, A.C., Quart. J.R. Met. Soc., 76, 302, 1950.

66. Langmuir, I. and Blodgett, K.B.: Army Air Forces Technical Report, 5418, Washington, 1946.

67. Fonda, A. and Herne, H. : 'Hydrodynamic Capture of particles by spheres', Min.Res.Est. Report No. 2608, 1957.

68. Walton, W.H. and Woolcock, A. : 'The suppression of air-borne dust by water spray', Min.Res.Est. Rep. No. 2163, 1960.

69. Das, P.K. : Ind. J. Met. Geophys., 1, 137, 1950.

70. Bosanquet, C.H.: "Impingement of particles on obstacles in a stream", Trans.Inst.Chem.Eng., 28, 136, 1950.

71. Vasseur, M., Rech. Aero, 9, 1, 1949.

72. Sell, W., Forschungsh. Ver. Dtsch. Ing., 347, 1931.

73. Brown, D.J., N.C.B., C.R.E. Rep. 1265, 1955.

74. Massie, W.H., Ph.D. Thesis, University of Glasgow, 1951.

75. Deshpande, A.K., Ph.D. Thesis, University of Glasgow, 1961.

76. Hutcheson, R.J. and Sweetin, R.M. : Research Report No. 11, Dust Research Group, Royal College of Science and Technology, 1958, 12.

77. Hattersley, R., Maguire, B.A. and Tye, D.L. : A Laboratory dust cloud producer, SMRE Res. Rep. No. 103, 1954.

78. Weir, G., Homogenisers, Publication No. 7011, G. and J. Weir Ltd., Glasgow.

79. Casella, C.F. and Co.Ltd., Thermal Precipitator, Instruction Leaflet No. 3019/RD, London.

80. Green, H.L. and Watson, H.H.; Physical methods for the estimation of the dust hazard in industry, Medical Res. Coun. Sp.Rep.Ser. No. 199, 1935, London, H.M.S.O.

81. Prewitt, W.C. and Walton, W.H.; The efficiency of the thermal precipitator for sampling large particles of unit density, M.O.S. Porton Technical paper No. 63, 1948.

82. Dawes, J.G.; Notes on Physics of Dust dispersion, SMRE 3, 1958.

83. Withers, A.G.: "Gravimetric sampling technique", Coll. Guar. 1946, 172, 627-32, 661-4.

84. Flow Measurement. BS. 1042: B.S.I., 18, 1943.

85. Martin, G. : A treatise on Chem. Engineering; 3, 6.

86. Honeycomb manufactured by Messrs. Dufaylite Developments Ltd., Essex Road, Borehamwood, Herts., made of standard 5/1000 Resinated kraft paper.

87. Stairmand, C.J. : Sampling of dust-laden gases: Trans. Inst. Chem. Eng., 29, 1, 16, 1951.

88. Stairmand, C.J. : Salicylic-acid crystals for sampling filters; Private Communication, 1960.

89. Stairmand, C.J. : Aerodynamic capture of particles; Proc. Conf. B.C.U.R.A., 1960, p.53.

90. Pereles, E.G., The theory of dust deposition from a turbulent airstream by several mechanisms, S.M.R.E. Res. Rep. No. 144, 1958, p.9.

91. Dawes, J.G. and Slack, A. : Deposition of Air-borne dust in a wind tunnel, SMRE Res. Rep. No. 105, 1954.

92. Page, A. and Townend, H.C.H. : 'An examination of turbulent flow with an ultramicroscope', Proc. Roy. Soc., A, 135, 656, 1932.

93. Biggs, R., and Macmillan, R.L., J.Clin.Path., 1, 288, 1948.

94. The Physics of Particle Size Analysis, Brit.J.Appl. Phys., Supp. 3, 1954.

95. Herdan, G. : Small particle Statistics, Butterworths, 1960, 340.

96. Hawksley, P.G.W., Blackett, J.H., Meyer, E.W., and Fitzsimmons, A.E. : 'The design and construction of a photoelectronic scanning machine for sizing microscopic particles', British Jour. Appl. Phys., Paper G6, S165.

97. Automatic Particle Counter and Sizer, Casella (Electronics)Ltd., Leaflet No. 872, now merged with Cooke, Troughton and Simms Ltd.

98. Stewart, A.W.K. of the Mining Department, Royal College of Science and Technology. Private Communication.

99. Non-drying Immersion oil ALP 1, supplied by Cooke, Troughton and Simms Ltd., York, ND = 1.524 at 20°.

100. Cadle, R.D., Particle Size Determination, Interscience Pub.Inc., New York, 1955.

101. Potter, N.M. : Micro and semi-micro methods for investigation of air-borne dust, Colliery Guardian, 173, 145-149, 179-185, 1946.

102. Giffen, E. and Muraszew, A. : Atomisation of liquid fuels, Chapman and Hall, London, 19-26, 1953.

103. May, K.R. : 'The measurement of air-borne droplets by the Magnesium Oxide Method', Journ. Scient. Instruments, 27, 123, 1950.

104. Fraser et.al. : Liquid Atomisation in Chemical Engineering, Brit.Chem.Eng., October, 1957.

105. Cited by Griffen, E. and Muraszew, A. : Atomisation of Liquid Fuels, Chapman and Hall, London, 192, 1953.

106. Joyce, J.R. 'The atomisation of liquid fuels for Combustion', Jour.Inst.Fuel, 22, 150, 1949.

107. 'Surface active agents', Publication No. 30, I.C.I. Dyestuffs Division, 1959.

108. Harmsen, G.T., van Schooten, J., and Overbeck, J.Th.G, J. Colloid Sci., 8, 64, 72 (1953).

109. Retel, R., Contribution to the study of injection in Diesel engines, Publications Scientifiques et Techniques due Ministere de l'Air, B.S.T., No. 81, 1938.

110. Owings, C.W., Control of airborne dust in bituminous - coal mines in U.S.; Proc. Fifth intern. Conf. of Dir. of Mine Safety Research, Bureau of Mines Bull., 489, 183 - 192, 1950.

111. Terrel, Iron and Coal Trade Review, 149, 871.

112. Pemberton, C.S., "Scavenging action of rain on non-wettable particulate matter suspended in the atmosphere", Proc. Conf. on 'Aerodynamic Capture of Particles', Pergamon Press, 168, 1960.

113. Lamb, H., Hydrodynamics, 6th edition (Cambridge) 1932.

114. Stairmand, C.J., Symposium on particle size analysis, Inst.chem.Engrs., 58, 1947.

115. Shale, C.C.; 'Laboratory dust feeder', Chemical Engineering, Nov. 1959.

SUMMARY

This study is concerned with the capture of airborne dust particles by sprayed liquid droplets, with particular reference to the airborne coal dust encountered in mining practice. The particle size range 0.5 - 5.0 microns, of physiological importance in causing occupational health hazard, has been investigated.

The significance of dusts and their harmful particle-size and concentration are discussed and the incidences of coal-miners' pneumoconiosis and existing methods of dust suppression in mines are surveyed. The general mechanism of liquid spray formation from nozzles is investigated and the theoretical probability of capture of dust particles by spray droplets is discussed.

Experiments on dust suppression were carried out on moving dust clouds in a wind-tunnel of 45.72 cm. (18 in.) diameter and 20 metres (65 ft.) long, under controlled conditions. Dust clouds, of concentrations in the range 300 and 3000 p.p.c.c., were produced using Hattersley's laboratory type dust generator. A three-throw reciprocating pump provided spray pressures up to about 210 kg./sq.cm. (3,000 p.s.i.g.) and the spray nozzles were

operated at the axis of the tunnel against the flow of dust-laden air. Simultaneous dust sampling was done by two thermal precipitators located ahead of and beyond the spray nozzle.

Distribution of air velocity in the tunnel was studied and modifications in the tunnel were made to straighten out the air flow. The effect on air flow pattern of baffle plates suitably placed in the tunnel is illustrated in the form of iso-velocity curves.

Distribution of dust concentration in the tunnel was studied with salicylic acid filters and the rate of decay of dust concentration with distance along the tunnel was found to be constant. The probable mechanisms of dust fall-out are discussed.

A system for counting the thermal precipitator dust slides using a five-channel Automatic Particle Counter and Sizer was developed and an analysis of variance for the machine was made.

Simultaneous dust sampling by thermal precipitator and salicylic acid filter was carried out in the tunnel and a correlation factor was derived on the basis of proportional number percentage size frequencies in both the samples.

Measurment of Average Droplet Size was carried out for water sprays in the range 35.15 - 190.16 kg./sq.cm. (500 - 2,750 p.s.i.g.) using a solid cone spray nozzle and the relationship

$$A.D.S. \quad \alpha \quad P^{(-0.28)}$$

was obtained. A functional non-dimensional relationship was also derived between the characteristics of the spray and the Average Droplet Size.

The dust suppression work was mainly concerned with small high pressure spray nozzles and the following issues were brought to focus: The effects on the efficiency of dust suppression of,

(a) hollow cone and solid cone spraying,

(b) high spray pressures,

(c) surface tension of sprayed liquid,

(d) counterflow air velocity, and

(e) a tandem arrangement of spray nozzles.

The effect of spray throughput on dust-water ratio was also studied. Solid cone spraying was found to be about 5 per cent more efficient than the hollow cone spray for the same nozzle. Maximum dust suppression was effected at 140.6 kg./sq.cm. in both the cases. (53.58 per cent and 48.5 per cent).

Surface active agent solutions were found to give only a small increase in dust suppression efficiency, E. The wetting power of different types of surface active agents is discussed. A relationship was obtained between the efficiency, spray pressure and the surface tension of the sprayed liquid.

Tandem spraying was found to give the best dust suppression efficiencies without much increase in water throughput. The rate of increase in E with number of spray nozzles in tandem was found to be maximum (about 6.5 per cent) at 140.6 kg./sq.cm.

An increase in air velocity resulted in a rapid decrease of E. The rapid deceleration of droplets on discharge into the gaseous medium, its lowered efficacy of impact on dust particles and the consequent reduction of the "capture cross-section" are discussed.

The dust-water ratio was calculated for all spray pressures and nozzles employed and was found to generally decrease with increase in throughput.

The sprayed droplets did not appear to be selective in suppressing any particular size-range of dust particles.

An improved type of dust feeding machine was put into operation and is discussed in the Appendix.